# GENOMIC AND BIOCHEMICAL INVESTIGATION OF SOYBEAN ANTIOXIDANT METABOLISM IN RESPONSE TO GROWTH AT ELEVATED CARBON DIOXIDE AND ELEVATED OZONE

BY

KELLY MARIE GILLESPIE

DISSERTATION

Submitted in partial fulfillment of the requirements
for the degree of Doctor of Philosophy in Biology
with a concentration in Physiological and Molecular Plant Biology
in the Graduate College of the
University of Illinois at Urbana-Champaign, 2010

Urbana, Illinois

Doctoral Committee:

Assistant Professor Elizabeth A Ainsworth, Director of Research, Chair
Professor Steven Huber
Professor Donald Ort
Assistant Professor Steven Clough

## ABSTRACT

Metabolism in an environment containing of 21% oxygen ($O_2$) has a high risk of oxidative damage due to the formation of reactive oxygen species (ROS). Therefore, plants have evolved an antioxidant system consisting of metabolites and enzymes that either directly scavenge ROS or recycle the antioxidant metabolites. Ozone ($O_3$) is a temporally dynamic molecule that is both naturally occurring as well as an environmental pollutant that is predicted to increase in concentration in the future as anthropogenic precursor emissions rise. It has been hypothesized that any elevation in $O_3$ concentration ($[O_3]$) will cause increased oxidative stress in plants and therefore enhanced subsequent antioxidant metabolism, but evidence for this response is variable. Along with increasing atmospheric $O_3$ concentrations ($[O_3]$), atmospheric carbon dioxide concentration ($[CO_2]$) is also rising and is predicted to continue rising in the future. The effect of elevated $[CO_2]$ on antioxidant metabolism varies among different studies in the literature. Therefore, the question of how antioxidant metabolism will be affected in the most realistic future atmosphere, with increased $[CO_2]$ and increased $[O_3]$, has yet to be answered, and is the subject of my thesis research. First, in order to capture as much of the variability in the antioxidant system as possible, I developed a suite of high-throughput quantitative assays for a variety of antioxidant metabolites and enzymes. I optimized these assays for *Glycine max* (soybean), one of the most important food crops in the world. These assays provide accurate, rapid and high-throughput measures of both the general and specific antioxidant action of plant tissue extracts. Second, I investigated how growth at either elevated $[CO_2]$ or chronic elevated $[O_3]$ altered antioxidant metabolism, and the ability of soybean to respond to an acute oxidative stress in a controlled environment study. I found that growth at chronic elevated $[O_3]$ increased the antioxidant capacity of leaves, but was unchanged or only slightly increased following an

acute oxidative stress, suggesting that growth at chronic elevated [$O_3$] primed the antioxidant system. Growth at high [$CO_2$] decreased the antioxidant capacity of leaves, increased the response of the existing antioxidant enzymes to an acute oxidative stress, but dampened and delayed the transcriptional response, suggesting an entirely different regulation of the antioxidant system. Third, I tested the findings from the controlled environment study in a field setting by investigating the response of the soybean antioxidant system to growth at elevated [$CO_2$], chronic elevated [$O_3$] and the combination of elevated [$CO_2$] and elevated [$O_3$]. In this study, I confirmed that growth at elevated [$CO_2$] decreased specific components of antioxidant metabolism in the field. I also verified that increasing [$O_3$] is highly correlated with increases in the metabolic and genomic components of antioxidant metabolism, regardless of [$CO_2$] environment, but that the response to increasing [$O_3$] was dampened at elevated [$CO_2$]. In addition, I found evidence suggesting an up regulation of respiratory metabolism at higher [$O_3$], which would supply energy and carbon for detoxification and repair of cellular damage. These results consistently support the conclusion that growth at elevated [$CO_2$] decreases antioxidant metabolism while growth at elevated [$O_3$] increases antioxidant metabolism.

## ACKNOWLEDGEMENTS

I first and foremost thank my advisor, Dr. Lisa Ainsworth, for allowing me the opportunity to work in her lab and for always moving toward excellence. She has been a brilliant mentor and a model scientist. I thank my Department of Energy mentor, Dr. Alistair Rogers, for allowing me to visit his lab and for patiently teaching me about robots and enzyme assays. His assistance and input on writing the chamber experiment mauscript were invaluable. I thank Dr. Steve Long, first for allowing me to conduct my undergraduate honors research project at SoyFACE, and then for welcoming me into his lab during my first semester of graduate school. He was always generous and encouraging with his time and input. I thank the rest of my committee members, Drs. Don Ort, Steve Huber, and Steve Clough. They have all given helpful suggestions along the way. I thank Dr. Andrew Leakey for his invaluable knowledge of primary metabolism and his ability to critically assess new ideas before I got carried away. This work would not have been possible without generous funding from the Department of Energy, Global Change Education Program's Graduate Research for the Environment Fellowship, the USDA-ARS, the UIUC Program for Physiological and Molecular Plant Biology and the UIUC Department of Plant Biology.

I thank all members of Team Ainsworth, both past and present, for their friendship, guidance, proof-reading abilities, and most of all for not running away when I needed help grinding leaf tissue. I especially thank Justin McGrath and Amy Betzelberger for their friendship, humor, sarcasm and their coffee-break and lunch companionship. I thank Justin for reminding me to be more critical and Amy for reminding me to be more open-minded. I thank June Chae, Bob Koester, Jessica Chiang and Carrie Ramig for being my right-hand people. This work would not have been possible without their attention to detail and stellar pipetting skills. I thank Tim Mies, Jaime Howard, Charlie Mitsdarfer, and Jesse McGrath for maintaining the SoyFACE facility and

growth chambers. I thank Craig Yendrek for his PCR expertise and helping me through the molecular biology. I also thank the myriad of graduate and undergraduate students who also conducted research at SoyFACE and traded field work favors with me. Without them, the massive sampling campaigns and long summers of field work would not have been successful or as fun.

Finally, I thank my family, Joshua and Ashlyn Gillespie, for being patient, encouraging and silly. They have kept me grounded and sane through this entire process, and I could not have finished this work without them. I would like to thank my sister, Carrie Ramig, for being a great friend, a great chemist and for reminding me to appreciate things besides science. I thank my brother, Jimmy Ramig, for being ridiculously smart and for challenging me in our race to become ‘the first doctor in our family’. I thank my parents, Jim and Nancy Ramig, for their constant encouragement and support. They have always prized education as a noble goal and are responsible for my early and unstoppable academic exploration by teaching me to read that first book, ‘Go, Dog. Go!’

**TABLE OF CONTENTS**

## LIST OF ABBREVIATIONS

| | |
|---|---|
| 1 h Max [$O_3$] | 1 hr maximum [$O_3$] on the day of sampling |
| 14 d 1 h Max [$O_3$] | Maximum 1 hr [$O_3$] averaged over 14 days prior to sampling |
| 14 d AOT40 | 14 d accumulated ozone over a threshold concentration of 40 ppb |
| 14d 8h Ave [$O_3$] | 8 hr (10:00-18:00) average [$O_3$] for the 14 days prior to sampling |
| $1O_2$ | Singlet oxygen |
| 8 h Ave [$O_3$] | 8 hr average [$O_3$] on the day of sampling |
| *A* | Photosynthetic carbon assimilation |
| ALA | 5-aminolevulinic Acid |
| ASA | Reduced ascorbic acid |
| CAT | Catalase |
| MDHAR | Monodehydroascorbate reductase |
| DHAR | Dehydroascorbate reductase |
| GR | Glutathione reductase |
| APX | Ascorbate peroxidase |
| AAO | Ascorbate oxidase |
| $CO_2$ | Carbon dioxide |
| DHA | Dehydroascorbic acid |
| FACE | Free Air gas Concentration Enrichment |
| GPX | Glutathione peroxidase |
| $g_s$ | Stomatal conductance to water |
| GSA | Glutamate-1-semialdehyde |
| $H_2O_2$ | Hydrogen peroxide |
| HO | Hydroxyl radical |
| MDA | Monodehydroascorbic acid |
| $O_2$ – | Superoxide anion |
| $O_2$ | Molecular oxygen |
| $O_2H$ | Perhydroxyl radical |
| $O_3$ | Ozone |
| $PAR_{max}$ | Maximum daily photosynthetically active radiation |
| PCMI | Palmer Crop Moisture Index |
| PEPCase | Phosphoenol-pyruvate carboxylase |
| $RH_{max}$ | Maximum relative humidity |
| ROS | Reactive oxygen species |
| SOD | Superoxide dismutase |
| $T_{max}$ | Maximum daytime temperature |
| $T_{min}$ | Minimum nighttime temperature |

# CHAPTER 1: GENERAL INTRODUCTION

*Oxidative Stress and Antioxidant Metabolism in Plants*

Plants have evolved a vast array of signaling networks and survival strategies to deal with a variety of potentially stressful conditions. One such situation is the inevitable consequence of metabolism in an atmosphere with 21% oxygen, generation of toxic reactive oxygen species (ROS; (Asada and Takehashi, 1987; Finkel and Holbrook, 2000). ROS are forms of oxygen that are more reactive than molecular oxygen ($O_2$), and they include the superoxide anion ($O_2^-$), hydroxyl ($HO^{\cdot}$) and perhydroxyl ($HO_2^{\cdot}$) radicals, hydrogen peroxide ($H_2O_2$), singlet oxygen ($^1O_2$) and ozone ($O_3$). ROS can be generated *in planta* as a result of normal metabolism such as chloroplastic and mitochondrial electron transport, and can also be generated in a controlled manner by plant cells through NADPH oxidases and cell-wall peroxidases (Bolwell *et al.*, 2002; Mittler, 2002; Neill *et al.*, 2002). The concentration of ROS in unstressed plant cells is low, approximately 1-200 µM (Foyer and Noctor, 2005; Polle, 2001) and ROS act as key signaling molecules for cellular responses to developmental and environmental stimuli (Carol and Dolan, 2006; Pei *et al.*, 2000). However, practically all adverse environmental conditions, including drought, salt stress, chilling, heat stress, exposure to heavy metals and UV radiation, $O_3$ and $SO_2$ pollution, mechanical stress, low nutrient availability, high-light levels and pathogen attack, can disrupt the reduction/oxidation (redox) homeostasis of cells by enhancing the endogenous production of ROS (De Gara *et al.*, 2003; Mittler, 2002; Noctor and Foyer, 1998; Polle, 2001). High concentrations of ROS can result in unrestricted oxidation of DNA, proteins and membrane lipids, which in turn leads to oxidative destruction of the cell (Asada and Takehashi, 1987; Bolwell *et al.*, 2002; Dat *et al.*, 2000; Desikan *et al.*, 2001).

Plants have evolved a range of enzymatic and non-enzymatic antioxidant mechanisms, which collectively constitute the total antioxidant capacity of cells (Ghiselli *et al.*, 1995; Larson, 1988). Major ROS scavenging enzymes include catalase (CAT), superoxide dismutase (SOD), and ascorbate peroxidase (APX; Figure 1.1). CAT is generally localized in the peroxisome and therefore might not be as sensitive to changes in cytoplasmic redox status as other antioxidant enzymes (Mittler, 2002). SOD and APX localize to many cellular compartments including the apoplast, and may play a larger role in scavenging ROS during oxidative stress (Mittler, 2002).

Another key component of the antioxidant system is the metabolite pool. Studies have shown that mutants deficient in ascorbic acid (ASA) biosynthesis or with altered levels of glutathione are hypersensitive to stress (Foyer and Noctor, 2005) implying that the enzymes involved in the ascorbate-glutathione cycle, such as APx, dehydroascorbate reductase (DHAR), monodehydroascorbate reductase (MDHAR), and glutathione reductase (GR), are also crucial to maintaining a balanced redox status (Noctor and Foyer, 1998). This flexible system of redox control in plants allows distinction between small fluctuations, such as changes in the light environment, from sustained oxidative stress conditions, such as pathogen attack or elevated $O_3$ concentration ($[O_3]$). When the plant is able to sense small changes in redox balance and induce acclimation responses, irreversible damage is avoided. Acclimation responses can be short-term controls including redox poising mechanisms, or long-term control, such as changes in gene expression (Barth *et al.*, 2006; Scheibe *et al.*, 2005). Redox poising mechanisms include cyclic-electron flow, the water-water cycle and the malate valve in the chloroplast (Scheibe *et al.*, 2005). However, when cellular redox imbalance exceeds a certain threshold, a specific 'life-saving' hypersensitive response may be initiated in attempt to contain the stress to the site of contamination (Scheibe *et al.*, 2005). Once this threshold is crossed, irreversible damage occurs.

*Antioxidant Metabolism Response to Elevated Tropospheric Ozone*

Ozone diffuses into the leaf apoplast via the stomata where it is rapidly converted into other ROS that signal a diverse metabolic response (Fig. 1.1; (Kangasjarvi *et al.*, 2005; Long and Naidu, 2002). Ozone stress has been characterized as either acute or chronic, depending on the concentration and the exposure duration (Fiscus *et al.*, 2005; Sandermann, 1996). While the actual concentration and duration threshold for $O_3$ damage varies among species and sometimes even among genotypes of the same species (Burkey *et al.*, 2000), it is commonly accepted that acute damage results from a very high concentration of $O_3$ (>150 ppb) over a short period of time, and chronic $O_3$ damage results from a lower concentration of exposure over a long period of time. Acute $O_3$ damage mimics the biochemical defence response of plants to pathogen attack (Kangasjarvi *et al.*, 2005; Overmyer *et al.*, 2003), but the cellular mechanism that leads to damage resulting from chronic $O_3$ exposure has yet to be clearly defined.

Exposure to acute [$O_3$] elicits a biphasic burst of endogenous ROS and increased concentrations of the signalling hormones salicylic acid, ethylene, and jasmonic acid (Puckette *et al.*, 2007), and leads to localized cell death within the leaf tissue (Baier *et al.*, 2005). Because $O_3$ enters the leaf through the stomata, the quenching capacity of apoplastic antioxidants is an important determinant of $O_3$ damage (Kangasjarvi *et al.*, 2005). In particular, apoplastic ASA appears to play an important role in removing ROS generated by $O_3$ (Conklin and Barth, 2004; Luwe *et al.*, 1993; Sanmartin *et al.*, 2003). However, a number of other initial targets of $O_3$ sensing in the cell have been suggested, including oxidative activation of calcium channels, lipid oxidation, $H_2O_2$ flux from the apoplast to symplast, and glutathione redox status (Baier *et al.*, 2005).

The physiological response of plants to chronic ozone exposure has also been studied in depth; however the biochemical mechanisms that lead to tissue and whole plant damage has not yet been clarified (Fiscus *et al.*, 2005). The physiological effects of elevated atmospheric [$O_3$] on plant systems include decreased photosynthetic productivity, decreased Rubisco and chlorophyll content, reduced stomatal conductance, leaf chlorosis, accelerated senescence and a general decrease in green leaf area and crop yield (Ashmore, 2005; Held *et al.*, 1991; Morgan *et al.*, 2004). Although the molecular and biochemical basis for tolerance to chronic $O_3$ is unknown, it is thought that the endogenous antioxidative metabolism plays a key role in quenching the low levels of ROS generated from chronic $O_3$ exposure (Burkey *et al.*, 2003). Therefore, the expectation is that any elevation in [$O_3$] will cause an up regulation of antioxidant metabolism. However, the direct evidence for this up regulation is highly variable and dependent on the duration and method of $O_3$ fumigation, and the species under investigation (Burkey *et al.*, 2000; Iglesias *et al.*, 2006; Robinson and Britz, 2000).

Modern day annual average background [$O_3$] over the midlatitudes of the Northern Hemisphere range between 20-45 ppb, which is roughly double the pre-Industrial Revolution concentration (Vingarzan, 2004). Global background [$O_3$] is predicted to continue increasing by 0.5-2% per year over the next century mainly due to increases in precursor emissions from anthropogenic sources (Solomon *et al.*, 2007). Ozone is a spatially and temporally heterogeneous pollutant and local concentrations depend heavily on upwind precursor emissions and local $O_3$-generating environmental conditions. This leads to a dynamically changing [$O_3$] above average background concentrations, which already have detrimental effects on plants (The Royal Society, 2008).

*Antioxidant Metabolism Response to Elevated Carbon Dioxide*

The unprecedented rise in atmospheric carbon dioxide concentration ($[CO_2]$) since the Industrial Revolution is one of the most well-documented global atmospheric changes. $CO_2$ concentration has risen from 280 parts per million (ppm) in 1750 to the present-day concentration of 387 ppm and is projected increase to over 700 ppm by the end of this century (Solomon *et al.*, 2007). It follows that the effects of such an environmental change on individual organisms, communities, and whole ecosystems have been well documented (Long *et al.*, 2006). Specifically, several of the well-characterized effects of elevated $[CO_2]$ on plant physiology include stimulated photosynthesis and growth in $C_3$ species, decreased Rubisco concentration, and decreased stomatal conductance (Ainsworth and Long, 2005; Ainsworth and Rogers, 2007; Bowes, 1991; Drake *et al.*, 1997). These physiological effects have led to the general hypothesis that the antioxidant metabolism will be down regulated in plants grown at elevated $[CO_2]$. This hypothesis has led to many predictions, including: 1) ROS production will be suppressed by lower rates of the Rubsico oxygenase reaction and subsequent photorespiration at elevated $[CO_2]$ (Polle *et al.*, 1993); 2) lower rates of the Mehler reaction at elevated $[CO_2]$ will decrease the electron leakage from photosystem I to oxygen and decrease chloroplastic oxidative stress (Polle, 1996); and 3) decreased incidence of drought as a result of lower stomatal conductance will reduce ABA-mediated up regulation of antioxidant metabolism (Jiang and Zhang, 2002). However, direct evidence to support any of these predictions is not consistent in the literature and most studies show mixed increases and decreases of individual biochemical components of the antioxidant metabolism in plants exposed to elevated $[CO_2]$ (di Toppi *et al.*, 2002; Polle *et al.*, 1997; Pritchard *et al.*, 2000; Rao *et al.*, 1995).

In tobacco, elevated $[CO_2]$ decreased CAT activity but had no effect on SOD activity (Havir and McHale, 1987). In aspen grown under elevated $[CO_2]$ at a Free Air gas Concentration

Enrichment (FACE) experiment, all measured antioxidant enzyme activities were decreased in plants grown at elevated [$CO_2$] compared to plants grown at ambient [$CO_2$] (Wustman *et al.*, 2001). A study conducted with plants grown in naturally occurring elevated [$CO_2$] springs demonstrated a mix of up and down regulation of antioxidant enzyme activities, with SOD and GR up regulated; and CAT, APX, DHAR, and MDHAR down regulated (Badiani *et al.*, 1998). Previous work with soybean suggests that antioxidant enzymes are generally down regulated at elevated [$CO_2$] (Pritchard *et al.*, 2000). In contrast, an alternative hypothesis has emerged that suggests endogenous ROS production will increase in plants grown at elevated [$CO_2$] leading to greater oxidative stress. Plants grown at elevated [$CO_2$] have higher rates of respiration (Leakey *et al.*, 2009b), increased number of mitochondria (Griffin *et al.*, 2001) and higher levels of protein carbonylation (Qiu *et al.*, 2008). Therefore, the question, how will the plant antioxidant system be affected by growth at elevated [$CO_2$], has yet to be clearly answered.

Only a handful of studies have investigated the interaction of elevated [$CO_2$] and [$O_3$] on antioxidant metabolism, but the results from these studies are conflicting. Generally two hypotheses emerge from the literature about how the interaction of elevated [$CO_2$] and [$O_3$] will affect antioxidant metabolism. The first hypothesis suggests that elevated [$CO_2$] will reduce the negative effects of elevated [$O_3$] based on decreased stomatal conductance limiting the amount of $O_3$ that enters a leaf (Booker and Fiscus, 2005). The second opposing hypothesis suggests that elevated [$CO_2$] will amplify the negative effects of elevated [$O_3$] because plants grown under elevated [$CO_2$] have a reduced need for cellular detoxification by the antioxidant system, and thus have less capacity to deal with increased levels of ROS resulting from concurrent elevated [$O_3$] (Wustman *et al.*, 2001).

*Research Objectives*

The aim of this thesis was to determine the molecular and biochemical response of the antioxidant system to elevated [$CO_2$] and [$O_3$]. Using controlled environments and an open air climate change facility, I tested the hypotheses outlined above. In order to understand the long-term effects of elevated [$CO_2$] and [$O_3$] on antioxidant metabolism, I first needed to develop accurate, high throughput methods for assessing key components of the antioxidant system. Chapter 2 describes rapid, microplate-based assays for measuring total antioxidant capacity, total phenolic content and ascorbate pools in soybean leaf tissue. The resulting assays from Chapter 2 have provided a valuable tool to easily and accurately scale up any experiment focused on examining components of the antioxidant system. In Chapter 3, I investigate how growth environment alters plant antioxidant metabolism and response to an acute oxidative stress in a controlled environment study. Soybeans were grown under chronic high [$CO_2$], chronic high [$O_3$] or control [$CO_2$] and [$O_3$] to test the hypotheses that growth at elevated [$CO_2$] or elevated [$O_3$] alters the total antioxidant capacity of plants, and therefore alters the capacity to respond to an acute oxidative stress. I also tested the hypothesis that growth environment would change the timing after acute stress exposure over which plants return to steady-state antioxidant levels.

I tested key findings from Chapter 3, that elevated [$O_3$] increases total antioxidant capacity while elevated [$CO_2$] decreases total antioxidant capacity, in the field in Chapter 4. In addition, I hypothesized that an increase in antioxidant metabolism for plants exposed to elevated [$O_3$] would require a shift in carbon metabolism to supply reducing power and carbon skeletons for repair and detoxification processes (Dizengremel *et al.*, 2009). Previous research has demonstrated that the transcriptional response of field-grown plants to stress is not easily duplicated in controlled environments (Miyazaki *et al.*, 2004; Pelloux *et al.*, 2001) Furthermore, the magnitude of the effect of elevated [$CO_2$] on plant physiological responses has been shown to

be dependent on environmental conditions that vary throughout a growing season, such as temperature and water deficit (Bernacchi *et al.*, 2006; Leakey *et al.*, 2006). Therefore, I used a genomic ecology approach, where field-grown soybeans were used for genomic studies in order to understand impacts of climate change over the entire life histories of the plants and to investigate transcriptional changes to climate change responses (Leakey *et al.*, 2009a). The Soybean Free Air Concentration Enrichment (SoyFACE) facility at the University of Illinois at Urbana-Champaign (UIUC) is the best open-air $CO_2$ and $O_3$ enrichment facility for annual crops in the world (http://soyface.illinois.edu). Using FACE technology, soybean was exposed to elevated [$CO_2$] and [$O_3$] without any physical enclosures; therefore, there was no perturbation of the soil-plant-atmosphere continuum. The effect of elevated [$CO_2$] and elevated [$O_3$] on the physiological, biochemical and genomic components of the antioxidant metabolism and resulting shifts in carbon metabolism in field-grown soybean is reported in Chapter 4.

FIGURE

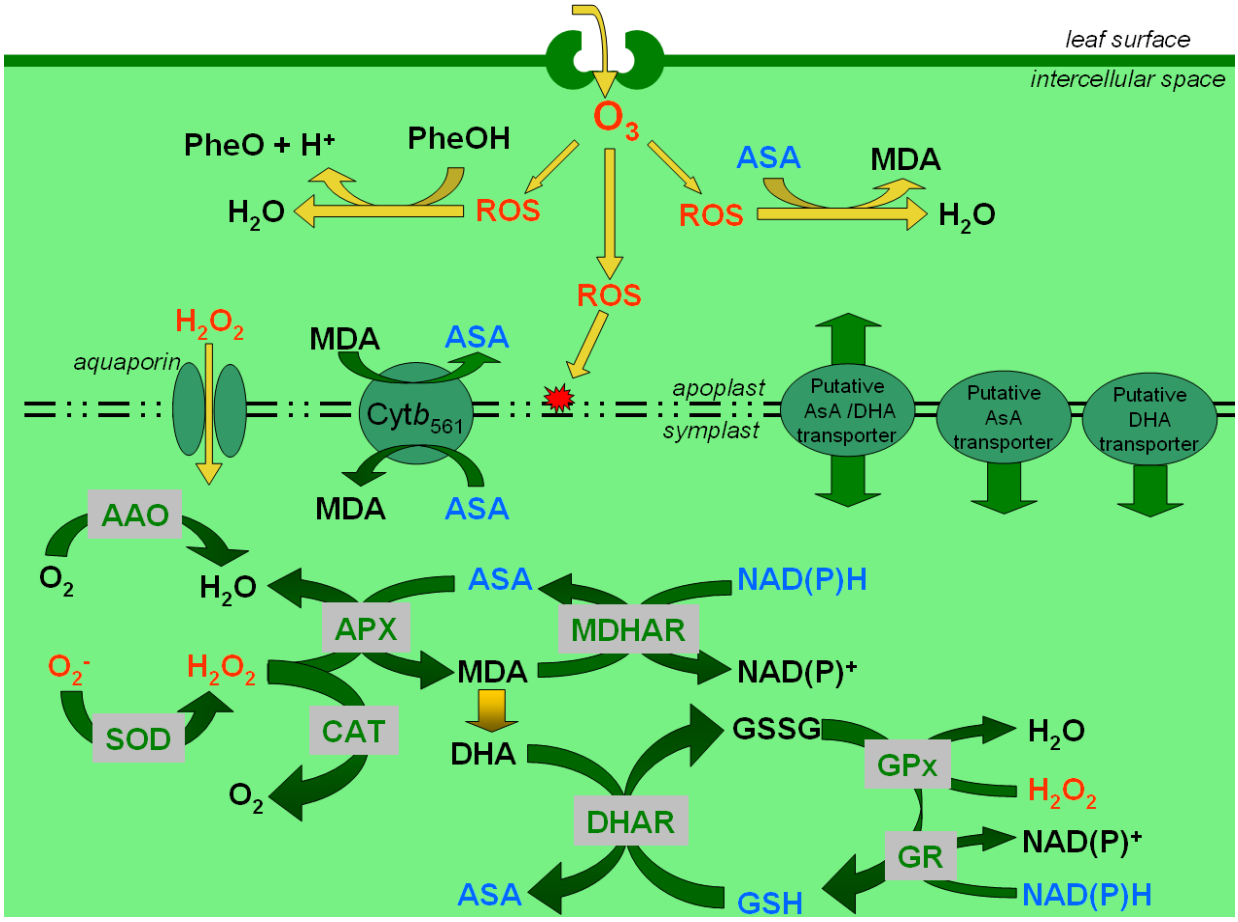


**Figure 1.1 Redox balance across the plasma membrane.** Ozone enters plant cells through open stomata and dissolves in the apoplastic fluid where it spontaneously converts to other ROS (Laisk *et al.*, 1989). Ascorbate (ASA) or phenolic compounds (Phe-OH) in the apoplast can react with ROS directly (Luwe *et al.*, 1993; Ranieri *et al.*, 1996). The resulting monodehydroascorbate (MDA), dehydroascorbate (DHA) can be reduced by cytochrome b561 (Griesen *et al.*, 2004) or possibly transported across the plasma membrane (Horemans *et al.*, 2000) to be reduced enzymatically. ROS can also react with the plasma membrane directly, causing oxidative damage, or hydrogen peroxide ($H_2O_2$) can possibly be transported through aquaporins(Bienert *et al.*, 2007). Within the symplast, ROS will react with metabolic antioxidant pools such as ASA and glutathione (GSH) or they can be enzymatically reduced. Ascorbate Oxidase (AAO) will oxidize ASA using electrons from $O_2$. Superoxide dismutase (SOD) converts superoxide to hydrogen peroxide, which can be reduced via catalase (CAT) or ascorbate peroxidase (APX). MDA can be immediately re-reduced via monodehydroascorbate reductase (MDHAR) utilizing NADPH, or spontaneously convert to DHA, which can then be re-reduced to ASA via dehydroascorbate reductase (DHAR) oxidizing one molecule of glutathione (GSH). Oxidized glutathione (GSSG) can be re-reduced via glutathione reductase (GR) utilizing NADPH.

# CHAPTER 2: DEVELOPMENT OF RAPID, HIGH THROUGHPUT TECHNIQUES FOR ANALYSIS OF ANTIOXIDANT METABOLISM[1]

## INTRODUCTION

The plant antioxidant system is dynamic, consisting of a range of metabolite and enzymatic components (Foyer and Noctor, 2009). It also has the potential to change rapidly in response to diverse environmental conditions (Scheibe *et al.*, 2005). The importance of studying this system under environmental conditions predicted for the future has been discussed in Chapter 1. Studying such a system under field conditions requires precise, quantitative measurements on a high-throughput scale that can capture as much of the variability in the system as possible. In order to meet this challenge, rapid, 96-well microplate-based assays of total antioxidant capacity, ascorbic acid pool size and phenolic pool size were developed.

### *Total Antioxidant Capacity*

The oxygen radical absorbance capacity (ORAC) assay has been widely used to measure the antioxidant activity of nutraceuticals, pharmaceuticals and foods (Huang *et al.*, 2002). The ORAC assay measures free radical oxidation of a fluorescent probe through the change in its fluorescence intensity (Cao and Prior, 1999). The assay is run to completion and the dynamic change in fluorescence of the probe over time is accounted for by calculating the area under the fluorescence decay curve (AUC). By comparing the integral of the fluorescence loss caused by each sample and standard with that of a blank solution, the ORAC assay considers both

[1] Adapted from **Ainsworth EA, Gillespie KM**. 2007. Estimation of total phenolic content and other oxidation substrates in plant tissues using Folin-Ciocalteu reagent. *Nature Protocols* **2**, 875-877.
, **Gillespie KM, Ainsworth EA**. 2007. Measurement of reduced, oxidized and total ascorbate content in plants. *Nature Protocols* **2**, 871-874.
, **Gillespie KM, Chae JM, Ainsworth EA**. 2007. Rapid measurement of total antioxidant capacity in plants. *Nature Protocols* **2**, 867-870.

inhibition degree and inhibition time, which is an improvement over previous assays of total antioxidant capacity that assume zero-order kinetics in their quantification (Ghiselli *et al.*, 1995; Glazer, 1990; Miller *et al.*, 1993; Wayner *et al.*, 1985). The ORAC assay measures the classical ability of an antioxidant to quench free radicals by hydrogen donation, and is thus a measure of both general and specific antioxidant action (Prior *et al.*, 2005). Although the ORAC assay has been widely used in the nutritional field (Prior *et al.*, 2005), it has not yet been widely used to assess the total antioxidant capacity of plants exposed to environmental stresses.

*Ascorbic Acid*

Ascorbate (L-ascorbic acid) is a critical metabolite in plants that is involved in cell expansion (Horemans *et al.*, 2000; Tabata *et al.*, 2001) cell division (Horemans *et al.*, 2000; Noctor and Foyer, 1998) growth (Horemans *et al.*, 2000), defense (Horemans *et al.*, 2000; Noctor, 2006) and, best known, antioxidant metabolism (Horemans *et al.*, 2000; Noctor, 2006; Smirnoff, 2005). Ascorbate also plays a role as a co-factor for many enzymes, including many dioxygenases, ascorbate peroxidase and violaxanthin de-epoxidase (Noctor, 2006). In leaves, ascorbate has been measured in greater concentration than chlorophyll (Noctor and Foyer, 1998). At physiological pH, the ascorbate anion (ASA) is the predominant form (Smirnoff, 2005). The anion loses an electron from its ene-diol group to form the monodehydroascorbate (MDA) radical. Further oxidation of MDA forms the uncharged molecule dehydroascorbate (DHA). This basic oxidation reaction explains the important biological role of ascorbate as an antioxidant metabolite. DHA can be reduced back to ASA by DHA reductase (DHAR), with GSH as the reducing substrate (Foyer and Halliwell, 1976). Despite our highly oxidizing environment with 21% oxygen, approximately 90% of the ascorbate pool in healthy leaves is present in the reduced

form (Noctor, 2006). However, when faced with further environmental stress, this pool can become more oxidized (Conklin and Barth, 2004; Dat *et al.*, 1998). Recently, evidence has accumulated that the redox status of the ascorbate pool is an environmental sensor and mediator between changes in environmental conditions and plant development and aging (Barth *et al.*, 2006; Chen and Gallie, 2006; Pastori *et al.*, 2003).

Different methods for detecting reduced and oxidized forms of ascorbate in plant cells include HPLC (Conklin *et al.*, 2000; Horemans *et al.*, 1997), enzyme-cycling assays utilizing ascorbate oxidase (Foyer *et al.*, 1983) and assays that rely on the reduction or oxidation of a compound leading to a color change (Conklin *et al.*, 2000; Hewitt and Dickes, 1961). Although the HPLC and enzyme-cycling assay methods are more specific, both are time-intensive and expensive, so the number of samples that can be processed is limited. Therefore, I have optimized a protocol for easy, rapid analysis of both oxidized and reduced forms of ascorbate based on the method of Okamura (Okamura, 1980). In this assay, ferric ion is reduced by ASA to the ferrous ion, which when coupled with α-α-bipyridl, forms a complex with characteristic absorbance at 525 nm (Okamura, 1980). In the presence of DTT, DHA is chemically reduced to ASA. Excess DTT is then removed with the N-ethylmaleimide (NEM). Total ascorbate is subsequently assayed using the α-α-bipyridl method, and DHA is calculated by subtracting the reduced ASA from the total pool of ascorbate (Kampfenkel *et al.*, 1995; Okamura, 1980; Stevens *et al.*, 2006). A major consideration for interpretation of the α-α-bipyridl assay is that the reduction of ferric ion to ferrous ion is non-specific and other oxidation substrates present in leaf tissue can interfere in an inhibitory, additive or enhancing manner. However, by extracting the ascorbic acid in trichloroacetic acid (TCA), potential antioxidant proteins are precipitated. Also, the assay is conducted in the presence of orthophosphoric acid at pH 1–2, and other reducing metabolites,

such as α-tocopherol, glutathione, reductone, glucosone, reductic acid, Cys, acetol, methyl glyoxal and creatinine, are not effective reductants (Maickel, 1960; Omaye *et al.*, 1979).

*Phenolic Metabolites*

Plants also produce an extraordinary diversity of phenolic metabolites that contain one or more acidic hydroxyl residues attached to an aromatic arene (phenyl) ring (Croteau *et al.*, 2000). Hydroxycinnamic acids, flavonoids, anthocyanins and tannins represent the major classes of phenolics, which collectively account for approximately 40% of the organic carbon in the biosphere (Croteau *et al.*, 2000). Although structural phenolic compounds such as lignin, suberin and other structural polymers comprise much of this carbon pool, the amazing array of non-structural phenolics have many functions in plants, including acting as antioxidants (Grace, 2005; Grace and Logan, 2000). Phenolic compounds are excellent oxygen radical scavengers because the electron reduction potential of the phenolic radical is lower than the electron reduction potential of oxygen radicals (Grace, 2005; Grace and Logan, 2000) and also because phenoxyl radicals are generally less reactive than oxygen radicals (Bors *et al.*, 1990). Therefore, phenolic compounds can scavenge reactive oxygen intermediates without promoting further oxidative reactions (Grace, 2005). It follows that many environmental stresses that cause oxidative stress often induce the synthesis of phenolic metabolites (Dixon and Paiva, 1995; Grace, 2005; Pasqualini *et al.*, 2003).

Many available methods of quantification of total phenolic content in food products or biological samples are based on the reaction of phenolic compounds with a colorimetric reagent, which allows measurement in the visible portion of the spectrum (Magalhaes *et al.*, 2006; Robards and Antolovich, 1997). The Folin–Ciocalteu (F–C) assay is such a method (Folin and

Ciocalteu, 1927; Singleton and Rossi, 1965) and has been proposed as a standardized method for use in the routine quality control and measurement of antioxidant capacity of food products and dietary supplements (Prior *et al.*, 2003). The F–C assay relies on the transfer of electrons in alkaline medium from phenolic compounds to phosphomolybdic/ phosphotungstic acid complexes to form blue complexes that are determined spectroscopically at approximately 760 nm (Singleton *et al.*, 1999; Singleton and Rossi, 1965). Although the exact chemical nature of the F–C reaction is unknown, it is believed that sequences of reversible one- or two-electron reduction reactions lead to blue species (possibly $(PMoW_{11}O_{40})^{4-}$; (Huang *et al.*, 2005). Major considerations in the interpretation of the F–C assay are that the chemistry is non-specific and that other oxidation substrates in a given extract sample can interfere in an inhibitory, additive or enhancing manner (Huang *et al.*, 2005; Singleton and Rossi, 1965). Inhibition could occur as a result of oxidants competing with the F–C reagent or air oxidation after the sample is made alkaline. For this reason, the F–C reagent is added before the alkali (Singleton *et al.*, 1999; Singleton and Rossi, 1965). Additive effects occur from unanticipated phenols, aromatic amines, high sugar levels or ascorbic acid in the extract (Singleton *et al.*, 1999; Singleton and Rossi, 1965). Singleton and colleagues (Singleton *et al.*, 1999; Singleton and Rossi, 1965) discussed the potential additive effects of various compounds and methods for correcting these factors. Ascorbic acid readily reacts with the F–C reagent and therefore must be considered. It can be measured before adding the alkali or by a more specific assay and then subtracted from the F–C value (Singleton *et al.*, 1999; Singleton and Rossi, 1965). Sulfites and sulfur dioxide also react with the F–C reagent, and this has been a problem in wines, where $SO_2$ is a common additive (Singleton *et al.*, 1999; Singleton and Rossi, 1965). Owing to the general nature of the F–C chemistry, it is indeed a measure of total phenols and other oxidation substrates. However, the F–

C assay is simple and reproducible and has been widely used for studying phenolic antioxidants (Huang *et al.*, 2005; Singleton and Rossi, 1965). Therefore, I have optimized a rapid, small-scale, high-throughput method to measure the total phenolic pool in leaf tissue based on F-C reagent chemistry and using gallic acid as a standard.

## METHODS

### *Oxygen Radical Absorbance Capacity Assay*

Approximately 20 mg (12.5 mm diameter leaf discs) of soybean leaf tissue was harvested and flash-frozen in liquid nitrogen. Samples were stored at -80 °C until assayed. Tissue was homogenized in 50% acetone (vol/vol in water; Sigma) using a mixer-mill disruptor with 1-2 mL adaptor sets (Qiagen tissue lyser). Each 2 mL, screw-cap tube contained 3 tungsten carbide beads and 2 mL of 50% acetone, and was shaken at 30 Hz for 5 min. Samples were then centrifuged at 4,500g for 30 min at 4 °C and the supernatants collected in fresh 2 mL tubes. Each sample was diluted in series so that the final concentrations ranged from 1:20 to 1:100. A 25 μL aliquot of each sample dilution (or blank or Trolox standard) was added to a microplate with 150 μL of 0.08 μM fluorescein (Sigma). The plate was then covered and incubated at 37 °C. Immediately before beginning the kinetic fluorescence reading, 25 μL of 150 mM 2,2'-azobis-2-methyl-propanimidamide, dihydrochloride (AAPH; Cayman Chemical) was added to every well. The oxidative decay of the fluorescein was followed for 1 h at 37 °C with a multi-detection plate reader using an excitation wavelength of 485 nm and an emission wavelength of 530 nm (Synergy HT: Bio-Tek). In order to calculate the total antioxidant capacity of each sample, the AUC was determined for each sample standard or blank. Wells that did not decay to zero were not used. The average AUC of the blanks was subtracted from the AUC of each standard and

sample to obtain the net AUC. The total antioxidant capacity of each sample is reported in trolox equivalents and calculated using the regression equation between the trolox standards and their net AUCs (Fig. 2.1).

*Ascorbic Acid Assay*

Approximately 40 mg (22mm diameter disc) of soybean leaf tissue was harvested and immediately frozen in liquid nitrogen. Tissue samples were stored at -80 °C for 1-4 days. The ratio of reduced to oxidized ASA begins to change even at -80 °C so we tested the longevity of the frozen samples before analysis. The tissue was homogenized using a chilled mortar and pestle and 2 mL of 6% (vol./vol. in water) TCA (Sigma) was added. The slurry was transferred to a 2 mL screw-top tube and centrifuged at 13,000g for 5 min at 4 °C. All extracts and reagents were kept on ice throughout the preparation and assay. The assay was preformed immediately after extraction because the ASA pool begins to degrade and the ratio of oxidized-to-reduced ASA changes. Duplicate 200 μL aliquots of the supernatant from each sample (or standards, or blanks) were transferred to new 2 mL tubes and 100 μL of 75 mM 50 mM $KH_2PO_4$, 50 mM $K_2HPO4$ (Sigma; pH 7.0) was added. To reduce the oxidized portion of ASA and measure the total pool size, 100 μL of 10 mM DTT (Sigma) was incubated with one of the aliquots for 10 min at room temperature. After the incubation, 100 μL of 0.5% (wt/vol. in water) NEM (Sigma) was added to remove the excess DTT. To the other aliquot of sample, 200 μL of water was added to account for the volume of DTT and NEM added to the other assay tube. To both tubes, the following was added: 500 μl 10% (wt/vol in water) TCA, 400 μl 43% (vol/vol in water) $H_3PO_4$, 400 μl 4% (wt/vol in 70% ethanol) α-α-bipyridl and 200 μl 3% (wt/vol in water) $FeCl_3$. After the addition of $FeCl_3$, each tube was vortexed thoroughly to avoid formation of precipitate and

incubated at 37 °C for 1 h. A 200 μL aliquot of each tube was transferred to an optically clear 96-well microplate and the absorbance at 525 nm ($A_{525}$) was read with a microplate spectrophotometer (HT-Synergy; BioTek). Reduced and total ascorbic acid were calculated using the regression between the ASA standards and their blank-corrected $A_{525}$. Oxidized ASA was calculated as the difference between the total pool and the reduced pool (Fig. 2.2).

*Total Phenolic Metabolites Assay*

Approximately 20 mg (12 mm diameter disc) of soybean leaf tissue was harvested and flash-frozen in liquid nitrogen. Samples were stored at -80 °C until assayed. Tissue was homogenized in 95% methanol (Sigma) using a mixer-mill disruptor with 1-2 mL adaptor sets (Qiagen tissue lyser). Each 2 mL, screw-cap tube contained 3 tungsten carbide beads and 2 mL of 95% (vol./vol. in water) methanol and was shaken at 30 Hz for 5 min. After removing the beads with a magnet, the samples were incubated at room temperature in the dark for 48 h. Samples were then centrifuged at 13,000g for 5 min at room temperature. A 100 μL aliquot of each supernatant (or blank, or gallic acid standard) was added to 200 μL of 10% (vol./vol. in water) F-C reagent and vortexed thoroughly. An 800 μL aliquot of 700 mM $Na_2CO_3$ was added to each assay tube and incubated at room temperature for 2 h. The assay can be incubated at warmer temperatures for a shorter period of time to obtain faster color development, but this can increase the technical variability. For soybean leaf extracts, a 2 h incubation at room temperature resulted in low variability between technical replications. After the incubation period, 200 μL of each sample, standard or blank from the assay tube was transferred to an optically clear 96-well microplate and the absorbance at 765 nm ($A_{765}$) was determined using a microplate spectrophotometer (Synergy HT, Bio-Tek). Total phenolic content was determined in gallic acid equivalents by

using the regression equation between the gallic acid standards and their blank-corrected $A_{765}$ (Fig. 2.3).

## RESULTS AND DISCUSSION

There is considerable natural variability in antioxidant capacity, ascorbate and phenolic content in leaf tissues. Much of this variability is biological; however, experimental procedures (pipetting errors, inefficient extractions) can also introduce significant error. High variability between replicates of samples can be a considerable issue with these assays; therefore the use of automated pipetting systems or multi-channel pipettes with all procedures greatly increased accuracy. To increase the sample through-put, a mixer-mill with the 2 mL tube adapter (Qiagen tissue lyser) can be used to homogenize 48 samples simultaneously. Further, a mixer-mill with a 96-deep well plate adapter (Spex Geno Grinder 2000) can be used to homogenize 192 samples simultaneously. Simply add the extraction buffer, 2-3 tungsten carbide beads and the leaf tissue to each tube or well and shake at 30 Hz for 5 min. Accurate temperature control is critical for the ORAC assay because the reaction is initiated by the thermal decomposition of AAPH. Preheating the microplate and monitoring the homogeneity of temperature in the plate reader improved the assay performance. When assaying ascorbate, the rapidity and ease of the assay method were important because the molecule is easily degraded, particularly in the absence of an acid buffer or after freezing and thawing cycles. For the phenolics assay, it was important to remember that although the F–C assay has commonly been used to assay ‘total phenolic content’, the assay measures other readily oxidized substances as well. When I performed the F–C assay with a known amout of ASA or trolox, I found that 94–96% of the compounds were detectable, so there is potential for significant interference using these molecules. However, when I incubated the

ASA or trolox for 48 h in a way similar to that in which I extracted total phenolics from the leaf samples, the recovery was reduced to approximately 15%. Furthermore, soybean leaves have a very high content of phenolics (15–20 mg $g^{-1}$ DW), and therefore the results of the F–C assay from soybean leaves is largely a measure of phenolic content.

The ORAC, ASA and phenolic assays provide accurate, rapid and high-throughput measures of both the general and specific antioxidant action of plant tissue extracts. In soybean leaves, I found a significant positive correlation between ORAC and total phenolic content and total ascorbate content (Fig. 2.4), which are known major contributors to the total antioxidant capacity in plant leaves.

FIGURES

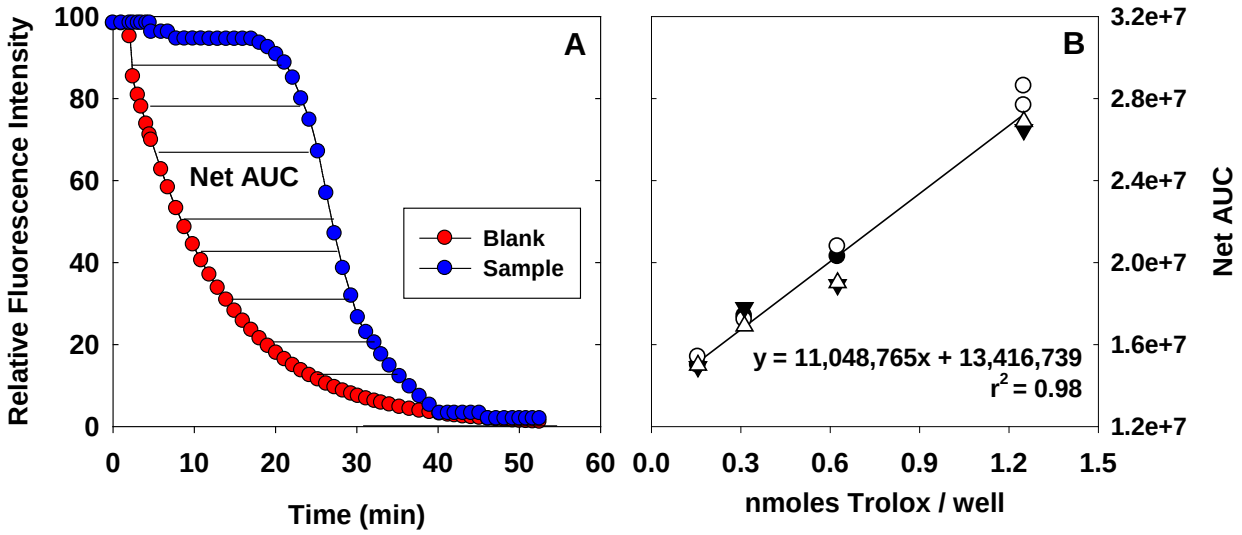


**Figure 2.1. Typical fluorescence curves and trolox standard curves for the ORAC assay.** **A.** Typical plot of fluorescence activity of a sample (blue) and a blank (red) (adapted from (Prior *et al.*, 2003). Each sample delays the oxidation of the fluorescent compound over time. The ORAC activity of a sample is calculated by subtracting the area under the blank curve from the area under the sample curve to obtain the net area under the curve (Net AUC). **B.** Using Trolox of known concentration, a standard curve is generated and the ORAC of the samples is calculated as Trolox equivalents. Each concentration is replicated four times.

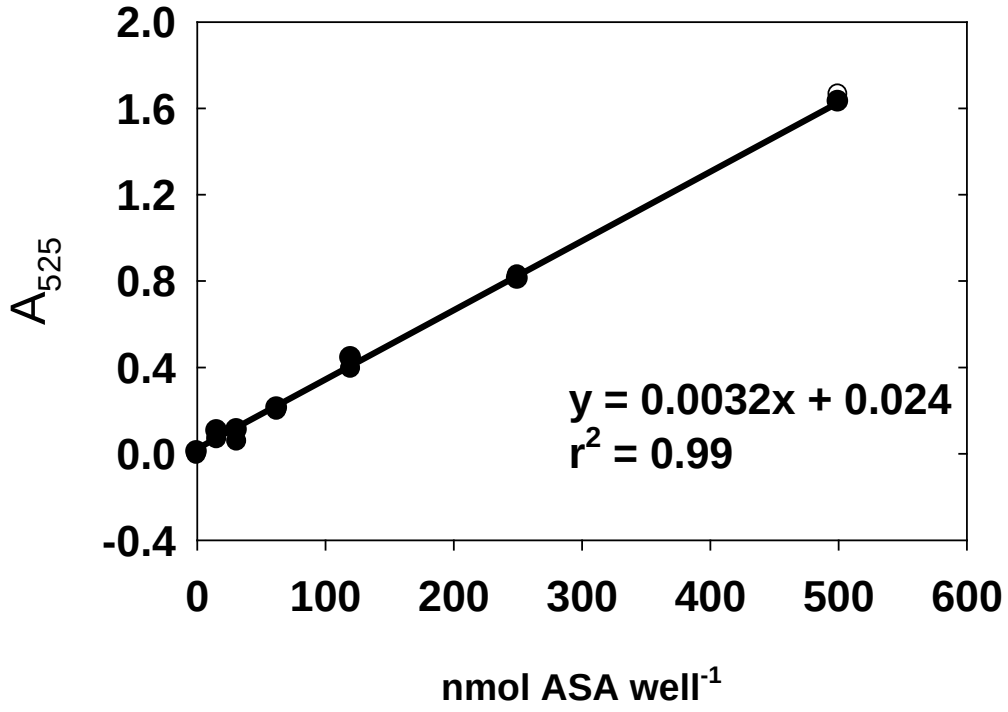


**Figure 2.2. An example of an ascorbate standard curve.** Reduced and total ascorbate are calculated directly utilizing the standard curve, and oxidized ascorbate is determined by subtracting the reduced portion from the total pool size. Each concentration is replicated twice.

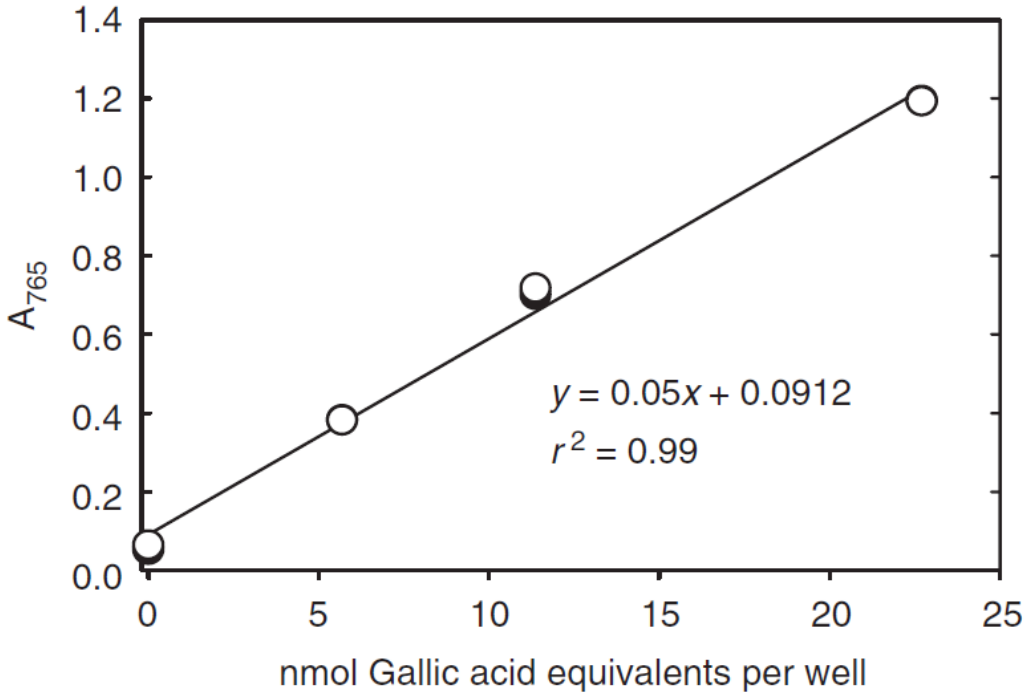


**Figure 2.3. An example of a phenolics standard curve.** Phenolic content was calculated using this standard curve and reported as gallic acid equivalents. Each concentration is replicated twice.

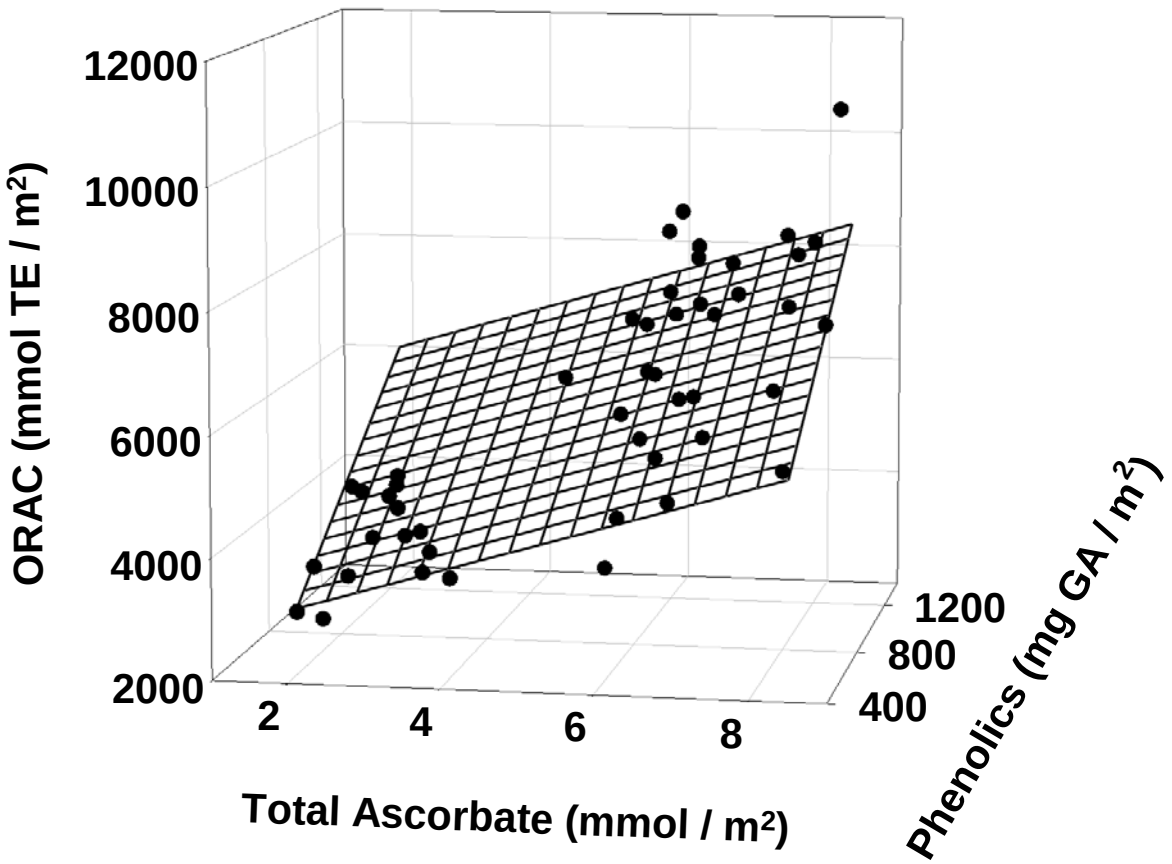


**Figure 2.4. Relationship between total antioxidant capacity (oxygen radical absorbance capacity, ORAC) and phenolic content and total ascorbate content in field-grown soybean leaves**. Multiple regression analysis revealed a highly significant relationship between ORAC and total ascorbate and total phenolic content (ORAC = 3.7 phenolics + 366.6 ascorbate + 406.8; $r^2 = 0.58$ $P < 0.001$).

# CHAPTER 3: GROWTH AT ELEVATED OZONE OR ELEVATED CARBON DIOXIDE CONCENTRATION ALTERS ANTIOXIDANT CAPACITY AND RESPONSE TO ACUTE OXIDATIVE STRESS[2]

## INTRODUCTION

Current background tropospheric [$O_3$] is already causing damage to a variety of plant species (Van Dingenen *et al.*, 2009) and background concentrations are predicted to increase throughout the rest of this century (Solomon *et al.*, 2007). The spatial and temporal heterogeneity of [$O_3$] above background levels as well as the mechanism by which $O_3$ enters and causes damage within leaf tissue was discussed in Chapter 1. Changes in environmental factors can easily disturb the steady-state redox balance by causing a rapid increase in ROS generation. The idea that cellular redox state can act as an environmental sensor and signal among various aspects of plant metabolism was also discussed in Chapter 1 (Fedoroff, 2006; Noctor, 2006). When a plant senses small changes in redox balance, an acclimation response is induced, and irreversible damage is avoided. Recently, there has been evidence suggesting that plants can 'remember' a stress event by existing in a primed metabolic state to more efficiently activate cellular defenses during a future stress (Conrath *et al.*, 2006). Most of this evidence comes from plant-pathogen interaction research, but plants responded with a faster and increased calcium signal to osmotic stress when pre-treated with $H_2O_2$ (Knight *et al.*, 1998). Furthermore, plantlets generated from $O_3$-treated tissue culture displayed increased oxidative stress tolerance (Nagendra-Prasad *et al.*, 2008), and $H_2O_2$ seed treatment led to increased salt tolerance in wheat seedlings (Wahid *et al.*, 2007).

[2] Adapted from **Gillespie KM, Rogers A, Ainsworth EA**. 2010. Long-term exposure to elevated ozone or elevated carbon dioxide alters antioxidant capacity and response to acute oxidative stress. *Journal of Experimental Biology* ***in review***.

Therefore, there is evidence that exposure to an abiotic stress can predispose plants for improved tolerance to another abiotic stress event.

This study investigated how growth environment alters plant antioxidant metabolism and response to an acute oxidative stress. Soybeans were grown under chronic high [$CO_2$], chronic high [$O_3$] or control [$CO_2$] and [$O_3$] to test the hypotheses that growth at elevated [$CO_2$] or elevated [$O_3$] alters the total antioxidant capacity of plants, and therefore alters the capacity to respond to an acute oxidative stress. I also hypothesized that growth environment would change the timing over which plants will return to steady-state antioxidant levels. The prevailing view is that elevated [$O_3$] causes an up regulation of the antioxidant metabolism in plants (Olbrich *et al.*, 2009; Puckette *et al.*, 2007; Ranieri *et al.*, 1996; Ranieri *et al.*, 2000; Scebba *et al.*, 2003; Xu *et al.*, 2008). However, the direct evidence for this up regulation is variable and dependent on the duration and method of $O_3$ fumigation, and the components of antioxidant metabolism investigated (Burkey *et al.*, 2000; Iglesias *et al.*, 2006; Robinson and Britz, 2000). Likewise, reports investigating the effects of growth at elevated [$CO_2$] show contrasting responses of individual components of the antioxidant system (di Toppi *et al.*, 2002; Polle *et al.*, 1997; Pritchard *et al.*, 2000; Rao *et al.*, 1995) and there is some evidence of increased oxidative stress in elevated [$CO_2$] (Qiu *et al.*, 2008). Therefore, in order to develop more holistic understanding of the effects of growth environment on the antioxidant system, this study investigated antioxidant metabolism at the metabolite, enzyme and transcript levels.

## METHODS

### *Leaf Material and Growth Chamber Conditions*

Soybean (*Glycine max*, cv. Pioneer 93B15*)* seeds were planted, four to a pot, in soil-less planting mix (Sunshine Professional Peat-Lite Mix LC1, SunGro Horticulture, Canada). Plants were maintained at a photosynthetic photon flux density (PPFD) of 300 µmol $m^{-2}$ $s^{-1}$ in a 10 h 25 °C light/14 h 22 °C dark cycle. Six growth chambers were used and each of three atmospheric treatments, control, high [$CO_2$] and high [$O_3$], was randomly assigned to two chambers. The control treatment averaged 409 ppm [$CO_2$] and 3 ppb [$O_3$], the high $CO_2$ treatment was 653 ppm [$CO_2$] and 3 ppb [$O_3$] and the chronic $O_3$ treatment was 93 ppb [$O_3$] for six hours daily and 409 ppm [$CO_2$] throughout the duration of the experiment. Ozone was produced by a variable output UV-C light bulb ballast (HVAC 560 ozone generator, Crystal Air, Langley, Canada), and a custom multi-port sampling system was used to measure and control chamber $CO_2$ and $O_3$ concentrations. $CO_2$ was continuously monitored with a $CO_2$ gas analyzer (SBA4, PP Systems, Amesbury, MA, USA) and $O_3$ was monitored with an $O_3$ analyzer (Thermo Electron 49i, Thermo Scientific, Waltham, MA, USA).

Fourteen days after planting (DAP), soybeans were thinned to two uniform plants per pot. Pots were well-watered with weekly additions of 5 mM potassium nitrate. At midday, 32 DAP, the second trifoliate leaf of three plants per chamber was sampled for initial measurements of antioxidant parameters. The measurements made in the subsequent days were also performed on the second trifoliate at midday to avoid any potential diurnal or developmental variation in measured parameters. Thirty-three DAP, all plants received an acute 200 ppb $O_3$ treatment for four hours, ending at midday. Leaf tissue was sampled from three plants per chamber, in two duplicate chambers, immediately following the acute $O_3$ treatment and again 24 h and 48 h post treatment. At each time-point and from each treatment, leaf tissue from three plants was excised

for metabolite and enzyme analysis, and three whole leaflets, from different plants, were sampled and pooled for gene expression analysis. The leaf tissue was immediately plunged into liquid nitrogen and maintained at -80 °C until analysis. After a plant was sampled, it was removed from the chamber.

*Antioxidant Metabolite and Enzyme Assays*

Total antioxidant capacity was measured with an ORAC assay (Gillespie *et al.*, 2007). Levels of ASA and DHA were measured using an α-α'-bipyridl based colormetric assay (Gillespie and Ainsworth, 2007). Total phenolic content was measured by a Folin-Ciocalteu assay (Ainsworth and Gillespie, 2007).

The activities of six antioxidant enzymes (Fig. 3.1), APX (EC 1.11.1.11), CAT (EC 1.11.1.6), GR (EC 1.8.1.7), DHAR (EC 1.8.5.1), MDHAR (EC 1.6.5.4), and SOD (EC 1.15.1.1) were measured in a common extract. Leaf discs (381 $mm^2$, approximately 20 mg FW) were macerated in microcentrifuge tubes using tungsten carbide beads in 50 mM $KH_2PO_4$, 50 mM $K_2HPO4$, pH 7.8. Samples were centrifuged at 14,000 g for 5 min at 4 °C. An aliquot of the supernatant was removed for the assessment of SOD, APX and MDHAR. Approximately 5 mg poly(vinylpolypyrrolidone) was added to the remaining supernatant and pellet to bind phenolics and alkaloids; the mixture was shaken and re-centrifuged. An aliquot of this second supernatant was used for the determination of CAT, DHAR, and GR activity. The extracts and temperature sensitive reagents were maintained at 4 °C until individual assays were initiated. All assays were completed within 2 h of extraction using a liquid handling robot (Janus, Perkin Elmer, Waltham, MA, USA) to allow rapid, accurate pipetting and the ability to initiate and stop reactions simultaneously in all 96-wells of the assay plates. In order to express enzyme activity on a

protein basis, the protein content of the extracts was determined using the Pierce Protein Determination Kit (Pierce, Rockford, IL, USA).

An established assay that measures CAT activity by determining $H_2O_2$ consumption (Summermatter *et al.*, 1995) was adapted for automation in 96-well format. In quadruplicate, 5 to 10 µL of enzyme extract was diluted with assay buffer (50 mM $Na_3PO_4$, pH 6.5) to a total volume of 50 µL and loaded on the 96-well assay plate with 50 µL standards (0, 3.5, 7, 35 mM $H_2O_2$). Fifty µL of assay buffer was added to standard wells and the reaction in the sample wells initiated by addition of 50 µL of 35 mM $H_2O_2$. After 1 min incubation at 25°C, reactions were stopped simultaneously in one half of the assay plate by addition of 50 µL 15% (w/v) tricholoroacetic acid (TCA). After an additional 2 min, TCA was added to the other half of the assay plate, stopping all remaining reactions. The amount of $H_2O_2$ remaining after incubation with CAT was determined by transferring 3 µL from the assay plate to a new 96-well determination plate and mixing it with 100 µL of determination mix (1 g $L^{-1}$ ABTS, 0.8 U $mL^{-1}$peroxidase). The determination plate was incubated for 10 min at room temperature and absorbance at 410 nm measured using a 96 well plate spectrophotometer (SynergyHT, Biotek, Winooski, VT, USA). Comparison of the amount of $H_2O_2$ consumed between the two TCA additions allowed the calculation of CAT activity.

An existing assay for GR activity based on measuring the rate of reduction of oxidized glutathione by NADPH oxidation was adapted for high throughput and automation in a 96-well format (Polle *et al.*, 1990; Pritchard *et al.*, 2000). The assay plate was prepared by loading 15-30 µL enzyme extract, and blanks (extract buffer) in quadruplicate. Half of the samples receive 98 µL of control buffer (50 mM tricine, pH 7.8, 0.5 mM EDTA) and the other half received 98 µL assay buffer (50 mM tricine, pH 7.8, 0.5 mM EDTA, 0.25 mM oxidized glutathione, prepared

immediately before use). The assay plate was equilibrated to 25 °C and the reaction started with the addition of 2 µL of 7.5 mM NADPH. The oxidation of NADPH was followed at 340 nm for 10 min. The rate of NADPH oxidation in the absence of oxidized glutathione was subtracted to account for non-enzymatic oxidation of NADPH by the extract. Both enzymatic and non-enzymatic rates were corrected by the rate of NADPH oxidation in the absence of leaf extract.

An existing assay for DHAR activity based on determining the rate of reduction of DHA to ASA was adapted for high throughput and automation in a 96-well format (Asada, 1984; Pritchard *et al.*, 2000). An aliquot of each extract was boiled at 95 °C for 10 min to denature all enzymes. One hundred µL of ASA standards (0, 0.1, 0.5, 1.0 mM in 50 mM $KH_2PO_4$, 50 mM $K_2HPO_4$, 0.5 mM EDTA, pH 7.8), 15 µL blanks (extraction buffer) and 15 µL of enzyme extracts were loaded onto a 96-well assay plate capable of absorbance measurements at UV wavelengths. Eighty-three µL of assay buffer (50 mM $KH_2PO_4$, 50 mM $K_2HPO4$, 0.5 mM EDTA, pH 7.8, 2 mM reduced glutathione) was added to the wells containing extracts and blanks. A second plate was prepared in the same manner using the boiled enzyme extracts. The assay was started by adding 2 µL of 7.5 mM DHA to sample and blank wells. The reduction of DHA to ASA was followed at 265 nm for 10 min. The rate and final absorbance were recorded. DHAR activity was determined by subtracting the rate of non-enzymatic reduction of DHA from enzymatic reduction.

Existing methods for measuring MDHAR activity (Dalton *et al.*, 1986) were adapted for high-throughput and automation in a 96-well format. MDHAR was determined by following the rate of reduction of monodehydroascorbate (MDA) to ASA by NADH oxidation. MDA was produced *in vitro* by the action of ascorbate oxidase on ASA in the presence of $O_2$. Previously MDA reduction in the absence of extract, ASA and ascorbate oxidase was found to be negligible

(Polle et al 1990). This was confirmed, and a common blank (extract buffer) was used to increase throughput. Ten µL aliquots of the enzyme extracts were added to a 96-well plate that included two 10 µL blanks. 88 µL of assay buffer (50 mM $KH_2PO_4$, 50 mM $K_2HPO_4$, pH 7.8, 0.25 mM NADH, 1.5 mM sodium ascorbate) was added to all wells except those containing the NADH standards (98 µl of 0, 0.1, 0.25 and 0.5 mM NADH in 50 mM $KH_2PO_4$, 50 mM $K_2HPO_4$, pH 7.8, 1.5 mM sodium ascorbate). The assay plate was equilibrated to 25 °C and the reaction initiated by adding 2 µL of ascorbate oxidase (0.01 U $\mu L^{-1}$ in 50 mM $KH_2PO_4$, 50 mM $K_2HPO_4$) to each well. MDHAR activity was determined from the rate of NADH oxidation measured at 340 nm over 10 min.

SOD activity was measured using a previously optimized 96-well assay (Ewing and Janero, 1995). Briefly, SOD activity was measured as the percent inhibition of total nitroblue tetrazolium (NBT) oxidation and compared to a standard curve of SOD purified from horseradish. Twenty-five µL of extract or SOD standard were loaded on a 96-well microplate followed by 173 µL of assay buffer 50 mM $KH_2PO_4$, 50 mM $K_2HPO_4$, pH 7.8, 0.4 mM EDTA, 0.2 mM NBT, 0.3 mM NADH). Immediately before beginning the kinetic assay, 2 µL of 0.33 mM phenazine methosulfate was added to every well. The oxidation of NBT was followed at 560 nm and the SOD activity was determined by comparing the inhibition of NBT oxidation in the plant extracts to that of the purified SOD. A unit of SOD activity was defined as the amount of SOD required to inhibit cytochrome c reduction by 50% in a coupled system with xanthine oxidase at pH 7.8 at 25 °C.

Existing methods for measuring APX activity by determining the rate of ASA oxidation by $H_2O_2$ were adapted for 96-well plates (Asada, 1984; Jahnke *et al.*, 1991). Duplicate 10 µL aliquots of extract and two blanks were loaded on a 96-well assay plate capable of absorbance

measurements at UV wavelengths. This was followed by addition of 80 µL assay buffer (50 mM $KH_2PO_4$, 50 mM $K_2HPO4$, pH 7.8, 0. 5 mM ascorbate, 0.2 mM DTPA). Duplicate 100 µL ASA standards were added to each plate (0, 0.1, 0.5, 1.0 mM ascorbate in 50 mM $KH_2PO_4$, 50 mM $K_2HPO4$, pH 7.8). The assay was initiated by adding 10 µl 20 mM $H_2O_2$ to all wells except those containing standards. The rate of ASA oxidation was determined by subtracting oxidation rates in the absence of extract and quantified with a standard curve.

*Gene Expression Analysis*

Total RNA was extracted following the methods of Bilgin *et al.*, 2009). The quantity and quality of RNA samples was determined with a spectrophotometer (Nanodrop 1000, Thermo Fischer Scientific) and a microfluidic visualization tool (Bioanalyzer, Agilent Technologies, Santa Clara, CA, USA). Contaminating DNA was removed with a DNA-free DNase treatment (Applied Biosystems/Ambion, Austin, TX, USA) following manufacturer's instructions. cDNA was prepared from 3 µg of RNA using Superscript II Reverse Transcriptase (Invitrogen, Carlsbad, CA, USA) and oligo(dT) primers according to manufacturer's instructions. qRT-PCR was performed using a quantitiative real-time PCR system (7900 HT, Applied Biosystems) using SYBR Green JumpStart Taq ReadyMix (Sigma) and 100 nM of each gene-specific primer in a 384-well plate. An initial denaturing step at 95 °C for 10 min was followed by 40 cycles of 95 °C for 15 sec and 60 °C for 1 min. Primers for each antioxidant gene are listed in Table 3.1. F-box protein, NCBI CD397253, was used as the control gene in these experiments (Libault *et al.*, 2008). After completion of PCR amplification, a dissociation curve was run to check for DNA contamination and to insure that a single gene product was amplified. The baseline-corrected delta-Rn values were used to calculate the PCR efficiency (E) and the cutoff value ($C_t$) in the

log-linear phase of the PCR reaction using LinReg PCR software (Ruijter *et al.*, 2009). The normalized expression level for each gene (G) was determined using the following equation: $G = (E_{control}^{Ct\text{-}control}) / (E_{gene}^{Ct\text{-}gene})$. Two replicate reactions were run for each sample, and their $E^{Ct}$ values were averaged. Data are expressed relative to control grown plants at time 0 h.

*Statistical Analysis*

For all parameters, a completely randomized, repeated measures, mixed model analysis of variance (PROC MIXED, SAS v9.2, SAS Institute) with the Satterthwaite option was used with atmosphere as a fixed effect. To assess differences among the parameters before the acute spike, an analysis of variance was run on the data at 0 h. For the time series data, time was treated as a repeated measure with an auto-regressive co-variance matrix structure. Chamber was not a significant source of variation and therefore statistical analysis for antioxidant metabolite and enzyme activity were performed on data from individual plants (n=6) and lsmeans were reported +/- one standard error. For gene expression data, only one pooled sample was analyzed per chamber (n=2). All statistics were performed on the control-gene normalized expression data. Effects were considered significant at $p < 0.05$.

## RESULTS AND DISCUSSION

Growth at elevated [$CO_2$] or elevated [$O_3$] significantly affected total antioxidant capacity. Long-term exposure to either gas also modified the response of the antioxidant system to a subsequent acute oxidative stress. In the following sections, these responses and the recovery of the antioxidant system following the acute stress are described.

*Chronic Growth Environment Alters Total Antioxidant Metabolism*

Growth at elevated [$O_3$] significantly increased total antioxidant capacity, measured by ORAC, by 24% compared to that of ambient grown soybean (Fig. 3.2A; Table 3.2). In contrast, growth at elevated [$CO_2$] significantly decreased the total antioxidant capacity by 20% compared to that of ambient grown soybean. These changes in total antioxidant capacity were reflected in the pool sizes of ASA (Fig. 3.2C), but not in phenolic content (Fig. 3.2E). Growth at elevated [$O_3$] significantly increased ASA by 42% (Fig. 3.2C). Growth at elevated $CO_2$ resulted in a 15% decrease in ASA, although it was not statistically significant (Fig. 3.2C). ASA is one of the most abundant antioxidants in plant tissue (Dalton *et al.*, 1986; Pritchard *et al.*, 2000) and high levels of ASA are essential to oxidative stress tolerance (Chen and Gallie, 2005; Conklin and Barth, 2004; Robinson and Britz, 2000; Smirnoff, 2000). Phenolic compounds also play a key role in antioxidant defense, but are more costly to manufacture and may not be synthesized as rapidly as ASA in response to acute oxidative stress (Grace, 2005). Trees have been shown to increase phenolic content and ASA content in response to elevated [$O_3$] (Di Baccio *et al.*, 2008). In contrast, soybean responded to long-term elevated [$O_3$] with higher levels of a rapid response compound, ASA, rather than through an increase in phenolic content (Fig. 3.2).

Consistent with the observation of a greater ASA pool, DHAR, an enzyme responsible for recycling DHA to ASA and regulating redox balance in plant cells (Fig. 3.1; Chen *et al.*, 2003), showed 120% higher activity in plants grown at chronic elevated [$O_3$] (Fig. 3.3A). None of the other enzyme activities measured responded to growth at chronic $O_3$ except GR, which showed a marked 43% decrease in response to elevated [$O_3$] (Fig. 3.3C). Additionally GR was the only enzyme to exhibit a response to elevated [$CO_2$], with a 29% decrease in rate (Fig 3.3C). GR is responsible for reducing glutathione (GSH), which provides reducing power to DHAR. In pea, GR is localized in the cytosol, chloroplast and mitochondria (Edwards *et al.*, 1990), with the

chloroplastic GR contributing approximately 80% to the total cellular GR activity. Therefore, a reduction in total GR activity does not directly indicate a reduction in activity of all isoforms or the availability of sufficient GSH to power DHAR activity. Increased DHAR activity may not require a matching increase in GR activity since GR activity is greater than DHAR activity (Fig. 3.2). Also the $K_m$ of GR for GSSG is approximately two orders of magnitude smaller than the $K_m$ of DHAR for GSH (Chang *et al.*, 2009), and the $K_m$ of GR was significantly lower in peas grown at high [$O_3$] (Edwards *et al.*, 1994). Therefore, ASA formation by DHAR is unlikely to be limited by the supply of reduced glutathione. Other antioxidant enzymes, CAT, SOD, MDHAR and APX, were not significantly changed by growth at either elevated [$CO_2$] or elevated [$O_3$] compared to control conditions (Fig. 3.3B, D, E, F). For CAT and SOD, this may reflect the very high capacities of these enzymes, which catalyze the initial steps in ROS scavenging (Chang *et al.*, 2009). Having an excess capacity for $O_2^-$ and $H_2O_2$ scavenging would be highly desirable since the consequences of a slow response to superoxides are severe (Foyer *et al.*, 1994).

This experiment measured total enzyme activity, so the contributions of each isoform to the total activity level were not distinguishable. In an attempt to parse the contribution of various isoforms localized in different cellular components, the transcript levels for genes annotated with antioxidant function and cellular localization were quantified (Table 3.2). Genes with a significant growth environment (atmosphere), time or interaction effect are shown in Fig. 3.4. Before the acute [$O_3$] treatment (Time 0 in Fig. 3.4), transcript levels were lower in plants grown at elevated [$CO_2$] for cytosolic GR1 by 93% (Fig. 3.4J), chloroplastic Cu-Zn SOD by 52% (Fig. 4D), GPX7 by 56% (Fig. 3.4F), and SOD copper chaperone by 59% (Fig. 3.4E). Transcript levels for two chloroplastic Cu-Zn SODs were 95% and 65% lower (Fig. 3.4B, 3.4D) and GPX7 was 50% lower(Fig. 3.4F) in plants grown at elevated [$O_3$]. Despite large decreases in two SOD

transcripts, no differences in SOD enzyme activities between the growth environments were found (Fig. 3.3F), suggesting compensatory contributions of the various SOD isoforms. Transcript levels for two genes, mitochondrial MDHAR (Fig. 3.4P) and ascorbate oxidase (AAO; Fig. 3.4L), were expressed at higher levels in plants grown at elevated [$O_3$]. Previous research has shown that the over-expression of cytosolic MDHAR led to increased ASA pool size in tobacco (Eltayeb *et al.*, 2007), which is consistent with the 42% increase in ASA pool size measured in response to growth at elevated [$O_3$] here (Fig. 3.2C). To date, at least 7 transcripts have been identified in soybean as having high homology to MDHAR genes (Schmutz *et al.*, 2010). Therefore, an increase in expression and possible enzyme activity of one isoform may be masked by the activity of the other isoforms when assaying total MDHAR enzyme activity. AAO transcript abundance was 15 times higher in elevated [$O_3$] than in the control condition (Fig. 3.4L). Over-expression of AAO has been demonstrated to oxidize the apoplastic ASA pool and enhance sensitivity to oxidative stress (Sanmartin *et al.*, 2003). However, my research did not find measurable differences in the DHA pool due to any growth treatment (data not shown). Evidence for significant regulation at the post-transcriptional level for antioxidant enzymes (May *et al.*, 1998; Pastori *et al.*, 2000; Schmidt *et al.*, 2002) is another factor that may explain discrepancies between transcript abundance and enzyme activity. Understanding the response of the antioxidant system would be improved by more extensive knowledge of the protein turnover rates, since the impact of large shifts in transcript abundance will be markedly reduced in enzymes with a large pool size.

In summary, high [$O_3$] grown plants demonstrate a primed antioxidant system consisting of high total antioxidant capacity, a large ASA pool, high total DHAR enzyme activity and increased MDHAR transcript abundance. Growth at elevated [$CO_2$] changed the composition of

the soybean antioxidant system by decreasing total antioxidant capacity, decreasing ASA content and decreasing the transcript abundance for cytosolic GR, chloroplastic Cu-Zn SOD, GPX7, and the SOD copper chaperone. Previous research has also demonstrated decreased levels of antioxidant enzyme levels in plants grown at elevated [$CO_2$] (Polle *et al.*, 1997; Pritchard *et al.*, 2000; Zhao *et al.*, 2009), suggesting decreased perceived oxidative stress. One proposed mechanism explaining why plants grown at elevated [$CO_2$] might be experiencing less oxidative stress is that plants exposed to elevated [$CO_2$] have lower rates of ROS production because of increased carboxylation rates and decreased oxygenation and subsequent photorespiration (Bowes, 1991; Pritchard *et al.*, 2000).

*Immediate Response to an Acute Oxidative Stress*

Immediately following a 200 ppb [$O_3$] spike for 4 h, plants grown under control atmospheric conditions shifted their antioxidant system to accommodate the increase in ROS (Table 3.2). MDHAR and DHAR, which recycle reduced ASA, increased activity levels by 162% and 250%, respectively (Fig. 3.5A, 3.5B, Time 24 h). Direct ROS scavenging enzymes, APX, CAT and SOD, responded differently (Fig. 3.5D, 3.5E, 3.5F). APX, which utilizes ASA to scavenge $H_2O_2$, decreased activity by 20% (Fig. 3.5D). CAT, which decomposes $H_2O_2$ into $H_2O$ and $O_2$, increased activity by 90% (Fig. 3.5E), and SOD, which dismutates $O_2^-$ into $H_2O_2$, decreased activity by 40% (Fig. 3.5F). This shift in enzyme activity toward the recycling and preservation of the ASA pool along with increased scavenging by CAT and decreased SOD maintained the total antioxidant capacity, which did not change immediately following the $O_3$ spike (Fig. 3.2B).

APX is sensitive to redox because its transcription and activity are regulated by its substrate, $H_2O_2$ (Ewing and Janero, 1995). The decrease in APX activity observed immediately following the $O_3$ spike indicates adequate reducing power provided by SOD, CAT and the soluble antioxidant molecules. When $O_3$ enters the leaf through the stomata, the first line of defense is the reducing capacity of the apoplast (Burkey *et al.*, 2003; Ranieri *et al.*, 1996). Measures of ASA within various compartments of the cell indicate that the concentration of ASA in the apoplast can be as much as 38 times higher than the concentration in the cytosol (Smirnoff, 2000). However, the volume of the apoplast is significantly less than that of the cytosol, suggesting that any changes in apoplastic ASA would not be detectable in total leaf ASA measurements (Smirnoff, 2000). Therefore, the cytosolic activity of APX, DHAR and MDHAR are important for regeneration of ASA for $O_3$ detoxification.

Transcript abundance for three chloroplastic Cu-Zn SOD enzymes decreased by 73%, 69%, and 57% (Fig. 3.4B, 3.4C, 3.4D) in plants grown at control conditions following an acute $O_3$ spike, which is consistent with previous experiments that showed that chloroplast-targeted genes are down-regulated immediately following acute $O_3$ stress (Mahalingam *et al.*, 2005). Transcript abundance increased for GR1 by 100% (Fig. 3.4J), for GR2 by 200% (Fig. 3.4K), MDHAR1 by 900% (Fig. 3.4M), and MDHAR by 600% (Fig. 3.4N), four antioxidant enzymes targeted to the cytosol, immediately following the $O_3$ spike, which supports a role for the cytosol in supplying reducing power for the apoplast.

Plants grown under chronic elevated [$O_3$] responded to the acute spike in a similar manner to the control plants. A 200% increase in MDHAR activity along with a 30% decrease in APX activity and a 38% decrease in SOD activity mirrored the response of the control grown plants (Fig. 3.5B, 3.5D, 3.5F). However, DHAR activity only increased by 60% and GR activity,

which did not change in the control plants, increased by 84% (Fig. 3.5A, 3.5C). Also, the significant increase in CAT activity measured in the control plants did not occur in the $O_3$-grown plants (Fig. 3.5E). In plants grown under chronic elevated [$O_3$], there was no change in total antioxidant capacity, phenolic content or ASA following the acute $O_3$ treatment (Fig. 3.2B, 3.2D, 3.2F). Also, the decrease in transcript abundance for chloroplastic antioxidant enzymes was not present in the elevated [$O_3$]-grown plants; however, the coordinated increase in transcripts coding for cytosolic antioxidant enzymes mirrored the increase observed in the control grown plants (Fig. 3.4J, 3.4K, 3.4M, 3.4N). In addition, the level of AAO transcript increased by 50% after the acute $O_3$ spike in the elevated [$O_3$]-grown plants (Fig. 3.4L). A large increase, 1660%, in the transcript abundance for the Cu-ZnSOD copper chaperone was also observed (Fig. 3.4E). Previous research has demonstrated that SOD requires a specific chaperone to facilitate copper transfer and the disproportion of superoxide (Chu *et al.*, 2005). Despite this large increase in transcript abundance for the copper chaperone, which has been shown to stimulate Cu-Zn SOD activity (Cohu *et al.*, 2009), a decrease in total SOD activity, which does not distinguish among Cu-Zn, Fe or Mn isoform contributions, was observed immediately following the $O_3$ spike (Fig. 3.5F).

The high [$CO_2$]-grown plants responded differently to the acute $O_3$ spike compared to the ambient and elevated [$O_3$]-grown plants. ORAC increased by 60%, but there were no observed changes in the ASA, DHA, or phenolic pool sizes (Figs. 3.2B, 3.2D, 3.2F). Activity levels increased for DHAR by 700%, MDHAR by 200% and CAT by 450% (Fig. 3.5A, 3.5B, 3.5E), while SOD activity decreased by 41% (Fig. 3.5F). The changes in transcript abundance for cytosolic and chloroplastic antioxidant enzymes following the acute $O_3$ spike that were observed in the elevated [$O_3$]- and control-grown plants were absent from the elevated [$CO_2$]-grown plants

(Fig. 3.4). Transcript abundance increased for one cytosolic enzyme, GR1, by 1400% (Fig.3. 4J), and the peroxisomal MDHAR4 by 161% (Fig. 3.4O). Previous research on the transcriptome responses of sensitive and tolerant *Medicago* cultivars to an acute $O_3$ spike demonstrated that the sensitive cultivar lacked the immediate induction of gene expression for a variety of defense and hormone related signaling pathways that were present in the tolerant cultivar (Puckette *et al.*, 2008). Therefore, the lack of coordinated transcription of antioxidant genes in the high [$CO_2$]-grown plants could indicate a delay in the immediate perception of the ROS signaling network.

Immediately following an acute oxidative stress, plants grown under control conditions responded by increasing ASA recycling and preservation (Fig. 3.2 & 3.5), down-regulating chloroplast-targeted antioxidant genes, and up-regulating cytosol-targeted antioxidant genes (Fig. 3.4). Previous research has shown that reducing equivalents are absent from the apoplast (Pignocchi and Foyer, 2003), suggesting that any reduced ASA required in the apoplast must be generated and reduced in the cytosol, then transported across the cell membrane. Thus, the cytosolic antioxidant system is integral to the ability of the apoplast to quench ROS (Chen and Gallie, 2005, 2006, 2008; Eltayeb *et al.*, 2006; Pignocchi and Foyer, 2003). The shift in antioxidant metabolism towards ASA recycling and preservation, as well as the up regulation of cytosolic antioxidant genes, was also present in the high [$O_3$]-grown plants although to a lesser degree (Figs. 3.2, 3.4 & 3.5). This may suggest that plants grown at elevated [$O_3$] were primed to quench the ROS influx following the acute $O_3$ stress. In contrast, the high [$CO_2$]-grown plants displayed a large stimulation of total antioxidant metabolism immediately following the acute $O_3$ spike (Fig. 3.2B), and notable increases in MDHAR, DHAR and CAT activity despite no changes in the majority of the antioxidant genes measured immediately following the oxidative stress (Fig. 3.5). Therefore, plants grown at high [$CO_2$] showed a different response to the acute

oxidative stress, with greater investment in total antioxidant capacity, greater relative changes to enzymatic activities and few immediate changes at the transcriptional level.

*Long-term Recovery from an Acute Oxidative Stress*

In the 2 days following the acute $O_3$ spike, the control-grown plants regulated the components of the antioxidant system in different ways. Despite no immediate change in total antioxidant capacity following the spike, a delayed increase was observed at 48 h, but antioxidant capacity returned to pre-spike levels by 72 h (Fig. 3.2B). The small decrease in phenolic content returned to baseline levels by 48 h and remained constant thereafter (Fig. 3.2F). The delayed increase in ORAC was mirrored by an increase in ASA at 48 h, which dropped slightly by 72 h (Fig. 3.2D). There was little consistency in the response of the enzymes following the acute $O_3$ spike (Fig. 3.5), suggesting distinct regulation mechanisms. The stimulation in CAT activity was sustained through 24 h but dropped back to pre-spike levels by 72 h (Fig. 3.5E). DHAR and MDHAR activity dropped after 48 h but a secondary stimulation was recorded at 72 h (Fig. 3.5A, 3.5B). While GR, SOD and APX activity all decreased immediately following the $O_3$ spike, the post-spike recovery of these activity levels varied. GR activity increased at 24 h back to pre-spike levels, but a second decrease in activity was recorded at 72 h (Fig. 3.5C). The decreased SOD activity was sustained through the remainder of the experiment and APX activity decreased even further at 48 h and remained low through 72 h (Fig. 3.5F). While evidence for post-transcriptional control of these enzymes exists, only a few of the mechanisms of control have been investigated. Work in rye has described one isoform of CAT as light-regulated (Schmidt *et al.*, 2002). However, at least 5 transcripts encoding genes with high homology to CAT have been identified in soybean (Schmutz *et al.*, 2010), and no work to date has been done on the post-

transcriptional control of these different isoforms. GR activity differs among cellular compartments (Edwards *et al.*, 1990) and cell-types, and recent work in maize suggests different protein turnover control mechanisms exist in different cell types (Pastori *et al.*, 2000). All transcripts that were immediately stimulated by the $O_3$ spike returned to pre-spike levels by 48h (Fig. 3.4J, 3.4K, 3.4M, 3.4N). Transcripts that were negatively affected by the acute $O_3$ spike remained low through 72 h except for the chloroplast Cu-Zn SOD (Fig. 3.4B), which increased 360%, and chloroplast APX4 (Fig. 3.H), which increased 77% over the pre-spike level at 72 h.

Although the immediate response of high [$O_3$]-grown plants to the acute $O_3$ spike was very similar to that of the control-grown plants, the post-spike regulation of the antioxidant system varied compared to the regulation observed in the control-grown plants. The initial high level of ORAC was sustained through 48 h but dropped by 46% at 72 h (Fig. 3.2B). The ASA pool remained fairly constant and significantly higher in elevated [$O_3$]-grown plants compared to ambient and elevated [$CO_2$]-grown plants throughout the experimental time-frame (Fig. 3.2D). The sustained antioxidant pools throughout the acute $O_3$ spike suggest that high [$O_3$]-grown plants were primed to deal with the acute stress better than the control or high [$CO_2$]-grown plants. CAT activity remained constant through the $O_3$ spike, but dropped at 48h and remained low through 72 h (Fig. 3.5E). DHAR and MDHAR activity deviated from the pattern observed in control grown plants. The increase in DHAR activity observed immediately following the $O_3$ spike was further increased at 48 h only dropping back to pre-spike levels by 72 h (Fig. 3.5A). The pattern of MDHAR regulation matched that observed in the control-grown plants (Fig. 3.5B). High [$O_3$]-grown plants were the only group to display an increase in GR activity immediately following the acute $O_3$ spike and that activity slowly returned to pre-spike levels by 72h (Fig. 3.5C). Mirroring the transcript response in the control-grown plants, all transcripts that

were immediately stimulated by the $O_3$ spike in high [$O_3$]-grown plants returned to pre-spike levels by 48 h (Fig. 3.4J, 3.4K, 3.4M, 3.4N). The initial stimulation in AAO transcript abundance dropped below the pre-spike levels, so that by 72 h, levels were no longer different among [$CO_2$]-, [$O_3$]- and control-grown plants (Fig. 3.4L).

High [$CO_2$]-grown plants responded to an acute $O_3$ spike with an immediate stimulation in total antioxidant capacity (Fig. 3.2B) and the largest stimulation in DHAR and CAT activity (Fig. 3.4A, 3.4E). Total antioxidant capacity slowly decreased so that by 72 h, it was not different from pre-spike levels (Fig. 3.2B). The stimulation of total antioxidant capacity was not reflected in changes in ASA pool size or phenolic content throughout the entire experimental time-frame (Figs. 3.2D, 3.2F). CAT activity returned to pre-spike levels by 48 h and remained low through 72 h (Fig. 3.5E). DHAR activity began to decrease at 48 and 72 h but remained higher than pre-spike levels through 72 h (Fig. 3.5A). The high [$CO_2$]-grown plants did not display the same immediate drop and sustained low APX activity observed in the control and [$O_3$]-grown plants. Instead, APX activity in high [$CO_2$]-grown plants decreased at 48h but returned to pre-spike activity levels by 72 h (Fig. 3.5D). While there was no immediate coordinated change in antioxidant transcript abundance in the high [$CO_2$]-grown plants due to the acute $O_3$ treatment, a delayed increase in abundance for some transcripts was observed (Fig. 3.4). Transcript abundance for mitochondrial MDHAR (Fig. 3.4P) and peroxisomal MDHAR4 (Fig. 3.4O) increased by 48 h and remained high through 72 h. GPX7 (Fig. 3.4F) increased at 48 h but dropped below pre-spike levels by 72 h. Transcript abundance for chloroplastic APX4 (Fig. 3.4H) and chloroplastic Cu-Zn SOD (Fig. 3.4B) only began to increase at 72 h. The sluggish increase in transcript abundance in the high [$CO_2$]-grown plants parallels the delay reported in

$O_3$-sensitive cultivars of *Medicago* (Puckette *et al.*, 2008) and *Arabidopsis* (Mahalingam *et al.*, 2005).

*Conclusions*

This study confirmed the hypotheses that growth environment alters the antioxidant system, the immediate response to an acute oxidative stress and the timing over which plants return to initial antioxidant levels. Previous research demonstrated that growth at elevated [$O_3$] caused a general up-regulation of the antioxidant metabolism in plants (Olbrich *et al.*, 2009; Puckette *et al.*, 2007; Ranieri *et al.*, 1996; Ranieri *et al.*, 2000; Scebba *et al.*, 2003; Xu *et al.*, 2008). However, direct evidence for this up-regulation has been variable and dependent on the duration and method of $O_3$ fumigation, and the components of antioxidant metabolism investigated (Burkey *et al.*, 2000; Iglesias *et al.*, 2006; Robinson and Britz, 2000). Likewise, reports investigating the effects of growth at elevated [$CO_2$] showed contrasting responses of individual components of the antioxidant system (di Toppi *et al.*, 2002; Polle *et al.*, 1997; Pritchard *et al.*, 2000; Rao *et al.*, 1995). In this study, it was demonstrated that growth in a chronic high [$O_3$] environment increased total antioxidant capacity, while chronic elevated [$CO_2$] decreased total antioxidant capacity. The growth environment also significantly altered the pattern of antioxidant transcript and enzyme response to an acute oxidative stress. Growth at high [$O_3$] increased the basal levels of components of the antioxidant system, which were then unchanged or only slightly increased following an acute oxidative stress, suggesting that growth at chronic elevated [$O_3$] allowed for a primed antioxidant system. Growth at high [$CO_2$] decreased the basal level of antioxidant capacity, increased the response of the existing antioxidant enzymes, but dampened and delayed the transcriptional response, suggesting an

entirely different regulation of the antioxidant system. The time-frame across which different components of the plant antioxidant system recover from an acute $O_3$ spike differed considerably as well, suggesting distinct mechanisms of control.

FIGURES AND TABLES

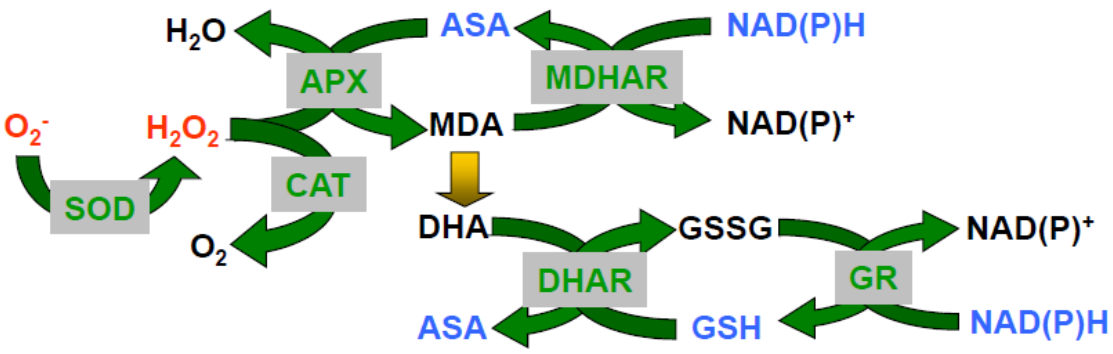


**Figure 3.1. Six antioxidant enzymes involved in recycling ascorbate and glutathione.** ROS (red text) react with metabolic antioxidant pools (blue text) such as ascorbic acid (ASA) and glutathione (GSH) or they can be enzymatically reduced (grey boxes). Superoxide dismutase (SOD) converts superoxide to hydrogen peroxide, which is then reduced via catalase (CAT) or ascorbate peroxidase (APX), which oxidizes one molecule of reduced ascorbate (ASA) to monodehydroascorbate (MDA). MDA can be re-reduced via monodehydroascorbate reductase (MDHAR) utilizing NADPH, or it will spontaneously convert to dehydroascorbate (DHA). DHA is re-reduced to ASA via dehydroascorbate reductase (DHAR), which oxidizes one molecule of glutathione (GSH). Oxidized glutathione (GSSG) can be re-reduced via glutathione reductase (GR) utilizing NADPH.

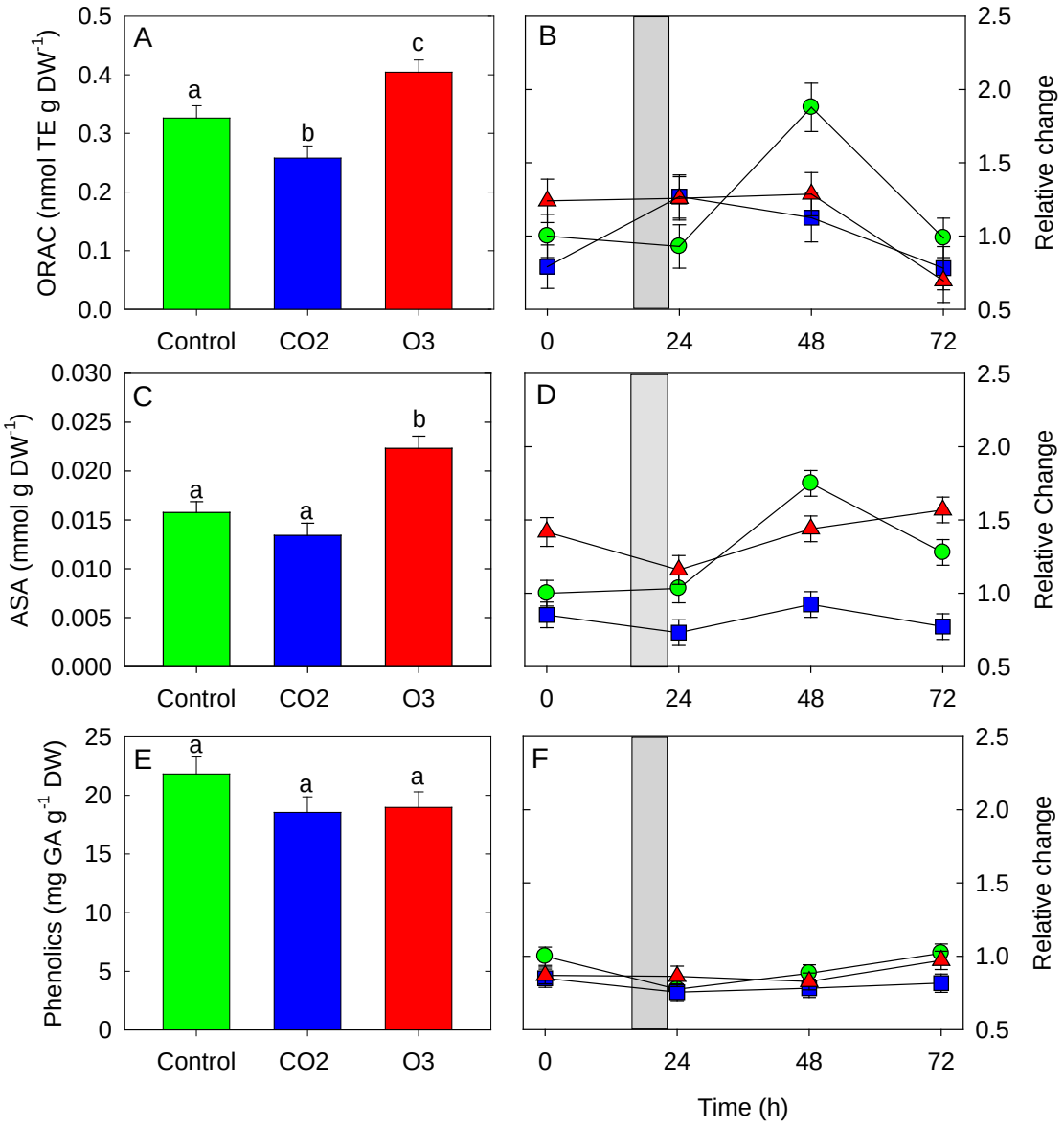


**Figure 3.2. The effects of atmospheric growth condition on the response of soybean total antioxidant capacity (panels A & B), reduced ascorbic acid (panels C & D) or phenolic content (panels E & F) due to an acute $O_3$ spike (200ppb [$O_3$] for 4h).** Growth conditions were control (green circles; 400ppm [$CO_2$] and 0ppb [$O_3$]), elevated $CO_2$ (blue squares; 650ppm [$CO_2$] and 0ppb [$O_3$]), and elevated $O_3$ (red triangles; 400ppm [$CO_2$] and 90ppb [$O_3$]). Panels A, C & E report the lsmean for each treatment (n=6) at time 0h, +/- standard error. Panels B, D & F report the relative change of each parameter compared to the control treatment at time 0h, +/- 1 standard error; the grey bar represents the timing of the 4h acute $O_3$ spike.

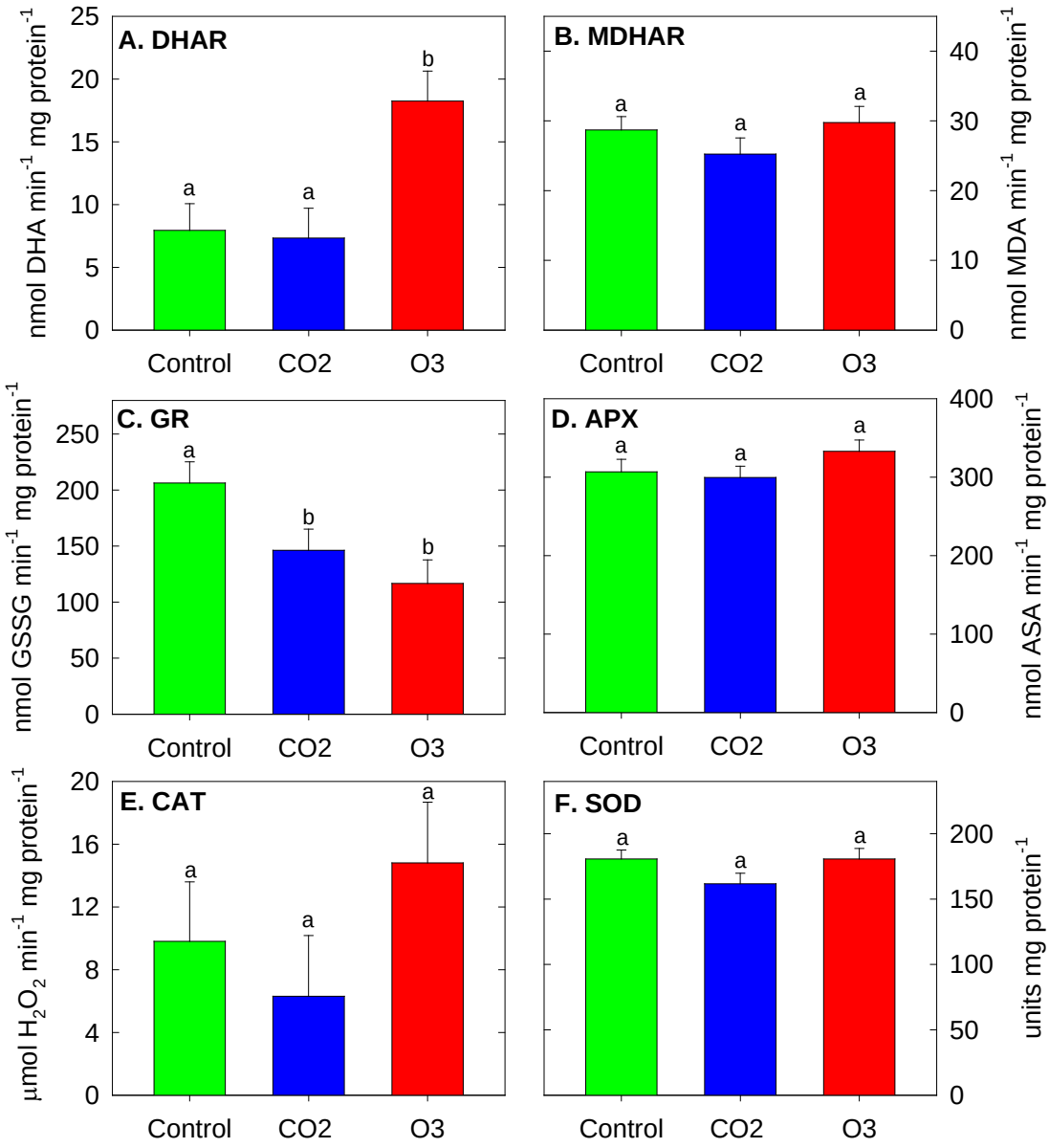


**Figure 3.3. The effects of atmospheric growth condition on the activity levels of six different antioxidant enzymes: dehyroascorbate reductase (DHAR; panel A), monodehydroascorbate reductase (MDHAR; panel B), glutathione reductase (GR; panel C), ascorbate peroxidase (APX; panel D), catalase (CAT; panel E), and superoxide dismutase (SOD; panel F).** Growth conditions were control (green; 400ppm [$CO_2$] and 0ppb [$O_3$]), elevated $CO_2$ (blue; 650ppm [$CO_2$] and 0ppb [$O_3$]), and elevated $O_3$ (red; 400ppm [$CO_2$] and 90ppb [$O_3$]). All panels report the lsmean for each treatment (n=6) at time 0h, +/- 1 standard error.

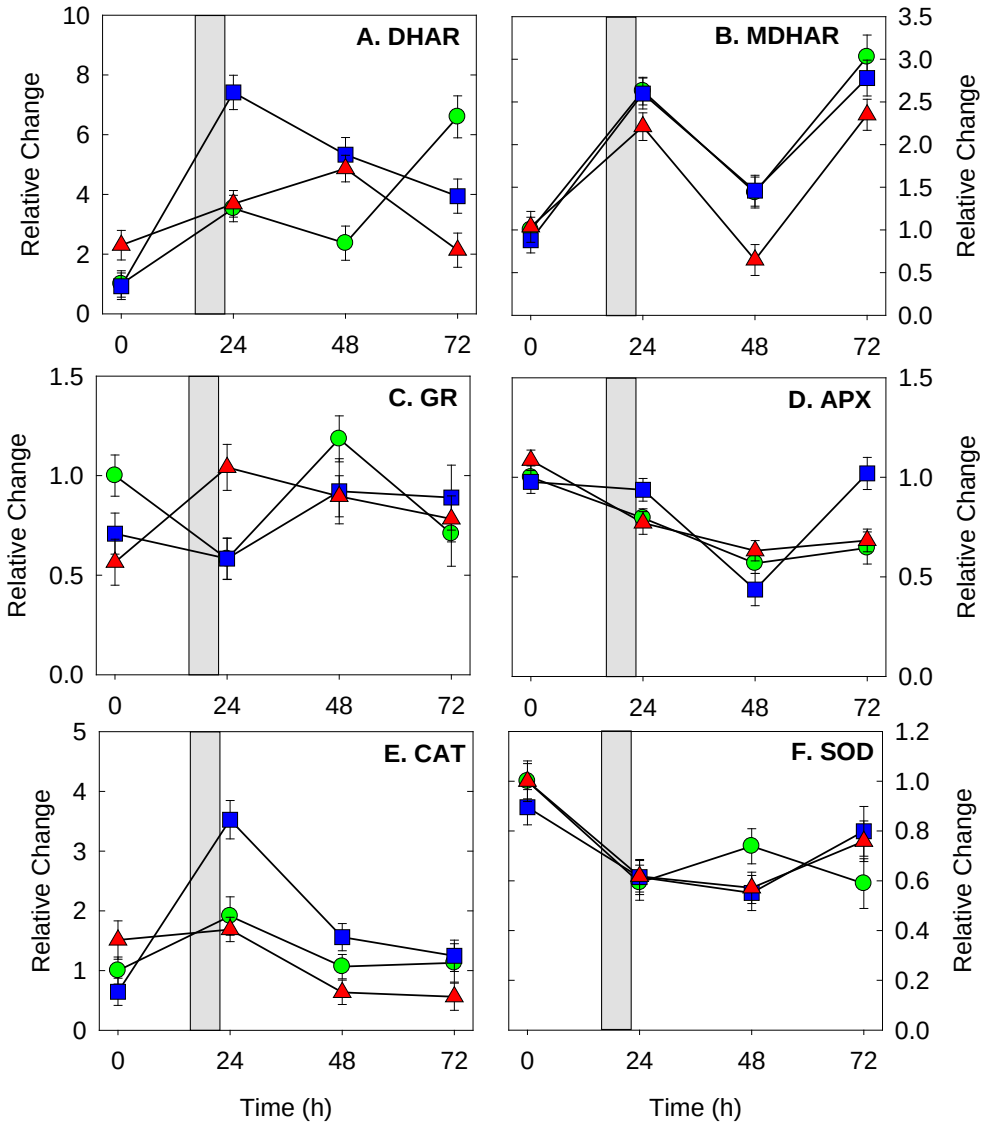


**Figure 3.4. The effects of atmospheric growth condition on the response of soybean enzyme activity levels of six different antioxidant enzymes due to an acute $O_3$ spike (200 ppb for 4h). The enzymes are: dehyroascorbate reductase (DHAR; panel A), monodehydroascorbate reductase (MDHAR; panel B), glutathione reductase (GR; panel C), ascorbate peroxidase (APX; panel D), catalase (CAT; panel E), and superoxide dismutase (SOD; panel F).** Growth conditions were control (green circles; 400ppm [$CO_2$] and 0ppb [$O_3$]), elevated $CO_2$ (blue squares; 650ppm [$CO_2$] and 0ppb [$O_3$]), and elevated $O_3$ (red triangles; 400ppm [$CO_2$] and 90ppb [$O_3$]). All panels report the relative change of each parameter compared to the control treatment at time 0h, +/- 1 standard error; the grey bar represents the timing of the 4h acute $O_3$ spike.

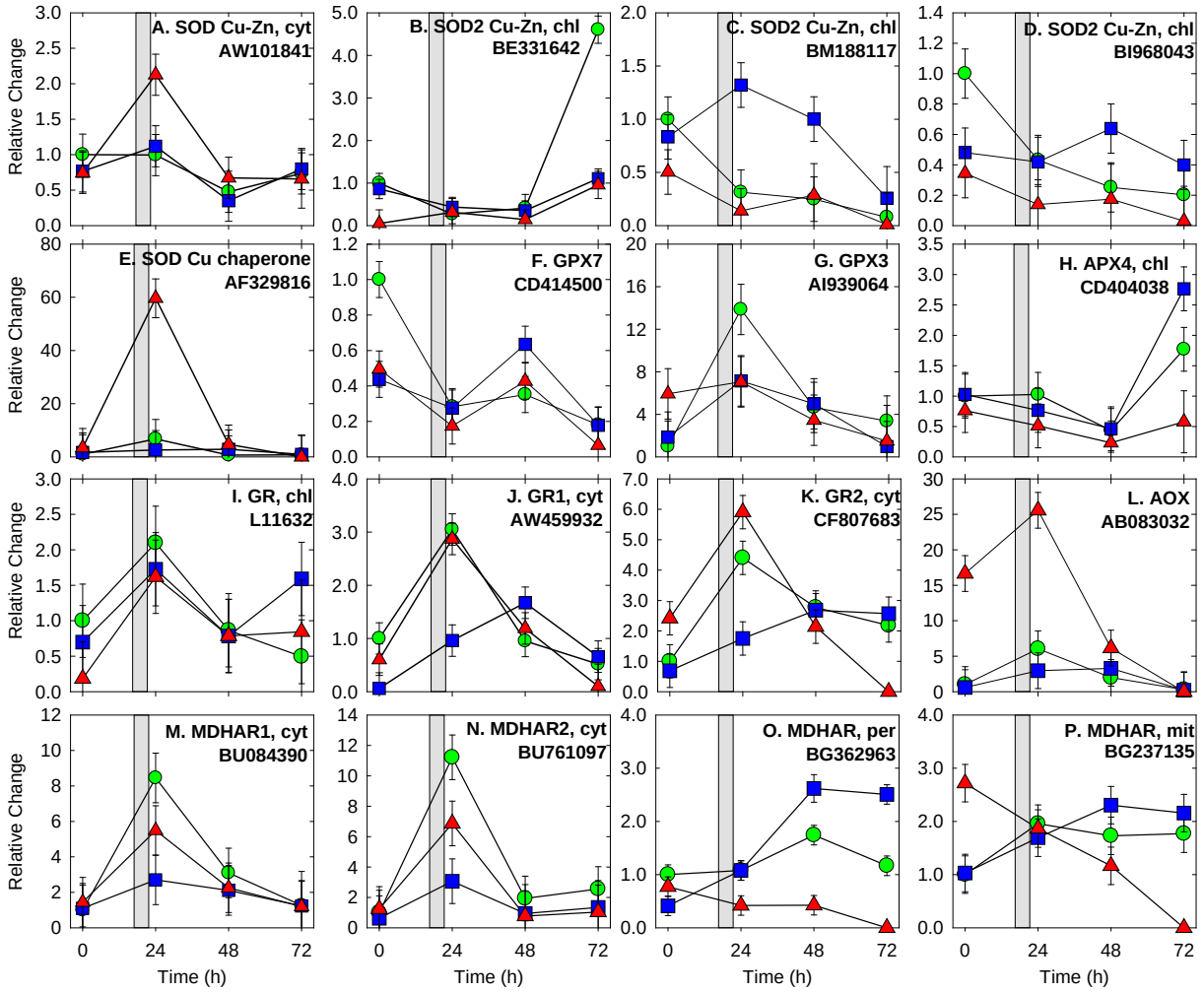


**Figure 3.5. The effects of atmospheric growth condition on the response of soybean transcripts involved in antioxidant metabolism due to an acute $O_3$ spike (200 ppb for 4h).** Each transcript is labeled with its annotated function and sub-cellular localization if one has been reported as well as the genbank identification number. Further information about the transcripts can be found in supp. Table 1. Growth conditions were control (green circles; 400ppm [$CO_2$] and 0ppb [$O_3$]), elevated $CO_2$ (blue squares; 650ppm [$CO_2$] and 0ppb [$O_3$]), and elevated $O_3$ (red triangles; 400ppm [$CO_2$] and 90ppb [$O_3$]). All panels report the relative change of each parameter compared to the control treatment at time 0h, +/- the standard error; the grey bar represents the timing of the 4h acute $O_3$ spike.

**Table 3.1.** Real-time PCR targets, Affymetrix Target ID, GenBank ID and primers for antioxidant transcript analysis.

| Target Description | Affymetrix ID | GenBank ID | Forward Primer | Reverse Primer |
|---|---|---|---|---|
| AAO | Gma.8447.1.S1_at | AB083032 | TGGGTATGGGAAGGGAAAGT | ATGAAAAGCCCACACTCCAG |
| APX4, chl. | Gma.2202.1.S1_at | CD404038 | CCAATATGGGAGAAGGCAAG | AGCAACATCAGGATCAGTGG |
| DHAR3, chl. | Gma.2041.1.S1_at | BE823473 | CAATGTCCGCTGTGAGAGTT | AGGAGGAACGGAAGACATTG |
| GPX | Gma.2338.4.S1_at | BQ252988 | CCAAGGTTCCAAAATCCGTA | GAAGGCACAATCAGGGAAAA |
| GPX3 | Gma.4312.2.S1_x_at | AI939064 | AAGAATGCAGCGCCACTTTA | TCGATTTTCAGAGGTGAGGTG |
| GPX6 | GmaAffx.93342.1.S1_s_at | CF809067 | AATCTCGCCGATTACAAAGG | CATGGGAATGCCAGAATTT |
| GPX7 | Gma.6855.1.S1_at | CD414500 | TGGACCATTTACAACTCCAGTG | GGAGACGTTGTTGGTGGGTA |
| GR, chl. | Gma.16708.1.S1_s_at | L11632 | AGGCTGACTTTGATGCCACT | CTGCAGCTTTTGCTTGAGAG |
| GR1, cyt. | GmaAffx.35832.1.S1_at | AW459932 | AAGGTTCTCGGAGCCTCAAT | CACTGACCGCATGGTTACAA |
| GR2, cyt. | GmaAffx.91958.1.S1_s_at | CF807683 | GCTGTTGGTGTTGAGCTTGA | AAGGCCACCGGAGTAAGATT |
| GSH synthetase | Gma.3133.1.S1_at | AJ272035 | GCCTGGTTTTGGAGTGGTAG | AGAAACAGCAATGCCTCCAT |
| MDHAR, cyt. | Gma.5803.2.S1_at | BU761097 | GTTGTTGGGGTCTTTCTGGA | GCAAACCACCAAGCATTTTT |
| MDHAR, mito. | GmaAffx.22568.1.S1_s_at | BG237135 | GTAAGCTGAAAGGAGTTCTTCTTGA | AGTTTGGCTTTATCAATCAGAGG |
| MDHAR1, cyt. | Gma.5803.1.S1_at | BU084390 | CTGGAAGGTGGAACTCCTGA | GCAAACCACCAAGCATCTTT |
| MDHAR4, perox. | GmaAffx.23473.2.S1_at | BM525801 | ACAATGGTCTTCCCTGAGGA | CCTTCCCATTGGAGTCAAAA |
| MDHAR4, perox. | GmaAffx.81725.1.S1_at | BG362963 | CCTGCATTGAGCAAAGGATT | TGGATTTAACTCCGGTTCCA |
| Cu-Zn SOD, copper chaperone | Gma.8498.1.S1_at | AF329816 | GCTGAGGGTGGCTGATCTTA | GGTGCCATCACACGTACAGA |
| Fe SOD, chl. | Gma.16827.1.S1_at | AF108084 | CCTGGGATGCAGTGAGTTCT | TATTCCTCATGACGCCATCC |
| Cu-Zn SOD1, cyt. | Gma.15464.1.S1_x_at | AW101841 | GAGAATCGTCATGCTGGTGA | CAGGATCAGCATGGACAACA |
| Cu-Zn SOD2, chl. | Gma.2513.2.S1_at | BE331642 | AATGCCGATGGTAATGCTTC | AGGAGCACCTGATTGTCCAC |
| Cu-Zn SOD2, chl. | Gma.6384.1.S1_at | BI968043 | CCACTCTCTGGCCCTAATTC | ATGCTGGAGTCAAACCAACC |
| Cu-Zn SOD2, chl. | Gma.2513.1.A1_at | BM188117 | TTTGAGCACTGGAAATGCTG | GAAGGATCGTGCTTCAGAGC |
| Fe SOD2, chl. | Gma.15794.1.S1_at | CD409698 | TGTAAACCCCCTTGTTTGGA | AGCTGACTGCATCCCAAGAC |
| Fe SOD2, chl. | Gma.3233.1.S1_s_at | M64267 | TTACCAGTGCATGATGCTGA | CAAAAGATGTGCCTGCTTACA |
| Cu-Zn SOD3, per. | Gma.15258.1.S1_at | CD412753 | AGTGACAGGGTTGTCCCAAG | CATGGCGCTTATCATCTGAA |

**Table 3.2.** Analysis of variance of antioxidant pools, enzymes and GenBank IDs of transcripts measured for soybeans grown under control conditions (400 ppm [$CO_2$], 0 ppb [$O_3$]), elevated [$CO_2$] (650 ppm [$CO_2$], 0 ppb [$O_3$]), and elevated [$O_3$] (400 ppm [$CO_2$], 90 ppb [$O_3$]), before and after an acute (200 ppb) $O_3$ spike. See Table 1 for descriptions of GenBank IDs. NS: not significant

| | Atmosphere | Time | Atmosphere x Time |
|---|---|---|---|
| ORAC | NS | 0.0001 | 0.0109 |
| Phenolic content | 0.0023 | 0.0292 | NS |
| ASA | <0.0001 | <0.0001 | 0.0012 |
| DHA | NS | <0.0001 | NS |
| CAT | 0.0065 | <0.0001 | 0.0065 |
| SOD | NS | <0.0001 | NS |
| APX | NS | <0.0001 | 0.0043 |
| GR | NS | 0.0496 | 0.0068 |
| DHAR | 0.0085 | <0.0001 | <0.0001 |
| MDHAR | 0.0023 | <0.0001 | NS |
| *Transcripts* | | | |
| AAO (AB083032) | <0.0001 | 0.0157 | 0.0364 |
| APX4 (CD404038) | *0.0537* | 0.0114 | NS |
| DHAR3 (BE823473) | NS | NS | NS |
| GPX3 (AI939064) | NS | 0.0153 | NS |
| GPX6 (CF809067) | NS | NS | NS |
| GPX7 (CD414500) | NS | 0.0005 | 0.0462 |
| GR (L11632) | NS | *0.0723* | NS |
| GR1 (AW459932) | *0.0687* | <0.0001 | 0.0077 |
| GR2 (CF807683) | 0.0188 | 0.0021 | 0.0210 |
| HGS (AJ272035) | NS | NS | NS |
| MDHAR (BU761097) | *0.0748* | 0.0015 | NS |
| MDHAR (BG237135) | NS | NS | 0.0268 |
| MDHAR1 (BU084390) | NS | 0.0101 | NS |
| MDHAR4 (BM525801) | NS | NS | NS |
| MDHAR4 (BG362963) | 0.0312 | 0.0018 | 0.0165 |
| SOD chaperone (AF329816) | 0.0088 | 0.0160 | 0.0158 |
| SOD-Fe (AF108084) | NS | NS | NS |
| SOD1 (AW101841) | NS | 0.0166 | NS |
| SOD2 (BE331642) | 0.0013 | 0.0002 | 0.0021 |
| SOD2 (BI968043) | *0.0751* | NS | NS |
| SOD2 (BM188117) | 0.0143 | *0.0505* | NS |
| SOD2 (CD409698) | NS | NS | NS |
| SOD2 (M64267) | NS | NS | NS |
| SOD3 (CD412753) | NS | NS | NS |

# CHAPTER 4: BIOCHEMICAL AND TRANSCRIPTIONAL EVIDENCE FOR INCREASED ANTIOXIDANT, CHLOROPHYLL AND RESPIRATORY METABOLISM IN FIELD-GROWN SOYBEAN EXPOSED TO ELEVATED OZONE[3]

## INTRODUCTION

A summary of the physiological effects of elevated [$CO_2$] and chronic elevated [$O_3$] were discussed in Chapter 1. The individual effects of elevated [$CO_2$] and elevated [$O_3$] were investigated in a controlled environment and discussed in Chapter 3. While that study identified some of the biochemical and transcriptional responses of the antioxidant system to elevated [$CO_2$] and [$O_3$], how the antioxidant system in a crop species will respond to future climate change in a field environment is unknown. Therefore, in this chapter, I examined the genomic and biochemical response of field-grown soybean to the atmospheric conditions predicted for 2050.

Many experiments investigating the interaction of concurrent elevated [$CO_2$] and [$O_3$] revealed some prevention or delay of $O_3$-mediated damage (Booker and Fiscus, 2005; McKee *et al.*, 1997; McKee *et al.*, 2000; Wustman *et al.*, 2001; Yan *et al.*, 2010). While this amelioration is highly dependent on fumigation levels, experimental duration and species, the resultant hypothesis is based on the physiological response. Decreases in stomatal conductance ($g_s$), as a result of growth at elevated [$CO_2$], lead to smaller fluxes of $O_3$ into the leaf and less subsequent damage. However, Booker and Fiscus (2005) demonstrated that setting the $O_3$ concentration to provide an equal flux of $O_3$ into leaf tissue grown at elevated and ambient [$CO_2$] suppressed photosynthesis at ambient [$CO_2$], but did not have detrimental effects at elevated [$CO_2$]. While an increase in substrate availability for repair and detoxification at elevated [$CO_2$] may reduce the negative

[3] These experiments were designed by Kelly Gillespie, Andrew Leakey, Don Ort, Elizabeth Ainsworth. Research was carried out by Kelly Gillespie, Fangxiu Xu, Justin McGrath, Andrew Leakey and Elizabeth Ainsworth. All data were analyzed by Kelly Gillespie and the chapter was written by Kelly Gillespie.

effects of elevated [$O_3$] (Rao *et al.*, 1995), there was no evidence that the elevated [$CO_2$] treatment caused up regulation of the antioxidant components measured in the Booker and Fiscus (2005) study. Studies have reported increased antioxidant activity in plants exposed to elevated [$O_3$] in both ambient and elevated [$CO_2$] (Sehmer *et al.*, 1998), while other studies have shown no change or a decrease in antioxidant activity in plants exposed to elevated [$CO_2$] and elevated [$O_3$] (McKee *et al.*, 1997; Niewiadomska *et al.*, 2009; Tausz *et al.*, 2004; Wustman *et al.*, 2001). Therefore, the mechanism for amelioration of $O_3$ damage by elevated [$CO_2$] may not be a simple matter of flux. Rather, the increased carbon available at elevated [$CO_2$] could provide more substrate for antioxidant metabolism to play a larger role as well.

An increase in antioxidant metabolism for plants exposed to elevated [$O_3$] is suggested to require a shift in carbon metabolism to supply reducing power and carbon skeletons for repair and detoxification processes (Dizengremel *et al.*, 2009). This hypothesis is supported by a number of studies showing increased respiration in plants grown at elevated [$O_3$] (Amthor, 1988; Amthor and Cumming, 1988; Biswas *et al.*, 2008; Kellomaki and Wang, 1998; Skarby *et al.*, 1987; Volin and Reich, 1996). However, other studies report decreases in photosynthetic carbon gain with associated decreases in respiration in plants grown at elevated [$O_3$] (He *et al.*, 2007; Low *et al.*, 2007; Velikova *et al.*, 2005; Wittig *et al.*, 2009). Therefore, there are two opposing hypotheses that emerge from the literature, the first that respiration will increase at elevated [$O_3$] in order to support detoxification and repair, and the second that respiration will decrease due to lower substrate supply.

The effects of elevated [$O_3$] on respiratory metabolism in plants grown at elevated [$CO_2$] have been investigated in a sink-limited species (Gandin *et al.*, 2009) and on root respiration (Grantz *et al.*, 2003), but little is known about the general response. Growth at elevated [$CO_2$] alone

increases respiration rates and alters the abundance of transcripts encoding enzymes throughout the respiratory pathway (Leakey *et al.*, 2009b). Changes in respiration in plants exposed to elevated [$CO_2$] are supported by the use of additional photoassimilate from enhanced photosynthetic C gain (Leakey *et al.*, 2009b) and by increased mitochondrial number (Griffin *et al.*, 2001). However, even in plants grown at elevated [$CO_2$], it is possible that changes in respiration due to growth at elevated [$O_3$] would support detoxification and repair of cellular damage (Amthor, 1988; Amthor and Cumming, 1988), and therefore decrease net C balance and overall plant productivity (Volin and Reich, 1996; Wittig *et al.*, 2009). How growth at both elevated [$CO_2$] and elevated [$O_3$] alter respiratory processes varies in different studies (Karnosky *et al.*, 2003; Loats and Rebbeck, 1999; Sehmer *et al.*, 1998; Volin and Reich, 1996), but has not been investigated at the biochemical and transcriptional level in field-grown plants exposed to atmospheric conditions anticipated for the middle of this century.

Previous research has demonstrated that the transcriptional response of field-grown plants to stress is not easily duplicated in controlled environments (Miyazaki *et al.*, 2004; Pasquer *et al.*, 2005). For example, Arabidopsis plants grown in the field showed significant up-regulation of transcripts involved in defense, photosynthesis and redox control, compared to plants grown in controlled environments (Miyazaki *et al.*, 2004). Wheat plants sprayed with a chemical to induce system resistance against pathogens showed significant up-regulation of defense-related genes in a greenhouse trial, but not in the field (Pasquer *et al.*, 2005). Additionally, the magnitude of the effect of elevated [$CO_2$] on plant physiological responses has been shown to be dependent on environmental conditions that vary throughout a growing season, such as temperature and water deficit (Bernacchi *et al.*, 2006; Leakey *et al.*, 2006). Therefore, the genomic ecology approach, where field-grown plants are used for genomic studies in order to understand impacts of climate

change over the entire life histories of subject species and to investigate transcriptional changes to ecologicaly relevant treatments (Leakey *et al.*, 2006), is becoming more common (Ainsworth *et al.*, 2006; Druart *et al.*, 2006; Leakey *et al.*, 2009b; Tallis *et al.*, 2010; Taylor *et al.*, 2005; Travers *et al.*, 2010). In this study, the transcriptional, biochemical and physiological response of soybean to elevated [$CO_2$] and elevated [$O_3$] was measured throughout the 2007 growing season in order to test the hypothesis that elevated [$O_3$] alters antioxidant metabolism with associated changes in respiratory metabolism to support detoxification and repair. I also hypothesized that elevated [$CO_2$] protects from the detrimental effects of elevated [$O_3$], and therefore, the up-regulation of antioxidant metabolism will be dampened with increasing [$O_3$].

## METHODS

### *Field Site Description*

Soybean (*Glycine max*, cv. Pioneer 93B15) was grown at the SoyFACE experimental facility (www.soyface.illinois.edu) during 2007. The field site, agronomic practices, $CO_2$ and $O_3$ fumigation methods have been described previously (Ainsworth *et al.*, 2004; Bernacchi *et al.*, 2006; Morgan *et al.*, 2004; Morgan *et al.*, 2006; Rogers *et al.*, 2004). The experiment was designed as a randomized complete block design (n = 4). Within each block, one ring was maintained at ambient [$CO_2$] and ambient [$O_3$], elevated [$CO_2$] (550 ppm) and ambient [$O_3$], ambient [$CO_2$] and elevated [$O_3$] (2x ambient), and both elevated [$CO_2$] (550 ppm) and elevated [$O_3$] (2x ambient). Treatments were chosen to simulate atmospheric conditions predicted for 2050 (Prentice *et al.*, 2001).

Fumigation started on 4 June 2007, shortly after crop emergence, and ended on 21 September 2007, after the soybeans were mature. Across the 2007 growing season, daytime average [$CO_2$]

was 386 ppm in the ambient [$CO_2$] treatment and 552 ppm in the elevated [$CO_2$] treatment. Based on 1-min averages, the [$CO_2$] in the elevated [$CO_2$] plots was within 10% of the target concentration for 80% of the time. Average 8 hr (10:00-18:00) [$O_3$] was 46.3 ppb ppb in the ambient and 82.5 ppb in the elevated [$O_3$] plots (Betzelberger *et al.*, 2010). Elevated [$O_3$] was within 10% of the target concentration for 70% of the time.

*Physiological, Biochemical and Transcriptional Analyses*

Mature, sun leaves of soybean were assessed on 5 dates in 2007 throughout the growing season (Figure 4.1). At midday, photosynthetic gas exchange under growth conditions was measured on 3 plants per plot using open gas-exchange systems (LI-6400; LICOR Inc.) as described in (Leakey *et al.*, 2009b). Directly after the photosynthetic measurements, tissue was excised from 3-5 plants per plot for determination of chlorophyll, soluble carbohydrates, starch, protein and total amino acid content (Ainsworth *et al.*, 2007), total antioxidant capacity (Gillespie *et al.*, 2007), reduced and oxidized ascorbic acid content (Gillespie and Ainsworth, 2007), total phenolic content (Ainsworth and Gillespie, 2007), and activity of six enzymes involved in antioxidant recycling (Gillespie *et al.*, 2010). Simultaneously, 6 leaflets from separate plants were excised, immediately plunged into liquid nitrogen in the field, and stored at -80 °C until RNA was extracted for global transcript analysis using soybean genechips (Affymetrix). RNA extraction, hybridization and data processing were performed as described in (Leakey *et al.*, 2009b).

*Statistical Analysis*

Photosynthesis and stomatal conductance were tested with a randomized complete block mixed model ANOVA, using the Kenward-Rogers option (PROC MIXED, SAS 9.2; SAS Institute; Leakey *et al*., 2009b). In the model, $CO_2$, $O_3$ and time were fixed effects and block was a random effect. A *P* value <0.05 was the threshold for significance and each day was analyzed independently (Fig 4.1).

The ANOVA approach is limited because it considers [$O_3$] to be a fixed variable, when in fact, [$O_3$] is heterogeneous and varies in both ambient and elevated plots in each day of sampling (Fig. 4.1). Moreover, other environmental variables (including light, temperature and relative humidity; Fig. 4.1) have strong effects on plant metabolism, vary over the growing season and are highly correlated (Janes and Yaffe, 2006; Travers *et al.*, 2010; Fig. 4.2). Therefore, principle components analysis (PCA) was used to collapse 10 environmental variables into two principle components that accounted for 76% of the variability in the environment data (Table 4.1). The 10 environmental variables included: maximum daytime temperature ($T_{max}$), minimum nighttime temperature ($T_{min}$), maximum relative humidity ($RH_{max}$), Palmer Crop Moisture Index (PCMI), maximum photosynthetically daily active radiation ($PAR_{max}$), maximum 1 hr [$O_3$] averaged over 14 days prior to sampling (14 d 1 h Max [$O_3$]), 8 hr (10:00-18:00) average [$O_3$] for the 14 days prior to sampling (14d 8h Ave [$O_3$]), 14 d accumulated ozone over a threshold concentration of 40 ppb (14 d AOT40), 1 hr maximum [$O_3$] on the day of sampling (1 h Max [$O_3$]) and 8 hr average [$O_3$] on the day of sampling (8 h Ave [$O_3$]). Ozone metrics were chosen because leaf development data collected at SoyFACE suggested that the measured leaves were unfolded ~14 days prior to sampling. AOT40 was calculated according to (Mauzerall and Wang, 2001).

The five different metrics of [$O_3$] loaded heavily onto principle component 1 (PC1), while $T_{max}$, $RH_{max}$ and $PAR_{max}$ loaded heavily onto PC2. Negative values of PC1 correspond to low [$O_3$] while positive and high values correspond to high [$O_3$] (Fig. 4.3). The five sampling dates displayed a negative correlation between $RH_{max}$ and $PAR_{max}$ (Fig. 4.2), such that the least humid days were the brightest. Therefore, PC2 accounted for this relationship with higher and $PAR_{max}$ loading heavily on negative values and higher $RH_{max}$ and temperature loading heavily on the positive values (Table 4.1).

The PCA multivariate technique effectively explains and parses the day-to-day variability in field environmental conditions from the day-to-day variability of [$O_3$] into orthogonal principle components. These PC values were used in all subsequent analyses of biochemical parameters and transcript changes. Biochemical parameters and transcript levels were tested with a mixed model analysis of covariance (SAS 9.2). In all tests, $CO_2$ was treated as a fixed effect while PC1 and PC2 were treated as covariates. Because a single test does not have enough degrees of freedom to determine whether the slopes of the covariate models were different from zero or different between [$CO_2$] treatments, an equal slopes model was used to test for differences among the slopes between $CO_2$ treatments and an unequal slopes model was used to determine whether the individual slopes at both $CO_2$ concentrations were different from zero (Littel *et al.*, 2006). The slope of the regression line between the dependent variable and PC1 or PC2 at both levels of $CO_2$ was obtained from the solution for the unequal model outputs. A $P$-value < 0.05 was used to reject the hypothesis that the slopes at either ambient or elevated [$CO_2$] equaled zero. Using the equal slopes model, a $P$-value < 0.1 was used to reject the hypothesis that the slope at ambient [$CO_2$] equaled the slope at elevated [$CO_2$].

*Construction of the Soybean Annotation Database for MapMan*

To aid in the visualization of the microarray results, I developed a soybean annotation database for use with MAPMAN software (Thimm *et al.*, 2004). The database is publicly available through the MAPMAN website (http://mapman.gabipd.org/web/guest/mapmanstore), and was first used to visualize the response of field-grown soybean to elevated [$CO_2$] in the field (Leakey *et al.*, 2009b). To construct the annotation database, I obtained the FASTA file containing the target sequences for each probe-set on the Affymetrix *Glycine max* genechip. To fit these target sequences into the existing hierarchical categories (BINs) originally created in the MAPMAN visualization software for Arabidopsis, I constructed a database with the TAIR 7 release of the Arabidopsis proteome and used a BlastX search to identify the best matches for each *G.max* probe set target sequence. This resulted in 21,363 target sequences with acceptable matches (E value $<10^{-6}$). These matches were assigned to the appropriate MAPMAN BIN based on the best-matched Arabidopsis protein in the ‘‘Ath_AGI_TAIR7’’ mapping file (http://mapman.gabipd.org/web/guest/mapmanstore). To double check the assigned function of the *G. max* probesets and to assign function to the remaining unmatched probe-sets, I performed a second BlastX search against the National Center for Biotechnology Information non-redundant protein database. I parsed the resulting file to retrieve the top 5 hits (E value $<10^{-6}$) for each target sequence. If a match from *Glycine*, *Phaseolus*, *Medicago* or another legume was among the top 5 hits, that annotation was used in place of the match from the Arabidopsis database. To determine the BIN placement, the bean annotation was compared with the annotation derived from the Arabidopsis search, and if they matched, the original BIN was kept. If the annotations did not match (or there were no hits in the Arabidopsis proteome), the appropriate BIN was chosen based on biological function. This search resulted in annotation of 4,712 target sequences, 1,159 of which had no hit in the Arabidopsis proteome database.

## RESULTS

### *Photosynthesis and Stomatal Conductance*

Elevated [$O_3$] decreased diurnal photosynthetic carbon assimilation (*A*) by 9% on average across the growing season, although this decrease was largely driven by the 26% decrease in photosynthesis on the last sampling date, 31 Aug (Fig. 4.1). Elevated [$CO_2$] increased *A* by 15% compared to ambient [$CO_2$], and the magnitude of the response varied from 5% on 3 July to 23% on 17 Aug (Fig 4.1). Growth at elevated [$O_3$] decreased $g_s$ by 14% on average throughout the growing season. Again, this was due to a large decrease (46%) in $g_s$ towards the end of the growing season. Growth at elevated [$CO_2$] decreased $g_s$ by 26% consistently throughout the growing season, and the combination treatment was similar to the elevated [$CO_2$] alone (Fig. 4.1).

These physiological data clearly show that the effects of [$O_3$] accumulated over the growing season (Fig. 4.1), and the impacts of [$O_3$] on leaf-level processes are therefore caused by a combination of the immediate [$O_3$] and the cumulative $O_3$ dose. Additionally, the magnitude of the effect of elevated [$CO_2$] on soybean photosynthesis varied with environmental conditions (Fig. 4.1; Bernacchi *et al.*, 2006). Therefore, to more appropriately characterize the $O_3$ treatment and the environmental variation, principle components analysis (PCA) was used to condense correlated $O_3$ metrics and environmental variables (Fig. 4.2) into two dimensions (PC1 and PC2; Table 4.1). PC1 and PC2 accounted for 50.4% and 26.2% of the variability in ten environmental variables (Table 4.1).

*Antioxidant Metabolism and Gene Expression*

Total antioxidant capacity was significantly lower in plants grown at elevated [$CO_2$] compared to ambient [$CO_2$] (Table 4.2), and positively correlated with PC1 at ambient [$CO_2$], indicating that total antioxidant capacity increased with increasing [$O_3$] (Fig. 4.4; Table 4.3). There was a marginally significantly correlation between total antioxidant capacity and PC1 at elevated [$CO_2$] (Fig. 4.4; Table 4.3). Ascorbate content was also positively correlated with PC1 at ambient [$CO_2$], but not in elevated [$CO_2$] (Table 4.3). MDHAR and SOD activity was lower in plants grown at elevated [$CO_2$] (Table 4.2). The only antioxidant enzyme that was significantly correlated with PC1 was CAT, which showed a negative correlation with PC1 in both ambient and elevated [$CO_2$] (Table 4.3).

A significantly larger fraction of genes involved in antioxidant metabolism were correlated with PC1 at ambient [$CO_2$] (19%) compared to the average response of all transcripts (14%; p=0.0375, 1-tailed fisher's exact test; Fig. 4.5). At elevated [$CO_2$], a larger fraction of antioxidant metabolism genes were also correlated with PC1 (18%) compared to the average response of all transcripts (11%; p=0.0012, 1-tailed fisher's exact test; Fig. 4.5). Moreover, 46 of the 56 genes that were significantly correlated with PC1 at ambient [$CO_2$] and 44 of the 52 genes that were significantly correlated with PC1 at elevated [$CO_2$] had a positive relationship, indicating higher transcript abundance at elevated [$O_3$]. More specifically, the majority of the genes coding for different isoforms of the antioxidant recycling enzymes were positively correlated with PC1 in plants grown at ambient and elevated [$CO_2$] (Fig. 4.6 and 4.7 respectively; Table 4.4), despite the lack of coordinated changes in enzyme activity. However, there was no significant correlation between PC1 and transcripts coding for CAT, which was the only enzyme that displayed a significant negative correlation with PC1 at both ambient and elevated [$CO_2$] (Fig. 4.6 & 4.7). Three genes coding for chloroplast localized Fe-SOD were negatively correlated with PC1 at

ambient [$CO_2$]. However, genes coding for chloroplastic and cytosolic Cu-Zn SOD were positively correlated with PC1 as was a SOD copper chaperone (Fig. 4.6). This trend is consistent at elevated [$CO_2$] with two transcripts coding for Fe-SOD negatively correlated with PC1, and three transcripts for Cu-Zn SOD positively correlated with PC1 (Fig 4.7).

This analysis also effectively parsed the effects of [$O_3$] from the effects of the other environmental factors that alter antioxidant metabolism. The activity levels of four antioxidant enzymes were more responsive to PC2 than PC1. SOD and GR activity were negatively correlated with PC2, while CAT and DHAR activity were positively correlated with PC2 (Table 4.3). In addition, a significantly larger portion of genes associated with redox metabolism were affected by PC2 (55% at ambient [$CO_2$] and 48% at elevated [$CO_2$]) compared to the average response of transcripts with other functions (38% at ambient [$CO_2$] and 35% at elevated [$CO_2$]; $p<0.0001$, 1-tailed Fisher's exact test; Fig. 4.8).

*Tetrapyrrole Synthesis Gene Expression and Chlorophyll Content*

A number of other functional categories were significantly over-represented when compared to the total population of transcripts changing with PC1 at both ambient [$CO_2$] and elevated [$CO_2$] (Fig. 4.5). The functional category that had the largest percentage of genes changing consistently with PC1 at ambient and elevated [$CO_2$] was tetrapyrrole synthesis. In ambient [$CO_2$], a significantly larger portion of tetrapyrrole synthesis genes were correlated with PC1 (57%) compared to the portion of genes responding that correspond to other functional categories (14%; $p <0.0001$, 1-tailed fisher's exact test; Fig 4.5). At elevated [$CO_2$], a significantly larger portion of 37% of tetrapyrrole synthesis genes were correlated with PC1 (37%) compared to the response of genes corresponding to other functions (11%; $p<0.0001$, 1-tailed fisher's exact test; Fig. 4.5).

Specifically, multiple genes encoding isoforms of the three key regulatory enzymes in chlorophyll biosynthesis were positively correlated with PC1 at both ambient and elevated [$CO_2$]. These three steps were: 1) the activation of glutamate by glutamyl tRNA synthetase; 2) the conversion of glutamate-1-semialdehyde (GSA) to 5-aminolevulinic acid (ALA) by GSA aminotransferase; and 3) the first step in the chlorophyll branch which consists of an ATP dependent insertion of $Mg^{2+}$ into protoporphyrin IX by magnesium chelatase (Fig 4.9 & 4.10; Tanaka and Tanaka, 2007). Chlorophyll content showed no relationship with PC1 at ambient or elevated [$CO_2$] (Table 4.3); however, the coordinated positive correlation of the genes involved in chlorophyll synthesis suggests that chlorophyll turnover may have been accelerated by elevated [$O_3$].

*Respiration Gene Expression and Carbohydrate Content*

Functional bins related to respiration had consistently larger percentages of genes correlated with PC1, including TCA metabolism (33% compared to 14% at ambient $CO_2$, $p<0.0001$ and 19% compared to 11% at elevated $CO_2$, $p=0.0356$, 1-tailed fisher's exact test; Fig. 4.5) and mitochondrial electron transport (38% compared to 14% at ambient $CO_2$, $p<0.0001$ and 34% compared to 11% at elevated $CO_2$, $p<0.0001$, 1-tailed fisher's exact test; Fig. 4.5). The vast majority of transcripts associated with TCA metabolism and mitochondrial electron transport displayed a positive correlation with PC1 (Table 4.4), indicating up-regulation at higher [$O_3$]. The gene coding for PEPCase, which carboxylates PEP to pyruvate, was positively correlated with PC1 at both ambient and elevated [$CO_2$] (Figs 4.11 & 4.12). Glucose, fructose, sucrose, starch, and amino acid content were all increased due to growth at elevated [$CO_2$] (Table 4.2),

but only sucrose content was positively correlated with PC1 and protein content negatively correlated with PC1 at both ambient and elevated [$CO_2$] (Table 4.3).

## DISCUSSION

The response of field grown soybean to elevated [$O_3$] at ambient and elevated [$CO_2$] was investigated in this study by combining genomic, biochemical and physiological analyses across the 2007 growing season. Sampling over an entire growing season and combining datasets across biological levels allows for the discovery of key mechanisms that drive the plant physiological responses to climate change (Stitt *et al.*, 2010). However, each sampling date had a unique set of environmental conditions that influenced the parameters being measured (Fig. 4.1). This variability in the environment is important and has been shown to alter the genomic (Miyazaki *et al.*, 2004) and physiological (Bernacchi *et al.*, 2006) response of plants to climate change treatments, but it also complicates the ability to identify common responses caused by the treatments of interest (Travers *et al.*, 2010). Two statistical techniques were used to partition the environmental variation and test changes that were dependent on the climate change treatments. PCA, a multivariate statistical technique, collapses co-varying values into a smaller number of 'super variables' that capture the maximal co-variation (Janes and Yaffe, 2006). In this study, PCA collapsed 10 co-varying environmental conditions into two orthogonal principle components that separated the variability in [$O_3$] from the variability in light, temperature and relative humidity (Table 4.2). Analysis of co-variance was subsequently used to model the effects of the continuous variables PC1 and PC2, and how they would alter the response to the fixed [$CO_2$] treatment (Littel *et al.*, 2006). This approach has provided a means to explain the

effects of [$O_3$] within each $CO_2$ environment, while accounting for the variability in other environmental factors.

An excellent example of a metabolic system that is known to be highly responsive to a variety of environmental variables, including [$O_3$], is antioxidant metabolism (Foyer and Noctor, 2005). Growth at elevated [$CO_2$] led to a generally lower antioxidant metabolism, which was manifested through lower total antioxidant capacity and DHA content, as well as lower total enzyme activity of SOD and MDHAR (Table 4.2). This is consistent with the results from Chapter 3 and previous studies of a number of species including soybean (Badiani *et al.*, 1993; Gillespie *et al.*, 2010), *Picea albies* (Polle *et al.*, 1993), *Citrus aurantium* (Schwanz *et al.*, 1996), and *Fagus sylvatica* (Polle *et al.*, 1997). However, there was no coordinated down-regulation of transcripts that code for the enzymes in the antioxidant recycling system at elevated [$CO_2$], suggesting a role for post-transcriptional regulation of the enzymes, which is also consistent with the results reported in Chapter 3 and other research (Dutilleul *et al.*, 2003). Growth at increasing levels of [$O_3$], as explained by PC1, was positively correlated with total antioxidant capacity, ASA content and the majority of genes coding for enzymes in the antioxidant recycling system (Figs 4.4, 4.6 & 4.7; Tables 4.3 & 4.4). This result was consistent regardless of $CO_2$ environment and supports a number of previous reports that elevated [$O_3$] increases antioxidant metabolism (Fiscus *et al.*, 2005; Heath, 2008). However, there were no correlations between PC1 and any of the maximum activity levels of any antioxidant enzyme (Table 4.3), suggesting that enzyme turnover may have been faster in elevated [$O_3$], but activity was supported by higher transcript abundance. There was also a negative correlation between PC1 and total protein content (Table 4.3). Cho *et al.*, (2008) reported higher levels of protein mis-folding and fragmentation in $O_3$-treated rice seedlings, which supports the conclusion of higher levels of protein turnover with increasing

[$O_3$]. We found the direction of the response of the antioxidant system to increasing [$O_3$] in either $CO_2$ environment to be similar. However, our results demonstrate that the slope of the line between total antioxidant capacity and PC1 was significant at ambient [$CO_2$] (Fig 4.4) and the overall transcriptional response to PC1 was greater at ambient [$CO_2$] than elevated [$CO_2$] (Fig 4.13), indicating a dampened response to increasing [$O_3$] at elevated [$CO_2$]. Together these results suggest that soybean responded to increasing [$O_3$] in a similar manner regardless of [$CO_2$] environment, and the dampened response at elevated [$CO_2$] may be explained by lower flux of [$O_3$] into the leaf (Fiscus *et al.*, 1997; Karnosky *et al.*, 2003; McKee *et al.*, 1995; Paoletti and Grulke, 2005; Vapaavuori *et al.*, 2009)

The results also suggest that some components of the antioxidant system responded to [$O_3$] while others responded to other environmental variables. Total antioxidant capacity and antioxidant metabolite pools (ASA) correlated with PC1, while the total activities of many antioxidant enzymes correlated with PC2 (Table 4.2). Previous research on a tobacco mutant with impaired respiratory metabolism also showed that maintenance of antioxidant metabolites was uncoupled from changes in enzyme activity (Dutilleul *et al.*, 2003). Thus, both environmental stress and genetic mutations can induce re-orchestration of the cellular antioxidant system. The negative correlation between SOD and GR and PC2 indicated that activity of these enzymes increased with higher $PAR_{max,}$ which is consistent with a strong correlation between light intensity and activity of antioxidant enzymes, namely SOD, reported for a number of plant species (Logan, 2006). The positive correlation of CAT with PC2 suggested that CAT activity was lower in high light, which is consistent with understanding that CAT is light sensitive (Schmidt *et al.*, 2002) and CAT turnover rates increase at higher photon flux densities (Hertwig *et al.*, 1992).

In addition to increases in antioxidant metabolism with higher [$O_3$], the gene expression results imply a coordinated up-regulation of tetrapyrrole synthesis in both ambient and elevated [$CO_2$] (Figs 4.9 & 4.10). While up regulation of senescence-associated genes and accelerated leaf senescence at elevated [$O_3$] has been widely reported in the literature (Gupta *et al.*, 2005; Heath, 2008; Kontunen-Soppela *et al.*, 2010; Miller *et al.*, 1999), coordinated changes in genes involved in chlorophyll biosynthesis have not been widely reported. An increase in chlorophyll content was not matched to the observed increases in abundance of genes involved in tetrapyrrole synthesis (Table 4.3). Therefore, the results suggest a possible increase in chlorophyll turnover in relatively young leaves exposed to elevated [$O_3$]. Leaf senescence is commonly characterized by chlorophyll degradation (Woo *et al.*, 2004; Zimmermann and Zentgraf, 2005), and this study did not investigate any of those products nor find a correlation between [$O_3$] and the genes coding for enzymes in the chlorophyll degradation pathway. Still, the coordinated up-regulation of transcripts at control points of chlorophyll biosynthesis (Fig. 4.9 & 4.10; Tanaka and Tanaka, 2007) is compelling and warrants further investigation.

The increase in antioxidant metabolism and chlorophyll synthesis with increasing [$O_3$] is energetically expensive and a corresponding coordinated up regulation of genes involved in mitochondrial respiration was observed (Fig 4.11 & 4.12; Table 4.4). This transcriptional evidence is consistent with previous research measuring higher respiration rates in plants exposed to elevated [$O_3$] (Amthor, 1988; Amthor and Cumming, 1988; Biswas *et al.*, 2008; Kellomaki and Wang, 1998; Skarby *et al.*, 1987; Volin and Reich, 1996). In addition, we measured higher transcript levels for PEPcase at increasing [$O_3$] in both ambient and elevated [$CO_2$] (Fig 4.11 & 4.12; Table 4.4). Up-regulation of PEPcase activity and content at elevated [$O_3$] has been suggested as a key metabolic shift for increasing reducing power for antioxidant

metabolism (Dizengremel *et al.*, 2008). Previous research at SoyFACE has demonstrated that growth at elevated [$CO_2$] also increased respiration rates and altered the abundance of transcripts encoding enzymes throughout the respiratory pathway (Leakey *et al.*, 2009b). As in Leakey et al., (2009b), our results showed that growth at elevated [$CO_2$] increased soluble carbohydrate and starch pools, which would fuel increased respiration. Yet even at elevated [$CO_2$], respiration increased with higher [$O_3$] suggesting that both the excess C availability and the increased demand for antioxidant metabolism was driving higher rates of respiration in the combination of climate change factors.

In conclusion, this study examined field-grown soybean exposed to elevated [$O_3$], elevated [$CO_2$], and the combination of both elevated [$CO_2$] and elevated [$O_3$] to test the hypothesis that soybean antioxidant metabolism is up regulated at high [$O_3$], requiring increased respiratory metabolism to fuel the higher energy demands, and that the response will be dampened by growth at elevated [$CO_2$]. This worked largely confirmed this hypothesis and also established that some components of antioxidant metabolism were more sensitive to changes in the light, temperature and relative humidity than to [$O_3$]. Genes involved in tetrapyrrole synthesis also increased with higher [$O_3$], which provided evidence for accelerated chlorophyll turnover in elevated [$O_3$]. Finally, the transcriptional evidence suggested that greater antioxidant and chlorophyll metabolism at elevated [$O_3$] was supported by increased respiratory metabolism.

FIGURES AND TABLES

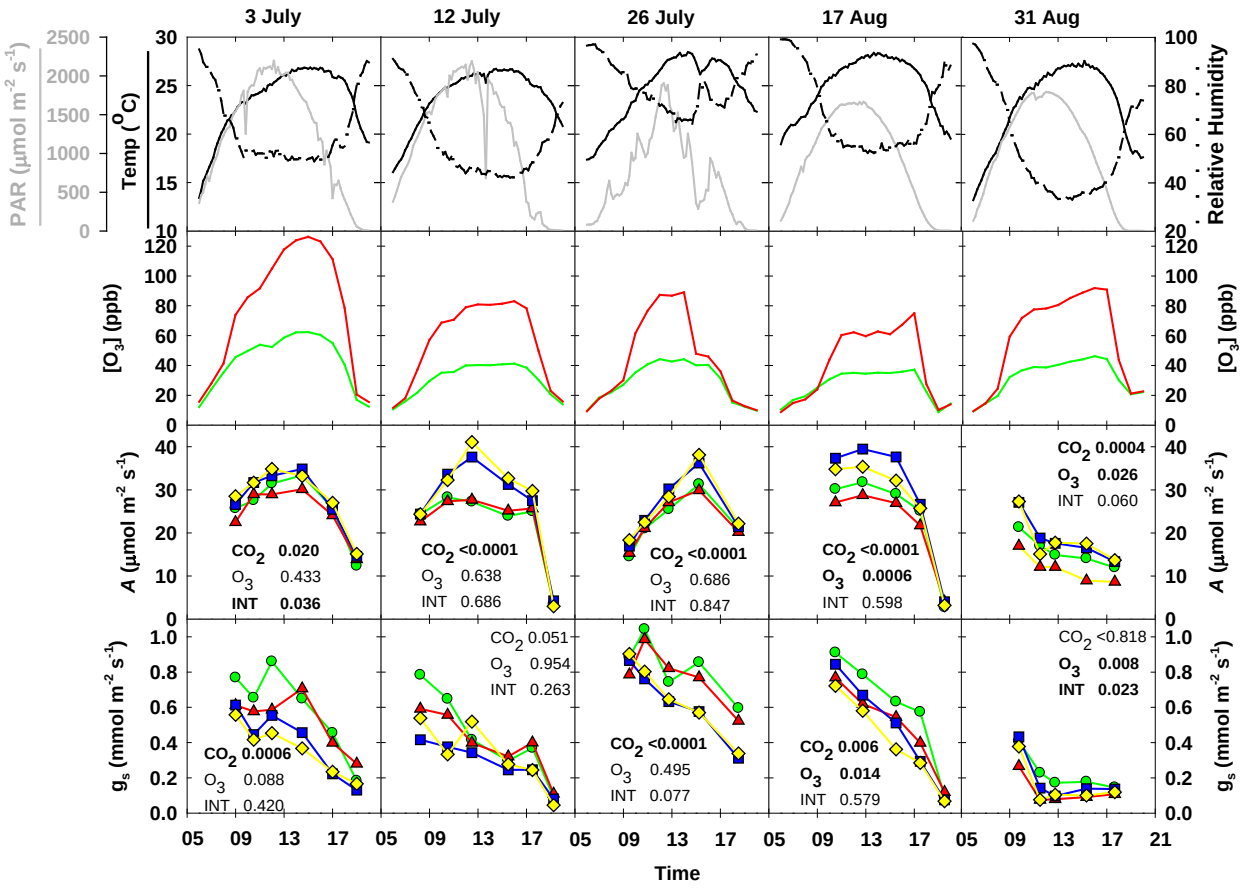


**Figure 4.1. Diurnal trends in photosynthetically active radiation (PAR), air temperature (Temp), relative humidity, hourly [$O_3$] in ambient air (green line) and elevated (red line) [$O_3$] treatments, photosynthesis (*A*) and stomatal conductance ($g_s$) measured on five days in 2007 at the SoyFACE experiment.** *A* and $g_s$ were collected on the most recently fully expanded soybean leaf at the top of the canopy. Growth conditions were ambient [$CO_2$] and [$O_3$] (green cirlces), elevated [$O_3$] (red triangles), elevated [$CO_2$] (blue sqares) and elevated [$CO_2$] and elevated [$O_3$] (yellow diamonds). Each point is the mean of the replicate plots (n=4) at that time. *P* values indicate statistical significance of $CO_2$, $O_3$, and $CO_2$ x $O_3$ interaction (INT) effects.

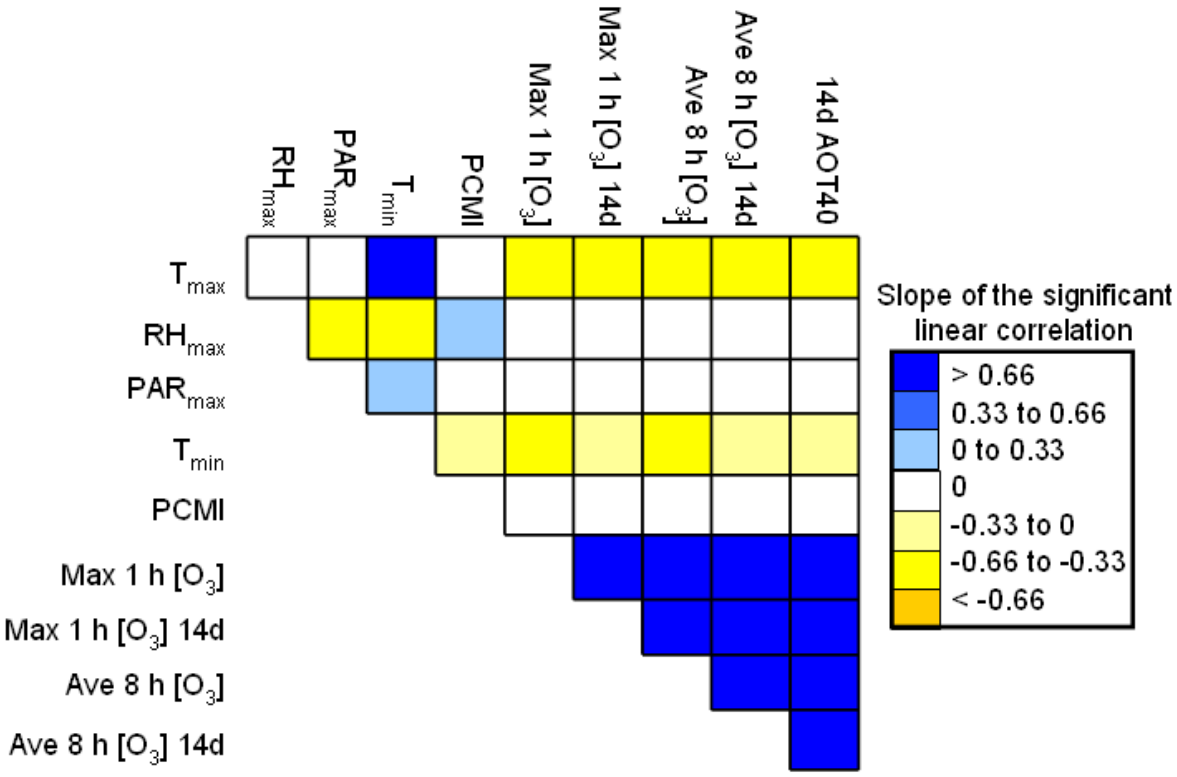


**Figure 4.2. Pearson Correlations between pairs of environmental variables.** Maximum temperature during daylight hours ($T_{max}$), maximum relative humidity during daylight hours ($RH_{max}$), maximum daily photosynthetically active radiation ($PAR_{max}$), minimum temperature during the night preceeding a sampling day ($T_{min}$), Palmer's Crop Moisture Index (PCMI), the 1 h maximum [$O_3$] during daylight hours (Max 1 h [$O_3$]), the average of the maximum 1 h [$O_3$] for the preceding 14 d before a sampling date (Max 1 h [$O_3$] 14d), the average 8 h [$O_3$] on the sampling date (Ave 8 h [$O_3$]), the average of the 8 h averages recorded for the preceding 14 d before a sampling date (Ave 8 h [$O_3$] 14d), and the accumulated dose of $O_3$ over a threshold of 40ppb for the preceding 14 d (14d AOT40). Significant correlations with a p-value less than 0.05 are displayed.

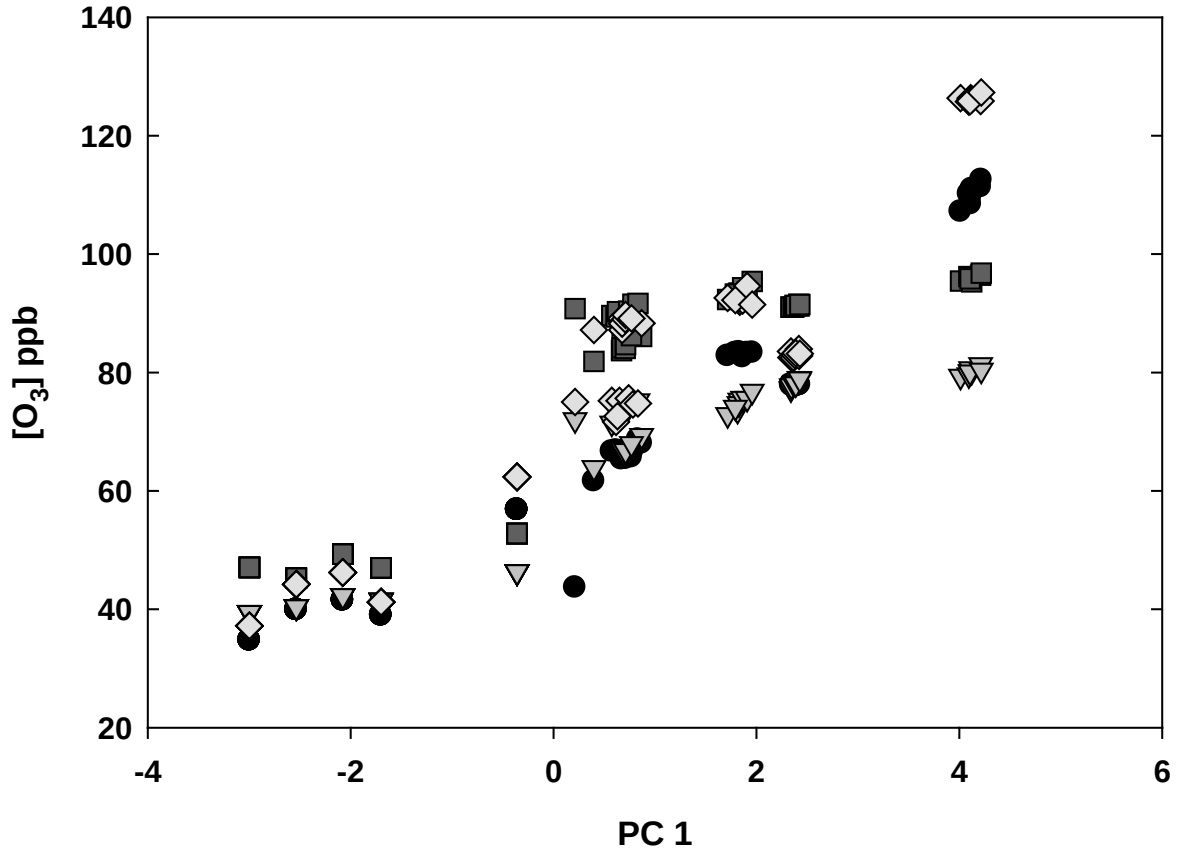


**Figure 4.3. Plot of four different measures of [$O_3$] against PC1.** The measures of [$O_3$] include: ave 8 h [$O_3$] (circles), ave 8 h [$O_3$] 14d (triangles), max 1 h [$O_3$] (squares), max 1 h [$O_3$] 14d (diamonds). PC1 accurately accounts for the variability in [$O_3$] across the 5 sampling dates, dealing with the larger variability in the measures of the highest [$O_3$] remarkably well.

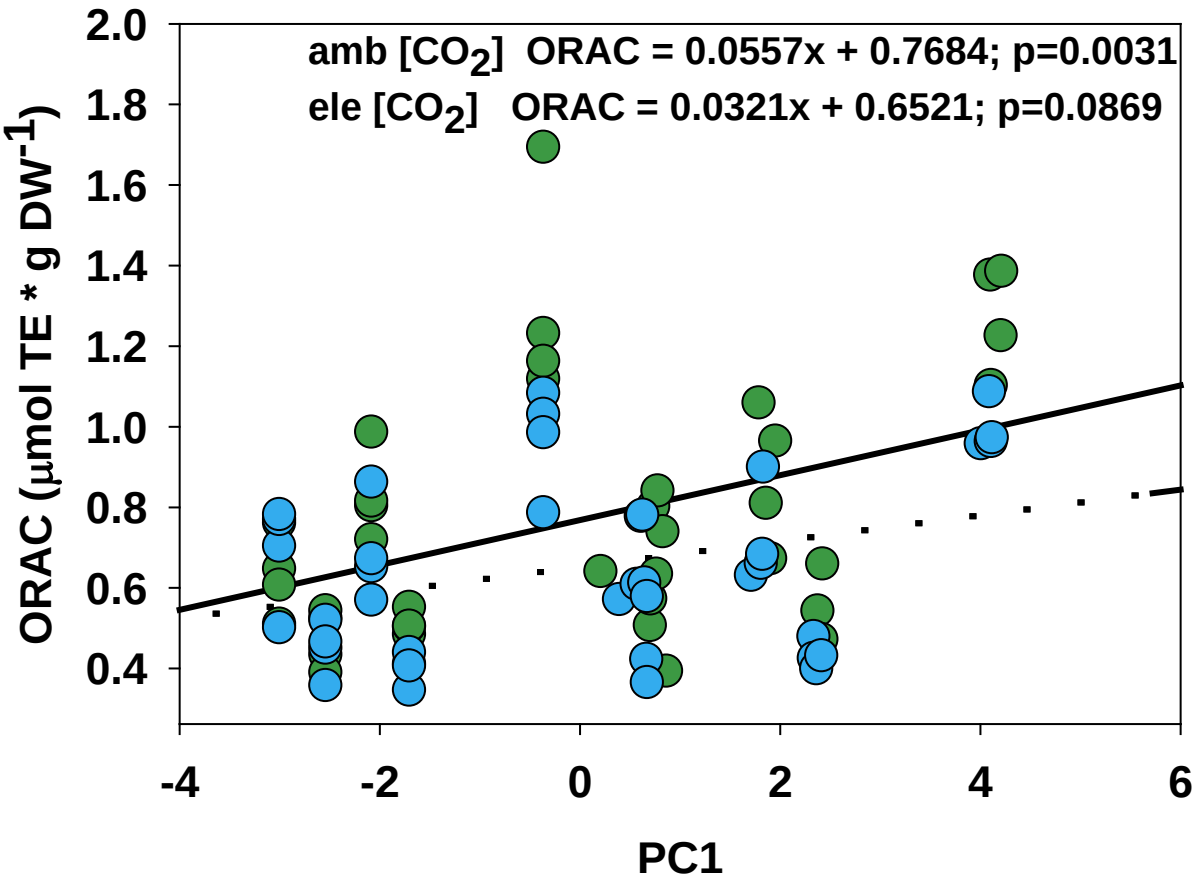


**Figure 4.4. Total Antioxidant Capacity as affected by PC1 ([$O_3$]).** The green circles depict the measurements recorded at ambient [$CO_2$] with the resulting linear regression (solid line). The blue circles depict the measurements taken at elevated [$CO_2$] with the resulting linear regression (dashed line). The slope of the regression line between ORAC and PC1 at ambient [$CO_2$] is significantly different from zero (p = 0.0031), while the regression between ORAC and PC1 at elevated [$CO_2$] is marginally significant (p=0.0869). However, the slopes of the two lines are not significantly different from each other (p=0.3633).

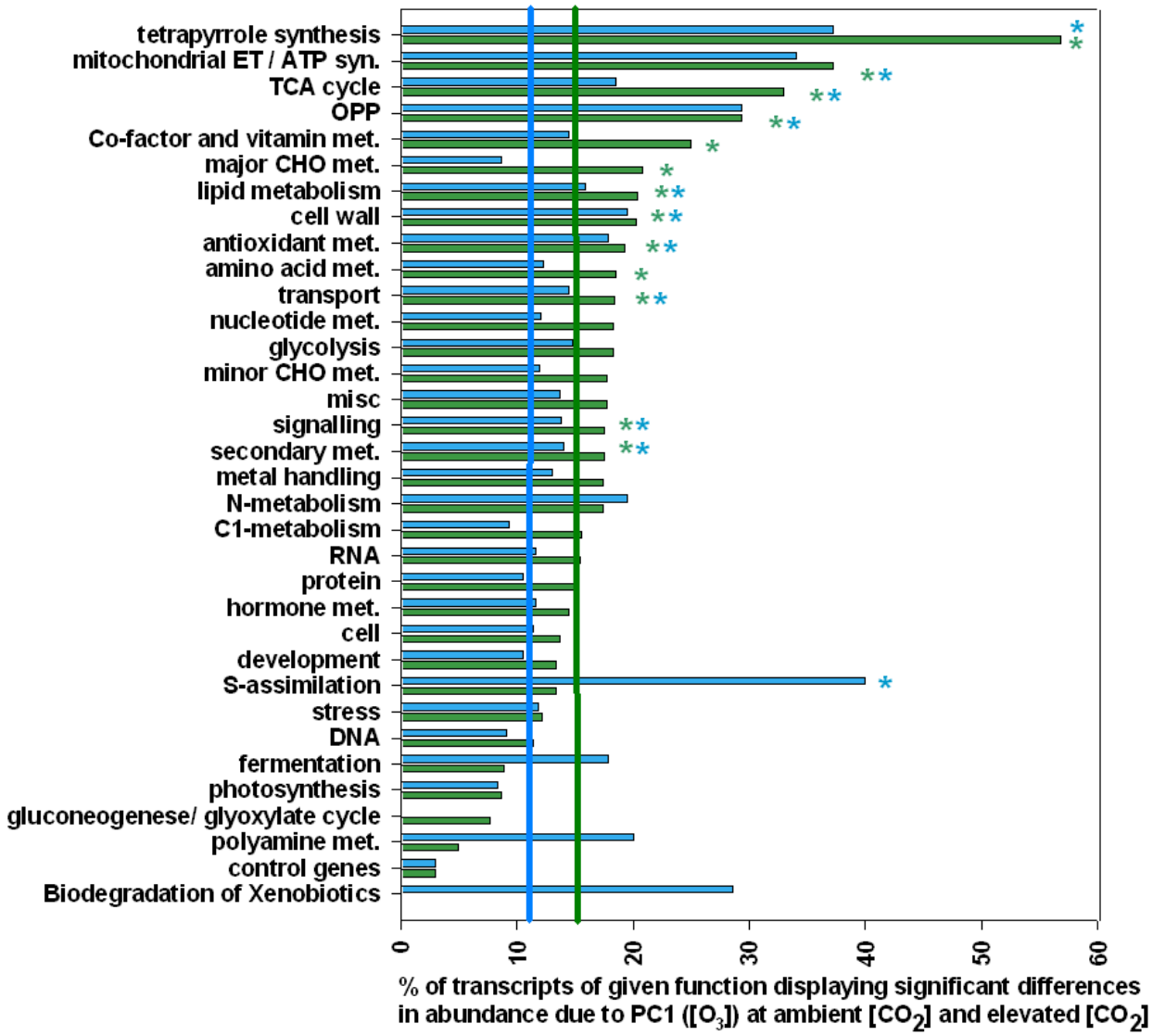


**Figure 4.5. Percentage of transcripts in each of 33 functional groups from MapMan software that displayed significant differences in abundance due to principle component 1 (PC1) in ambient [$CO_2$] (green bars) and elevated [$CO_2$] (blue bars).** The vertical blue line shows that 11% of all of the transcripts tested responded significantly to PC1 in the elevated [$CO_2$] treatment and the vertical green line shows that 15% responded significantly in ambient [$CO_2$]. Functional categories with significantly more genes responding than average were tested with the Fisher's exact test and are indicated with an asterisk.

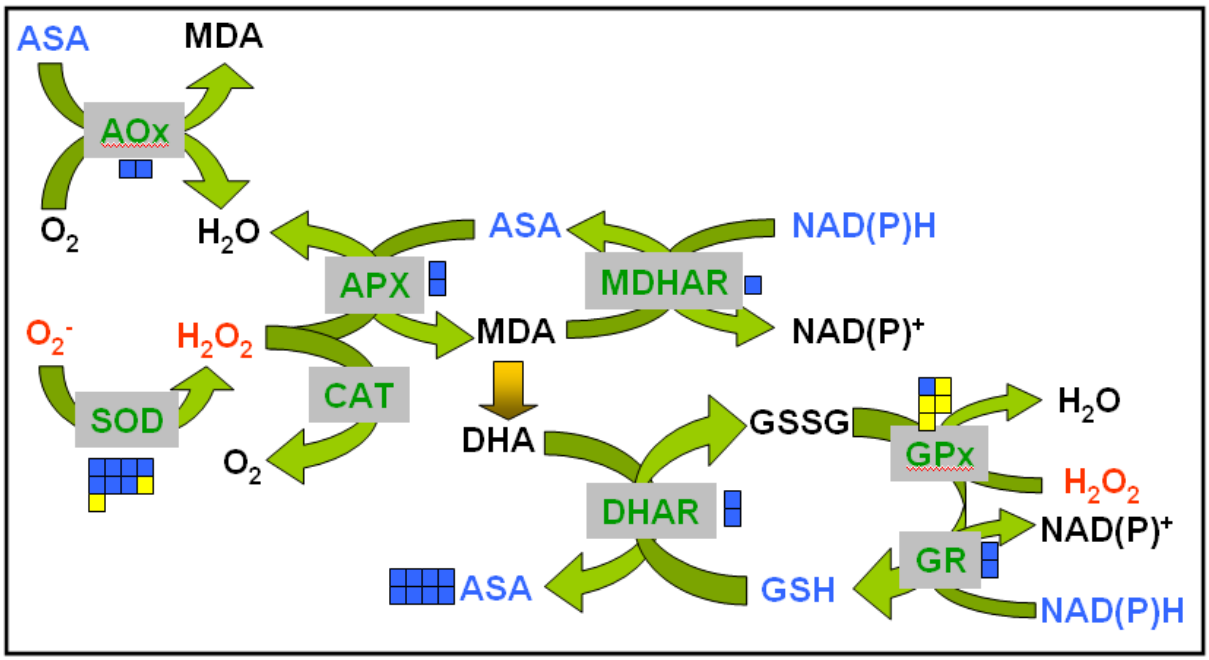


**Figure 4.6. Transcripts coding for antioxidant recycling components significantly affected by PC1 at ambient [$CO_2$].** Blue boxes denote a significant positive correlation between transcript abundance and PC1. Yellow boxes denote a significant negative correlation between transcript abundance and PC1. ROS (red text) react with metabolic antioxidant pools (blue text) such as ascorbic acid (ASA) and glutathione (GSH) or they can be enzymatically reduced (grey boxes). Superoxide dismutase (SOD) converts superoxide to hydrogen peroxide, which is then reduced via catalase (CAT) or ascorbate peroxidase (APX), which oxidizes one molecule of reduced ascorbate (ASA) to monodehydroascorbate (MDA). MDA can be re-reduced via monodehydroascorbate reductase (MDHAR) utilizing NADPH, or it will spontaneously convert to dehydroascorbate (DHA). DHA is re-reduced ASA via dehydroascorbate reductase (DHAR), which oxidizes one molecule of glutathione (GSH). Oxidized glutathione (GSSG) can be re-reduced via glutathione reductase (GR) utilizing NADPH.

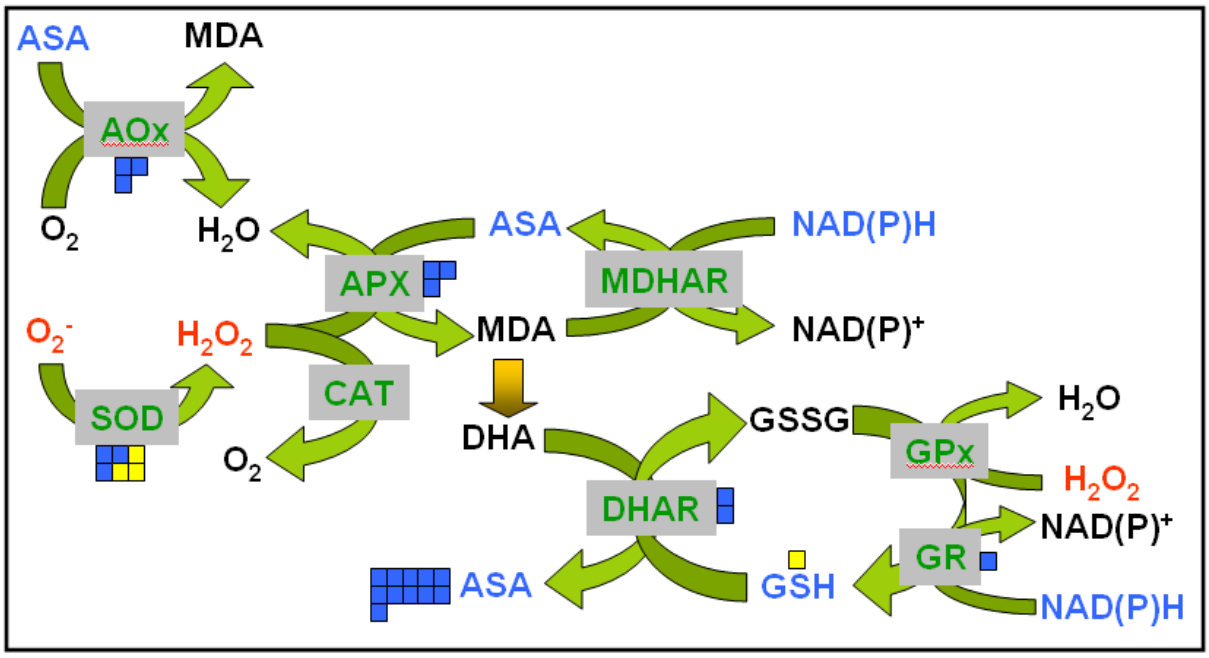


**Figure 4.7. Transcripts coding for antioxidant recycling components significantly affected by PC1 at elevated [$CO_2$].** Blue boxes denote a significant positive correlation between transcript abundance and PC1. Yellow boxes denote a significant negative correlation between transcript abundance and PC1. ROS (red text) react with metabolic antioxidant pools (blue text) such as ascorbic acid (ASA) and glutathione (GSH) or they can be enzymatically reduced (grey boxes). Superoxide dismutase (SOD) converts superoxide to hydrogen peroxide, which is then reduced via catalase (CAT) or ascorbate peroxidase (APX), which oxidizes one molecule of reduced ascorbate (ASA) to monodehydroascorbate (MDA). MDA can be re-reduced via monodehydroascorbate reductase (MDHAR) utilizing NADPH, or it will spontaneously convert to dehydroascorbate (DHA). DHA is re-reduced ASA via dehydroascorbate reductase (DHAR), which oxidizes one molecule of glutathione (GSH). Oxidized glutathione (GSSG) can be re-reduced via glutathione reductase (GR) utilizing NADPH.

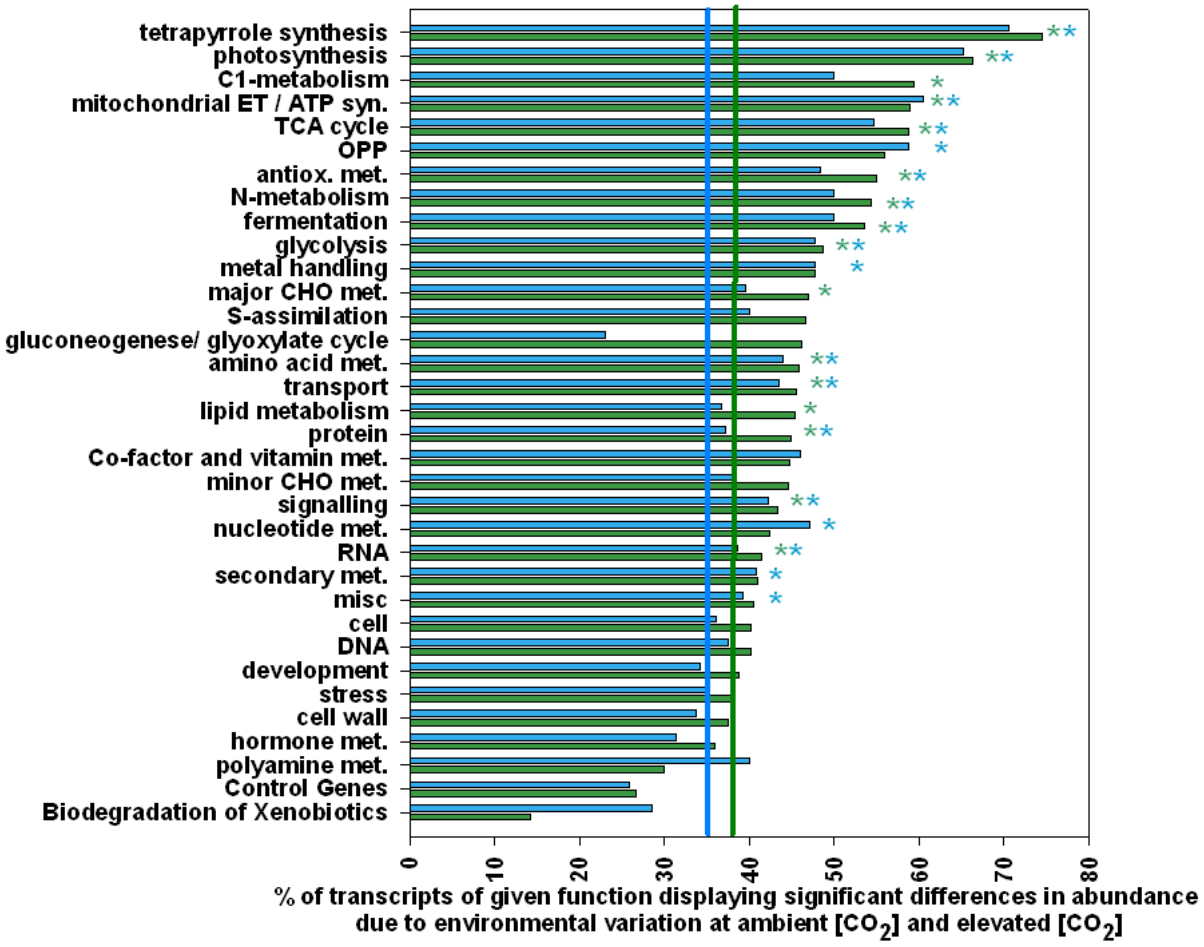


**Figure 4.8**. **Percentage of transcripts in each of 33 functional groups from MapMan software that displayed significant average differences in abundance due to principle component 2 (PC2) in ambient [$CO_2$] (green bars) and elevated [$CO_2$] (blue bars).** The vertical blue line shows that 35% of all of the transcripts tested responded significantly to PC2 in the elevated [$CO_2$] treatment and the verticalgreen line shows that 38% responded significantly in ambient [$CO_2$].

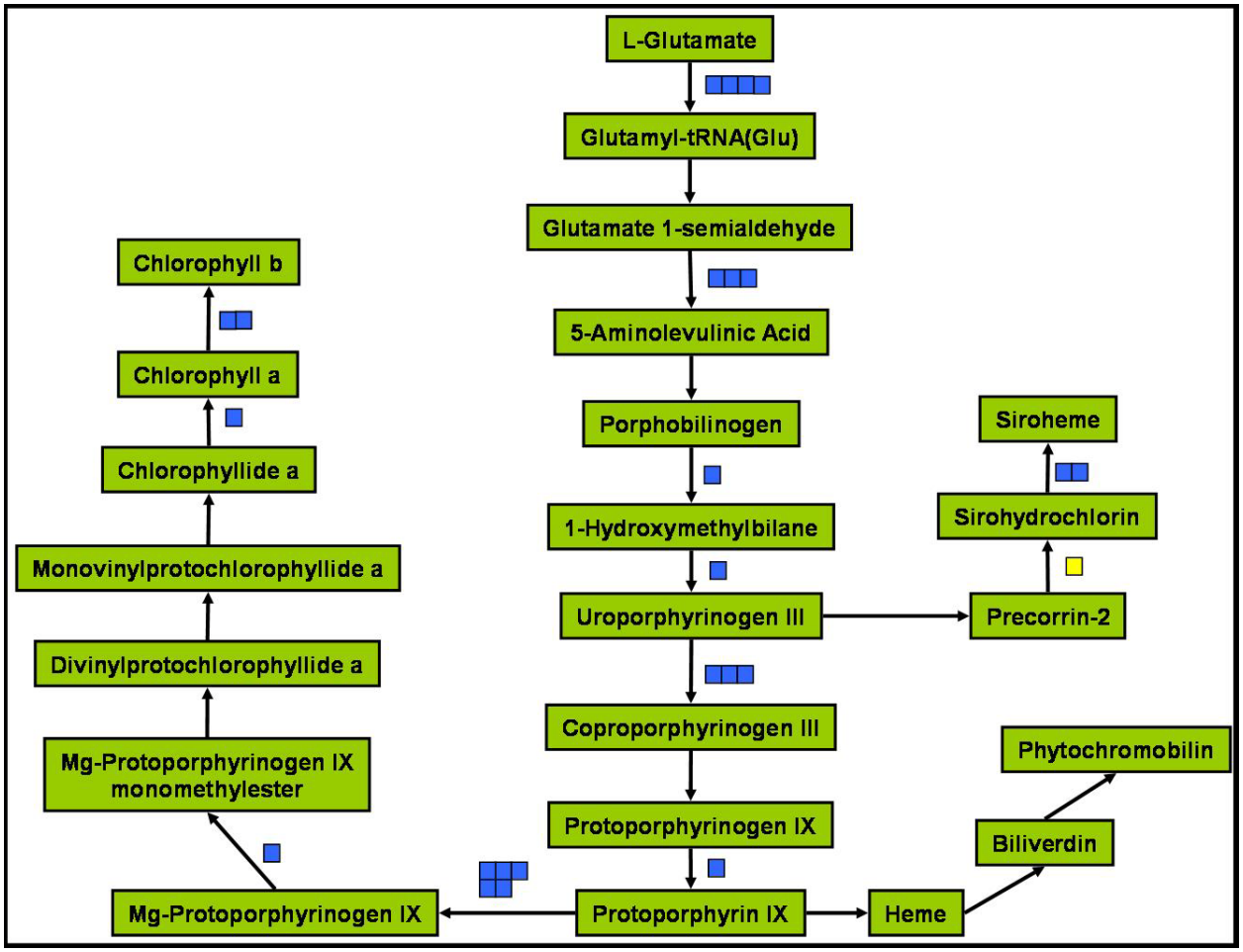


**Figure 4.9. Transcripts coding for components of tetrapyrrole synthesis significantly affected by PC1 at ambient [$CO_2$].** Blue boxes denote a significant positive correlation between transcript abundance and PC1. Yellow boxes denote a significant negative correlation between transcript abundance and PC1. Three key regulatory steps in this pathway are: 1) the activation of glutamate by Glutamyl tRNA synthetase; 2) the conversion of glutamate-1-smialdehyde to 5-aminolevulinic acid (ALA) by GSA aminotransferase; and 3) an ATP dependent insertion of $Mg^{2+}$ into protoporphyrin IX by magnesium chelatase (Tanaka and Tanaka, 2007).

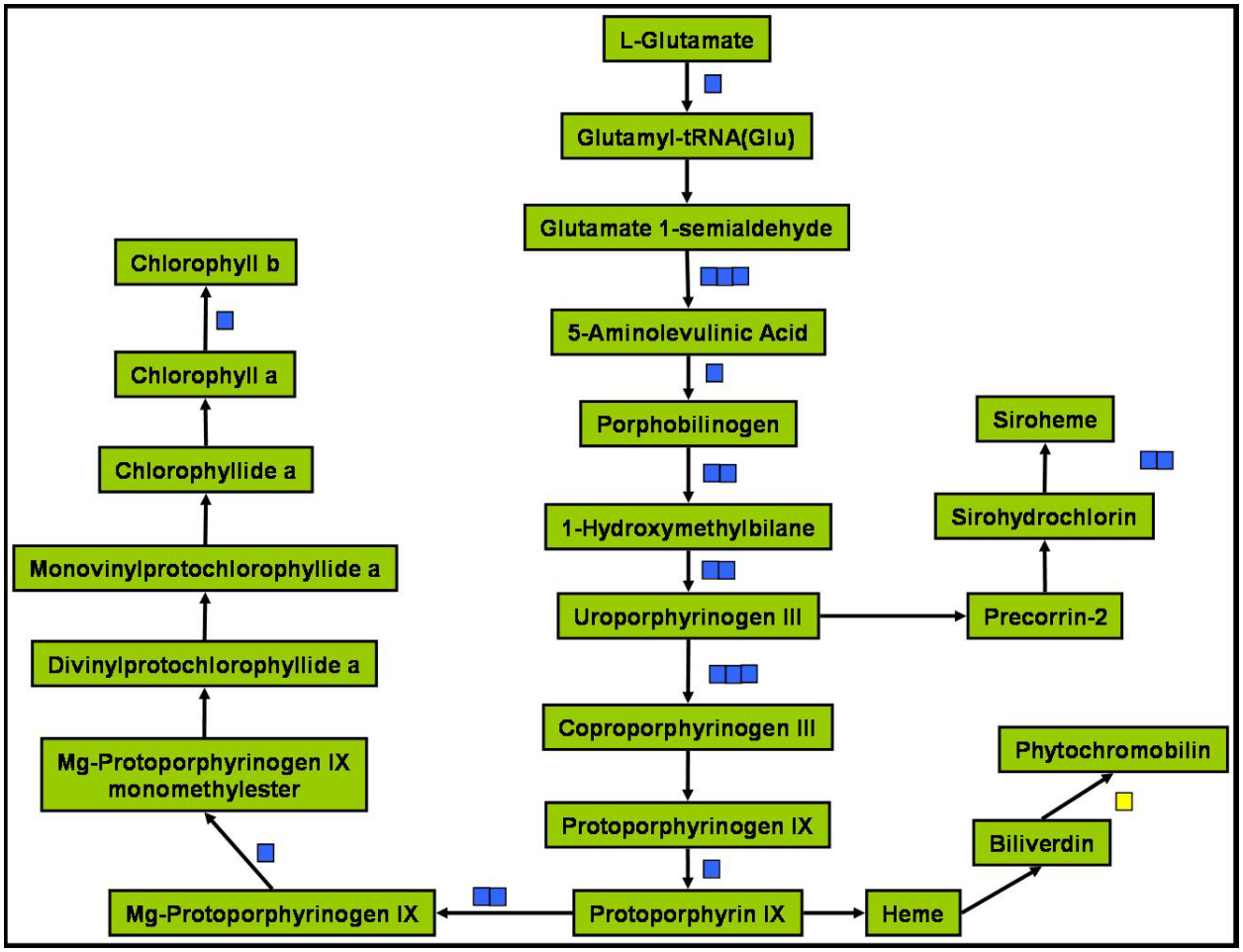


**Figure 4.10. Transcripts coding for components of tetrapyrrole synthesis significantly affected by PC1 at elevated [$CO_2$].** Blue boxes denote a significant positive correlation between transcript abundance and PC1. Yellow boxes denote a significant negative correlation between transcript abundance and PC1. Three key regulatory steps in this pathway are: 1) the activation of glutamate by Glutamyl tRNA synthetase; 2) the conversion of glutamate-1-smialdehyde to 5-aminolevulinic acid (ALA) by GSA aminotransferase; and 3) an ATP dependent insertion of $Mg^{2+}$ into protoporphyrin IX by magnesium chelatase (Tanaka and Tanaka, 2007).

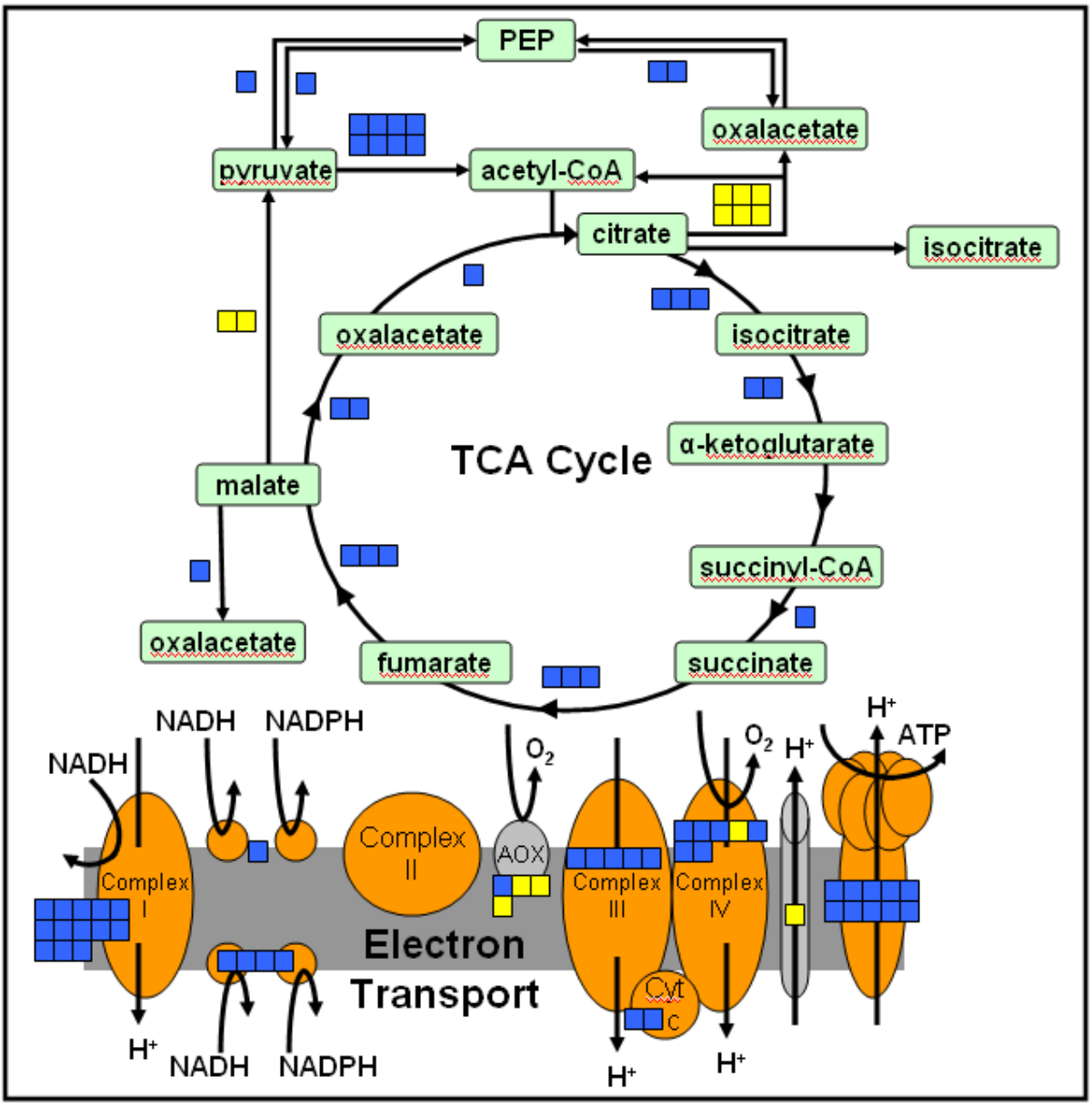


**Figure 4.11. Transcripts coding for components of the TCA cycle and mitochondrial electron transport significantly affected by PC1 at ambient [$CO_2$].** Blue boxes denote a significant positive correlation between transcript abundance and PC1. Yellow boxes denote a significant negative correlation between transcript abundance and PC1.

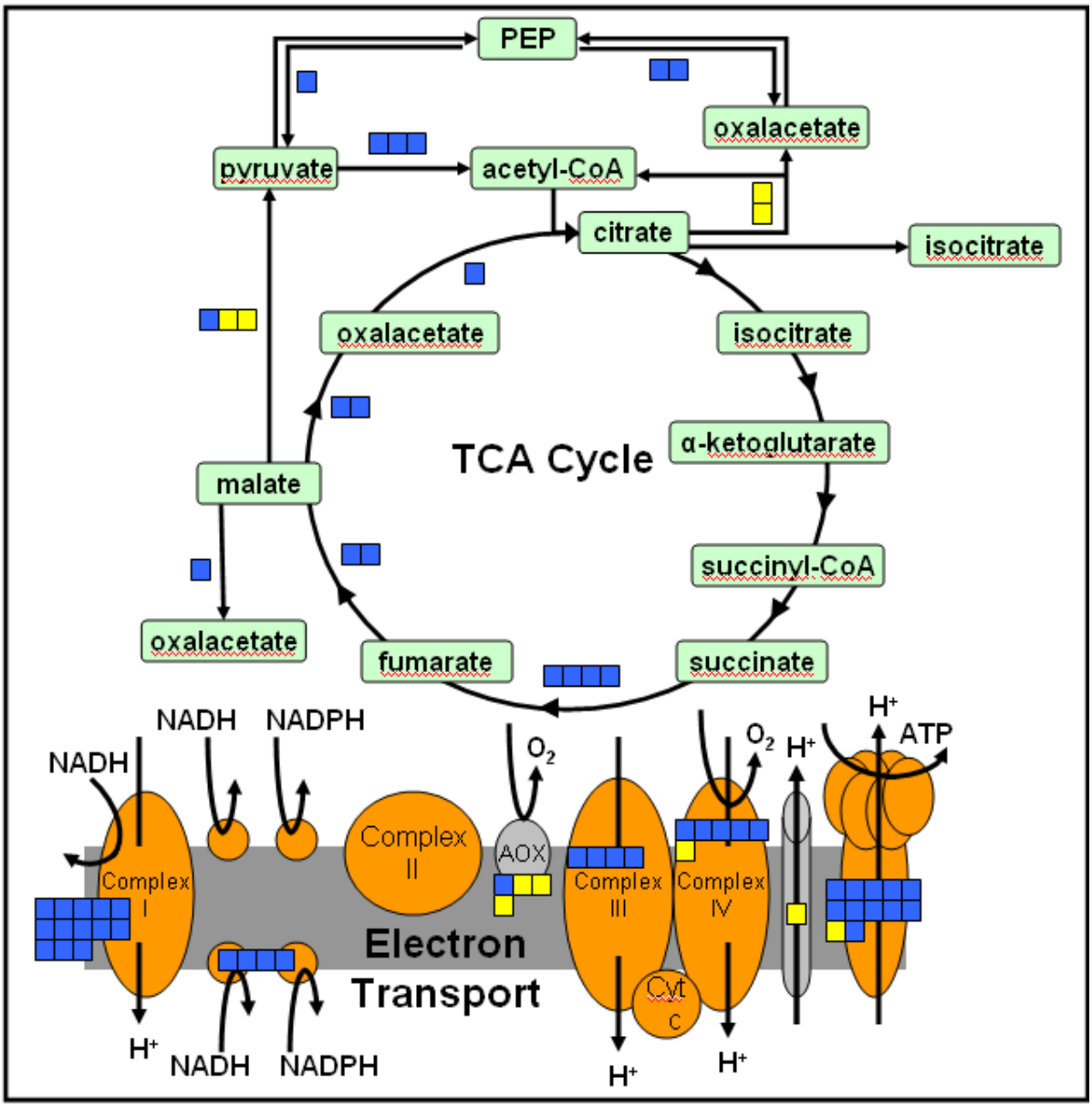


**Figure 4.12. Transcripts coding for components of the TCA cycle and mitochondrial electron transport significantly affected by PC1 at elevated [$CO_2$].** Blue boxes denote a significant positive correlation between transcript abundance and PC1. Yellow boxes denote a significant negative correlation between transcript abundance and PC1.

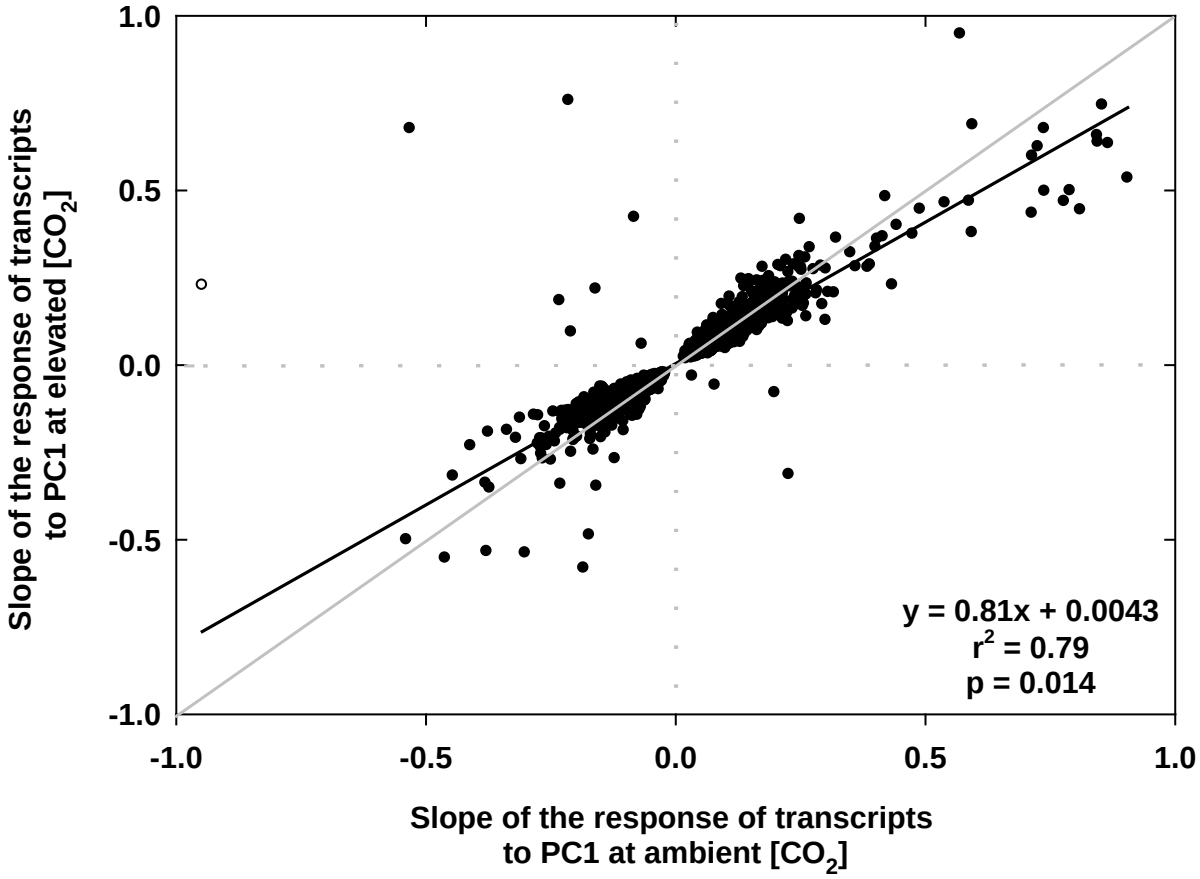


**Figure 4.13. The magnitude of the significant changes in transcripts to PC1 (slope) between ambient and elevated [$CO_2$].** The solid gray line indicates the 1:1 line and the black line indicates the best fit from linear regression. The slope of the regression line is significantly different from the 1:1 line, tested by a t-test ($p = 0.014$).

**Table 4.1. The Eigenvectors and Eigenvalues of the correlation matrix for the first two principle components.** Each principle component is an orthogonal, linear combination of the ten original environmental parameters. See text for abbreviations.

| | PC 1 | PC2 |
|---|---|---|
| **$T_{max}$** | -0.186 | 0.511 |
| **$T_{min}$** | -0.161 | 0.030 |
| **$RH_{max}$** | -0.106 | 0.542 |
| **PCMI** | -0.026 | 0.248 |
| **$PAR_{max}$** | 0.178 | -0.541 |
| **1 h max [$O_3$] 14 d** | 0.409 | 0.195 |
| **8h ave [$O_3$] 14 d** | 0.419 | 0.148 |
| **14d AOT40** | 0.423 | 0.136 |
| **1h max [$O_3$]** | 0.429 | 0.096 |
| **8h ave [$O_3$]** | 0.435 | 0.045 |
| **Eigenvalue** | 5.03 | 2.62 |
| **Percent Variability** | 50.38 | 26.20 |
| **Cumulative Percent Variability** | 50.38 | 76.58 |

**Table 4.2. Least-squared means (lsmeans) for the $CO_2$ treatment.** The lsmeans are reported for each variable at ambient [$CO_2$] and elevated [$CO_2$] after controlling for the co-variation in PC1 and PC2. Bold values indicate significant differences between ambient and elevated [$CO_2$] pairs at $p < 0.1$. See text for abbreviations.

| | ambient [$CO_2$] | elevated [$CO_2$] | p-value |
|---|---|---|---|
| **APX** (nmol ASA $min^{-1}$ mg $protein^{-1}$) | 93.1 | 100 | 0.510 |
| **SOD** (Units mg $protein^{-1}$) | **144** | **125** | 0.0131 |
| **CAT** (μmol $H_2O_2$ $min^{-1}$ mg $protein^{-1}$) | 18.3 | 20.9 | 0.292 |
| **DHAR** (nmol DHA $min^{-1}$ mg $protein^{-1}$) | 15.4 | 14.8 | 0.703 |
| **MDHAR** (nmol MDA $min^{-1}$ mg $protein^{-1}$) | **37.9** | **27.5** | 0.0308 |
| **GR** (nmol GSSG $min^{-1}$ mg $protein^{-1}$) | 75.7 | 79.4 | 0.764 |
| **ORAC** (nmol TE g $DW^{-1}$) | **0.768** | **0.652** | 0.0482 |
| **Phenolics** (mg GA g $DW^{-1}$) | 17.0 | 16.4 | 0.679 |
| **ASA** (mmol g $DW^{-1}$) | 0.0413 | 0.0391 | 0.141 |
| **DHASA** (mmol g $DW^{-1}$) | **0.00732** | **0.00631** | 0.081 |
| **Chl a** (μmol $m^{-2}$) | 523 | 532 | 0.640 |
| **Chl b** (μmol $m^{-2}$) | 103 | 105 | 0.592 |
| **Total Chl** (μmol $m^{-2}$) | 626 | 638 | 0.630 |
| **Glucose** (mmol $m^{-2}$) | **1.02** | **2.04** | < 0.0001 |
| **Sucrose** (mmol $m^{-2}$) | **2.02** | **2.84** | < 0.0001 |
| **Fructose** (mmol $m^{-2}$) | **0.848** | **1.25** | 0.0002 |
| **Starch** (mmol $m^{-2}$) | **28.3** | **54.1** | < 0.0001 |
| **Protein** (g $m^{-2}$) | **9.83** | **9.41** | 0.0787 |
| **Amino Acids** (mmol $m^{-2}$) | **3.09** | **3.53** | 0.00121 |

**Table 4.3**. **Results of the ANCOVA for biochemical parameters.** The slope of the regression between PC1 or PC2 and the measured variable at either ambient (amb [$CO_2$]) or elevated [$CO_2$] (ele [$CO_2$]) is displayed along with the p-value, which denotes whether that slope is significantly different from zero. Grey boxes highlight significant slopes at p <0.1. Values highlighted in bold denote slopes that are significantly different between ambient and elevated [$CO_2$] pairs.

| | **PC1** | | **PC2** | |
|---|---|---|---|---|
| | **slope at amb [$CO_2$], p-value** | **slope at ele [$CO_2$], p-value** | **slope at amb [$CO_2$], p-value** | **slope at ele [$CO_2$], p-value** |
| **APX** | 4.02, 0.222 | 3.873, 0.246 | -3.17, 0.484 | 4.08, 0.367 |
| **SOD** | -3.36, 0.154 | 0.994, 0.676 | **-16.5, <0.0001** | **-6.71, 0.0439** |
| **CAT** | -1.34, 0.0819 | -1.69, 0.0286 | 4.28, 0.000987 | 4.74, <0.0001 |
| **DHAR** | -0.0743, 0.886 | 0.286, 0.587 | 1.54, 0.0279 | 1.60, 0.0248 |
| **MDHAR** | -0.171, 0.911 | -0.337, 0.820 | -1.66, 0.422 | -3.08, 0.135 |
| **GR** | 6.39, 0.109 | -0.703, 0.863 | -7.30, 0.177 | -13.9, 0.0125 |
| **ORAC** | 0.0558, 0.00306 | 0.0321, 0.0869 | -0.0143, 0.575 | 0.01533, 0.550 |
| **Phenolics** | -0.08903, 0.8431 | -0.456, 0.319 | 0.520, 0.408 | 1.18, 0.0641 |
| **ASA** | **0.000942, 0.0428** | **-0.000319, 0.493** | -0.00009862, 0.877 | 0.0000256, 0.968 |
| **DHASA** | 0.0000159, 0.930 | -0.000133, 0.469 | 0.0007082, 0.0062 | 0.0009546, 0.0003 |
| **Chl a** | -7.20, 0.287 | -1.88, 0.783 | -5.486, 0.559 | -9.02, 0.341 |
| **Chl b** | -1.78, 0.179 | -0.760, 0.571 | 0.474, 0.797 | 0.341, 0.853 |
| **Total Chl** | -9.00, 0.263 | -2.64, 0.745 | -5.01, 0.653 | -8.68, 0.440 |
| **Glucose** | 0.0220, 0.726 | -0.0809, 0.206 | -0.0342, 0.695 | 0.0604, 0.492 |
| **Sucrose** | 0.116, 0.0635 | 0.234, 0.0003 | **-0.377, <0.0001** | **-0.674, <0.0001** |
| **Fructose** | **0.0442, 0.172** | **-0.0416, 0.204** | -0.0591, 0.190 | 0.00434, 0.923 |
| **Starch** | 0.711, 0.5642 | 1.354, 0.280 | **-3.35, 0.0534** | **-9.42, <0.0001** |
| **Protein** | -0.137, 0.0635 | -0.182, 0.0161 | 0.377, 0.0004 | 0.192, 0.0645 |
| **Amino Acids** | -0.00349, 0.933 | 0.0166, 0.693 | -0.0677, 0.241 | -0.136, 0.0210 |

**Table 4.4.** List of genes involved in antioxidant metabolism, mitochondrial electron transport, the TCA cycle and tetrapyrrole synthesis that showed significant correlations with PC1.

| Affymetrix Gene ID | Functional Category | Annotation | % change ele[$CO_2$] | p-value | slope at amb [$CO_2$] | p-value | slope at ele[$CO_2$] | p-value |
|---|---|---|---|---|---|---|---|---|
| GmaAffx.55339.1.S1_at | redox | 2-oxoglutarate-dependent dioxygenase, putative | 12.8 | 0.001 | n.s. | n.s. | n.s. | n.s. |
| GmaAffx.87031.1.S1_at | redox | AAO | n.s. | n.s. | 0.162 | 0.014 | 0.149 | 0.024 |
| Gma.10720.2.S1_x_at | redox | AAO, chl., thylakoid bound | n.s. | n.s. | 0.075 | 0.002 | 0.066 | 0.007 |
| GmaAffx.73877.1.S1_at | redox | APR-LIKE 5; protein disulfide oxidoreductase | 108.6 | 0.027 | 0.040 | 0.004 | n.s. | n.s. |
| Gma.16213.1.S1_at | redox | ascorbate oxidase precursor | n.s. | n.s. | n.s. | n.s. | 0.169 | 0.044 |
| Gma.4429.1.S1_at | redox | ascorbate oxidase precursor | n.s. | n.s. | n.s. | n.s. | 0.177 | 0.048 |
| GmaAffx.91272.1.S1_s_at | redox | ascorbate oxidase precursor | n.s. | n.s. | 0.157 | 0.027 | n.s. | n.s. |
| Gma.2202.1.S1_at | redox | ascorbate peroxidase 4 | n.s. | n.s. | 0.150 | 0.012 | 0.132 | 0.029 |
| GmaAffx.91474.1.S1_s_at | redox | ascorbate peroxidase, chl stroma | n.s. | n.s. | n.s. | n.s. | 0.059 | 0.049 |
| Gma.3317.2.S1_a_at | redox | ATPRX Q \| peroxiredoxin Q, putative | n.s. | n.s. | 0.074 | 0.017 | 0.070 | 0.025 |
| Gma.8498.1.S1_at | redox | Cu/Zn-SOD copper chaperone precursor | n.s. | n.s. | 0.128 | <0.001 | n.s. | n.s. |
| GmaAffx.62476.1.S1_at | redox | Cu-Zn SOD | -16.4 | 0.008 | n.s. | n.s. | n.s. | n.s. |
| GmaAffx.65064.1.S1_at | redox | Cu-Zn SOD | n.s. | n.s. | 0.048 | 0.019 | n.s. | n.s. |
| Gma.15464.2.S1_at | redox | Cu-Zn SOD1 | n.s. | n.s. | 0.067 | <0.001 | 0.046 | 0.006 |
| Gma.15464.1.S1_x_at | redox | Cu-Zn SOD1 | n.s. | n.s. | 0.071 | 0.001 | n.s. | n.s. |
| Gma.6384.1.S1_at | redox | Cu-Zn SOD2 | n.s. | n.s. | 0.111 | 0.009 | 0.094 | 0.030 |
| Gma.2513.1.A1_at | redox | Cu-Zn SOD2 | n.s. | n.s. | 0.110 | 0.042 | n.s. | n.s. |
| Gma.15258.1.S1_at | redox | Cu-Zn SOD3 | 10.38 | 0.046 | n.s. | n.s. | n.s. | n.s. |
| Gma.2513.2.S1_at | redox | Cu-Zn SOD3 | n.s. | n.s. | 0.105 | 0.010 | n.s. | n.s. |
| Gma.10919.1.S1_at | redox | Cytochrome b5 B | -35.8 | 0.003 | n.s. | n.s. | n.s. | n.s. |
| Gma.8645.1.S1_at | redox | cytochrome b5 family protein #5 | n.s. | n.s. | n.s. | n.s. | 0.061 | 0.032 |
| Gma.2041.1.S1_at | redox | DHAR | n.s. | n.s. | 0.121 | <0.001 | 0.091 | 0.002 |
| Gma.4366.1.S1_at | redox | DHAR2 | n.s. | n.s. | 0.062 | 0.037 | 0.067 | 0.026 |
| Gma.5685.1.S1_s_at | redox | electron carrier/ protein disulfide oxidoreductase | 25.6 | 0.032 | n.s. | n.s. | n.s. | n.s. |
| Gma.13363.1.A1_at | redox | electron carrier/ protein disulfide oxidoreductase | n.s. | n.s. | n.s. | n.s. | -0.146 | 0.025 |
| Gma.13363.1.S1_s_at | redox | electron carrier/ protein disulfide oxidoreductase | n.s. | n.s. | -0.041 | 0.024 | n.s. | n.s. |
| Gma.16827.1.S1_at | redox | Fe-SOD | n.s. | n.s. | -0.411 | <0.001 | -0.231 | 0.013 |
| Gma.3233.1.S1_s_at | redox | Fe-SOD | n.s. | n.s. | -0.311 | <0.001 | -0.152 | 0.045 |
| Gma.3233.1.S1_at | redox | Fe-SOD1 | n.s. | n.s. | n.s. | n.s. | -0.151 | 0.023 |

Table 4.4 (cont.)

| Affymetrix Gene ID | Functional Category | Annotation | % change ele[$CO_2$] | p-value | slope at amb [$CO_2$] | p-value | slope at ele[$CO_2$] | p-value |
|---|---|---|---|---|---|---|---|---|
| Gma.3523.1.S1_at | redox | galactono-1,4-lactone dehydorogenase | n.s. | n.s. | 0.046 | 0.001 | 0.038 | 0.006 |
| Gma.2292.2.S1_a_at | redox | GDP-mannose 3,5-epimerase | n.s. | n.s. | 0.186 | 0.009 | 0.175 | 0.015 |
| Gma.6917.1.S1_at | redox | glucose-6-phosphate isomerase, cytosolic | 7.4 | 0.007 | 0.036 | 0.010 | n.s. | n.s. |
| GmaAffx.76101.1.S1_at | redox | glucose-6-phosphate isomerase, cytosolic | n.s. | n.s. | 0.044 | 0.010 | n.s. | n.s. |
| GmaAffx.4537.1.S1_at | redox | glutaredoxin family | -49.5 | 0.034 | -0.189 | 0.007 | -0.167 | 0.018 |
| GmaAffx.90206.1.S1_s_at | redox | glutaredoxin family | -32.1 | 0.002 | -0.081 | 0.011 | -0.073 | 0.024 |
| GmaAffx.1832.1.S1_at | redox | glutaredoxin family | -11.4 | 0.022 | n.s. | n.s. | n.s. | n.s. |
| Gma.7926.1.S1_at | redox | glutaredoxin family | 35.9 | 0.040 | n.s. | n.s. | n.s. | n.s. |
| GmaAffx.86613.2.S1_at | redox | glutaredoxin family | n.s. | n.s. | 0.475 | <0.001 | 0.374 | <0.001 |
| GmaAffx.34785.21.S1_at | redox | glutaredoxin family | n.s. | n.s. | 0.171 | 0.037 | 0.236 | 0.005 |
| Gma.6855.1.S1_at | redox | GPx | n.s. | n.s. | 0.022 | 0.041 | n.s. | n.s. |
| Gma.4312.3.S1_a_at | redox | GPx 2 | n.s. | n.s. | -0.028 | 0.043 | n.s. | n.s. |
| GmaAffx.89649.1.A1_at | redox | GPx 3 | n.s. | n.s. | -0.077 | 0.032 | n.s. | n.s. |
| GmaAffx.89649.1.S1_s_at | redox | GPx 3 | n.s. | n.s. | -0.032 | 0.048 | n.s. | n.s. |
| GmaAffx.91533.1.S1_s_at | redox | GR | n.s. | n.s. | 0.026 | 0.023 | n.s. | n.s. |
| GmaAffx.35832.1.S1_at | redox | GR, cytosolic | n.s. | n.s. | 0.032 | 0.024 | 0.035 | 0.017 |
| Gma.8509.1.S1_x_at | redox | heme oxygenase 1 | n.s. | n.s. | 0.047 | 0.002 | n.s. | n.s. |
| Gma.540.1.S1_s_at | redox | heme oxygenase 3 | n.s. | n.s. | 0.047 | 0.008 | n.s. | n.s. |
| Gma.3133.1.S1_at | redox | GSH synthetase | 5.1 | 0.027 | n.s. | n.s. | n.s. | n.s. |
| GmaAffx.71453.1.S1_at | redox | GSH synthetase | n.s. | n.s. | n.s. | n.s. | -0.147 | 0.032 |
| GmaAffx.64454.1.S1_at | redox | L-galactose dehydrogenase | n.s. | n.s. | 0.082 | 0.003 | 0.085 | 0.003 |
| Gma.5576.1.S1_at | redox | Mn SOD | n.s. | n.s. | n.s. | n.s. | 0.028 | 0.012 |
| Gma.5151.1.S1_at | redox | mannose-6-phosphate isomerase | n.s. | n.s. | 0.092 | <0.001 | 0.060 | 0.008 |
| Gma.5803.2.S1_at | redox | MDHAR | n.s. | n.s. | 0.034 | 0.002 | n.s. | n.s. |
| Gma.5304.2.S1_at | redox | Membrane progesterone binding protein | 5.8 | 0.013 | n.s. | n.s. | n.s. | n.s. |
| GmaAffx.90559.1.S1_s_at | redox | membrane progesterone binding protein 5 | n.s. | n.s. | -0.041 | 0.003 | n.s. | n.s. |
| Gma.2650.1.S1_at | redox | NADH-cytochrome b5 reductase, putative | 20.2 | <0.001 | 0.038 | 0.015 | 0.032 | 0.043 |

Table 4.4 (cont)

| Affymetrix Gene ID | Functional Category | Annotation | % change ele[$CO_2$] | p-value | slope at amb [$CO_2$] | p-value | slope at ele[$CO_2$] | p-value |
|---|---|---|---|---|---|---|---|---|
| GmaAffx.92590.1.S1_at | redox | NADP-thioredoxin reductase C | -16.4 | 0.004 | 0.043 | 0.013 | 0.044 | 0.012 |
| GmaAffx.87753.1.S1_at | redox | NADP-thioredoxin reductase C | n.s. | n.s. | 0.066 | 0.001 | 0.059 | 0.004 |
| GmaAffx.41419.1.S1_s_at | redox | NADP-thioredoxin reductase C | n.s. | n.s. | 0.063 | 0.018 | 0.061 | 0.024 |
| GmaAffx.93215.1.S1_s_at | redox | nonsymbiotic hemoglobin | -9.6 | 0.034 | n.s. | n.s. | n.s. | n.s. |
| Gma.2350.1.S1_x_at | redox | PDI-LIKE 1-4; thiol-disulfide exchange intermediate | n.s. | n.s. | n.s. | n.s. | 0.051 | 0.007 |
| Gma.16343.1.S1_at | redox | PDI-LIKE 1-4; thiol-disulfide exchange intermediate | n.s. | n.s. | n.s. | n.s. | 0.102 | 0.009 |
| GmaAffx.88516.1.S1_at | redox | PDI-LIKE 1-6; thiol-disulfide exchange intermediate | -16.0 | 0.005 | n.s. | n.s. | 0.037 | 0.030 |
| GmaAffx.71811.1.S1_at | redox | PDI-LIKE 2-2; thiol-disulfide exchange intermediate | n.s. | n.s. | 0.046 | 0.014 | 0.052 | 0.006 |
| GmaAffx.90027.1.S1_s_at | redox | pectin methylesterase | n.s. | n.s. | n.s. | n.s. | 0.265 | 0.042 |
| Gma.2262.1.S1_at | redox | pectin methylesterase 3 | n.s. | n.s. | n.s. | n.s. | 0.203 | 0.014 |
| GmaAffx.26348.1.S1_at | redox | pectin methylesterase, putative | n.s. | n.s. | 0.148 | 0.004 | 0.107 | 0.026 |
| Gma.2182.1.S1_at | redox | pectinesterase family | n.s. | n.s. | n.s. | n.s. | 0.174 | 0.001 |
| Gma.7198.1.S1_at | redox | pectinesterase family | n.s. | n.s. | 0.191 | 0.002 | 0.191 | 0.002 |
| GmaAffx.78421.2.S1_at | redox | pectinesterase family | n.s. | n.s. | n.s. | n.s. | 0.091 | 0.027 |
| GmaAffx.78421.1.S1_at | redox | pectinesterase family | n.s. | n.s. | n.s. | n.s. | 0.119 | 0.043 |
| Gma.4362.1.S1_at | redox | peroxiredoxin | n.s. | n.s. | n.s. | n.s. | 0.052 | 0.042 |
| GmaAffx.77106.1.S1_s_at | redox | peroxiredoxin | n.s. | n.s. | 0.094 | 0.003 | 0.081 | 0.012 |
| Gma.4362.1.S1_a_at | redox | peroxiredoxin | n.s. | n.s. | 0.084 | 0.006 | 0.072 | 0.019 |
| Gma.11803.1.S1_at | redox | rubredoxin family protein | n.s. | n.s. | 0.121 | 0.008 | n.s. | n.s. |
| GmaAffx.76419.1.S1_at | redox | senescence-associated nodulin 1B | 319.7 | 0.044 | n.s. | n.s. | n.s. | n.s. |
| Gma.6029.1.S1_at | redox | thiol-disulfide exchange intermediate | n.s. | n.s. | 0.047 | <0.001 | n.s. | n.s. |
| Gma.5662.1.S1_at | redox | thioredoxin | 19.9 | 0.024 | n.s. | n.s. | n.s. | n.s. |
| Gma.15886.1.S1_x_at | redox | thioredoxin | n.s. | n.s. | 0.030 | 0.018 | n.s. | n.s. |
| Gma.11194.2.S1_at | redox | Thioredoxin domain 2 | -31.6 | 0.007 | n.s. | n.s. | n.s. | n.s. |
| Gma.11194.1.S1_at | redox | Thioredoxin domain 2 | -27.5 | 0.005 | n.s. | n.s. | n.s. | n.s. |
| GmaAffx.3670.1.S1_at | redox | thioredoxin family | 13.6 | 0.009 | n.s. | n.s. | n.s. | n.s. |
| GmaAffx.12188.1.S1_at | redox | thioredoxin family | n.s. | n.s. | 0.090 | <0.001 | 0.080 | <0.001 |
| GmaAffx.12188.2.S1_at | redox | thioredoxin family | n.s. | n.s. | 0.066 | 0.003 | 0.064 | 0.005 |

Table 4.4 (cont)

| Affymetrix Gene ID | Functional Category | Annotation | % change ele[$CO_2$] | p-value | slope at amb [$CO_2$] | p-value | slope at ele[$CO_2$] | p-value |
|---|---|---|---|---|---|---|---|---|
| Gma.3776.1.S1_at | redox | Thioredoxin fold | -22.5 | <0.001 | -0.090 | 0.008 | -0.068 | 0.044 |
| Gma.8119.1.S1_s_at | redox | thioredoxin h1 | 9.5 | <0.001 | n.s. | n.s. | n.s. | n.s. |
| GmaAffx.89881.1.A1_at | redox | thioredoxin h1 | 69.0 | 0.003 | n.s. | n.s. | n.s. | n.s. |
| Gma.8119.2.S1_at | redox | thioredoxin h2 | 5.9 | 0.006 | n.s. | n.s. | n.s. | n.s. |
| GmaAffx.89881.1.S1_s_at | redox | thioredoxin H-type | 10.1 | <0.001 | n.s. | n.s. | n.s. | n.s. |
| GmaAffx.50781.2.S1_s_at | redox | thioredoxin H-type 9 | n.s. | n.s. | 0.080 | <0.001 | 0.067 | <0.001 |
| Gma.5430.1.S1_at | redox | thioredoxin H-type 9 | n.s. | n.s. | n.s. | n.s. | 0.025 | 0.036 |
| GmaAffx.50781.2.S1_x_at | redox | thioredoxin H-type 9 | n.s. | n.s. | n.s. | n.s. | 0.061 | 0.037 |
| Gma.10845.1.S1_s_at | redox | thioredoxin M-type 2 | n.s. | n.s. | 0.045 | 0.037 | n.s. | n.s. |
| Gma.7165.1.S1_at | redox | thioredoxin M-type 3 | n.s. | n.s. | 0.051 | 0.006 | n.s. | n.s. |
| Gma.5401.1.S1_s_at | redox | thioredoxin-dependent peroxidase 1 | n.s. | n.s. | n.s. | n.s. | 0.037 | 0.003 |
| GmaAffx.18471.1.S1_at | redox | thioredoxin-related | -10.4 | 0.039 | n.s. | n.s. | n.s. | n.s. |
| Gma.3937.2.S1_at | redox | thioredoxin-related | 10.5 | 0.014 | n.s. | n.s. | n.s. | n.s. |
| Gma.15252.1.S1_at | tetrapyrrole syn. | chlorophyll a oxygenase | n.s. | n.s. | 0.047 | 0.012 | n.s. | n.s. |
| Gma.15252.2.S1_at | tetrapyrrole syn. | chlorophyll a oxygenase | n.s. | n.s. | 0.049 | 0.017 | n.s. | n.s. |
| Gma.17255.1.S1_at | tetrapyrrole syn. | chlorophyll synthetase | n.s. | n.s. | 0.074 | <0.001 | 0.061 | 0.002 |
| Gma.8074.1.S1_s_at | tetrapyrrole syn. | COX10; prenyltransferase | n.s. | n.s. | 0.078 | <0.001 | 0.055 | 0.001 |
| GmaAffx.44857.1.A1_at | tetrapyrrole syn. | FLU (FLUORESCENT IN BLUE LIGHT) | n.s. | n.s. | 0.064 | 0.011 | n.s. | n.s. |
| Gma.1779.1.S1_at | tetrapyrrole syn. | glutamate-1-semialdehyde 2,1-aminomutase | n.s. | n.s. | 0.107 | <0.001 | 0.098 | 0.001 |
| GmaAffx.91779.1.S1_s_at | tetrapyrrole syn. | glutamate-1-semialdehyde 2,1-aminomutase | n.s. | n.s. | 0.080 | 0.003 | 0.079 | 0.004 |
| GmaAffx.91779.1.S1_at | tetrapyrrole syn. | glutamate-1-semialdehyde 2,1-aminomutase | n.s. | n.s. | 0.069 | 0.002 | 0.063 | 0.006 |
| Gma.3336.1.S1_at | tetrapyrrole syn. | glutamate-tRNA ligase | n.s. | n.s. | 0.064 | <0.001 | 0.037 | 0.019 |
| Gma.8011.2.S1_a_at | tetrapyrrole syn. | glutamyl-tRNA(Gln) amidotransferase | n.s. | n.s. | 0.081 | <0.001 | n.s. | n.s. |
| Gma.8011.2.S1_at | tetrapyrrole syn. | glutamyl-tRNA(Gln) amidotransferase | n.s. | n.s. | 0.054 | 0.010 | n.s. | n.s. |
| GmaAffx.48451.1.S1_at | tetrapyrrole syn. | glutamyl-tRNA(Gln) amidotransferase, putative | 14.4 | 0.036 | 0.080 | 0.013 | n.s. | n.s. |
| Gma.13003.1.S1_at | tetrapyrrole syn. | GUN4 (Genomes uncoupled 4) | 694.8 | 0.005 | 0.148 | 0.006 | n.s. | n.s. |
| Gma.13003.1.S1_s_at | tetrapyrrole syn. | GUN4 (Genomes uncoupled 4) | n.s. | n.s. | 0.112 | 0.047 | n.s. | n.s. |
| Gma.6038.1.S1_at | tetrapyrrole syn. | HEMB1 | n.s. | n.s. | n.s. | n.s. | 0.049 | 0.046 |

Table 4.4 (cont)

| Affymetrix Gene ID | Functional Category | Annotation | % change ele[$CO_2$] | p-value | slope at amb [$CO_2$] | p-value | slope at ele[$CO_2$] | p-value |
|---|---|---|---|---|---|---|---|---|
| Gma.13182.2.S1_at | tetrapyrrole syn. | hydroxymethylbilane synthase | n.s. | n.s. | 0.064 | 0.002 | 0.088 | <0.001 |
| Gma.1986.1.S1_at | tetrapyrrole syn. | hydroxymethylbilane synthase | n.s. | n.s. | n.s. | n.s. | 0.073 | 0.032 |
| GmaAffx.73108.1.S1_at | tetrapyrrole syn. | Mg chelatase | n.s. | n.s. | 0.063 | 0.043 | 0.066 | 0.039 |
| Gma.5672.1.A1_at | tetrapyrrole syn. | Mg chelatase | n.s. | n.s. | 0.078 | 0.020 | 0.069 | 0.042 |
| Gma.12621.2.S1_at | tetrapyrrole syn. | Mg chelatase subunit | n.s. | n.s. | 0.084 | 0.010 | n.s. | n.s. |
| Gma.12621.1.A1_at | tetrapyrrole syn. | Mg chelatase subunit | n.s. | n.s. | 0.081 | 0.013 | n.s. | n.s. |
| Gma.1796.1.S1_at | tetrapyrrole syn. | Mg chelatase subunit | n.s. | n.s. | 0.104 | 0.015 | n.s. | n.s. |
| Gma.15868.2.A1_a_at | tetrapyrrole syn. | Mg-protoporphyrin IX methytransferase | n.s. | n.s. | 0.102 | 0.039 | 0.105 | 0.035 |
| Gma.3129.1.S1_at | tetrapyrrole syn. | protoporphyrinogen oxidase | n.s. | n.s. | 0.096 | <0.001 | 0.072 | 0.004 |
| GmaAffx.48616.1.S1_at | tetrapyrrole syn. | sirohydrochlorin ferrochelatase | n.s. | n.s. | 0.045 | 0.009 | 0.061 | 0.001 |
| GmaAffx.3890.1.A1_at | tetrapyrrole syn. | sirohydrochlorin ferrochelatase | n.s. | n.s. | 0.042 | 0.032 | 0.051 | 0.011 |
| GmaAffx.69778.1.S1_at | tetrapyrrole syn. | uroporphiryn-III C-methyltransferase | n.s. | n.s. | -0.114 | 0.022 | n.s. | n.s. |
| Gma.7747.1.S1_at | tetrapyrrole syn. | uroporphyrinogen decarboxylase | n.s. | n.s. | 0.068 | 0.003 | 0.067 | 0.004 |
| Gma.7747.2.S1_at | tetrapyrrole syn. | uroporphyrinogen decarboxylase | n.s. | n.s. | 0.078 | 0.009 | 0.071 | 0.020 |
| Gma.6694.1.S1_at | tetrapyrrole syn. | uroporphyrinogen decarboxylase | n.s. | n.s. | n.s. | n.s. | 0.054 | 0.043 |
| GmaAffx.85881.1.S1_at | tetrapyrrole syn. | uroporphyrinogen decarboxylase | n.s. | n.s. | 0.062 | 0.021 | n.s. | n.s. |
| Gma.4912.2.S1_a_at | tetrapyrrole syn. | uroporphyrinogen-III synthase | n.s. | n.s. | 0.042 | 0.030 | 0.042 | 0.033 |
| Gma.8415.1.S1_at | mito. ETC | alternative oxidase 2a | n.s. | n.s. | 0.044 | 0.003 | 0.039 | 0.008 |
| GmaAffx.91355.1.S1_s_at | mito. ETC | alternative oxidase 2b | n.s. | n.s. | -0.095 | 0.008 | -0.086 | 0.018 |
| Gma.11120.1.S1_at | mito. ETC | alternative oxidase 2b | n.s. | n.s. | -0.079 | 0.003 | -0.062 | 0.018 |
| GmaAffx.86361.1.S1_s_at | mito. ETC | alternative oxidase 2b | n.s. | n.s. | -0.067 | 0.003 | -0.049 | 0.030 |
| Gma.1312.1.S1_s_at | mito. ETC | ATP synthase beta chain 2 | n.s. | n.s. | 0.056 | <0.001 | 0.046 | 0.001 |
| GmaAffx.90801.1.S1_at | mito. ETC | ATP synthase beta chain 2 | n.s. | n.s. | 0.054 | <0.001 | 0.041 | 0.006 |
| GmaAffx.92910.1.S1_s_at | mito. ETC | ATP synthase D chain-related | n.s. | n.s. | 0.025 | 0.028 | 0.042 | <0.001 |
| GmaAffx.92392.1.S1_at | mito. ETC | ATP synthase delta' chain | n.s. | n.s. | 0.047 | 0.004 | 0.044 | 0.007 |
| GmaAffx.92392.1.S1_s_at | mito. ETC | ATP synthase delta' chain | n.s. | n.s. | 0.071 | <0.001 | 0.047 | 0.005 |
| Gma.17512.2.S1_at | mito. ETC | ATP synthase delta chain, | n.s. | n.s. | 0.051 | <0.001 | 0.044 | <0.001 |

Table 4.4 (cont)

| Affymetrix Gene ID | Functional Category | Annotation | % change ele[$CO_2$] | p-value | slope at amb [$CO_2$] | p-value | slope at ele[$CO_2$] | p-value |
|---|---|---|---|---|---|---|---|---|
| Gma.11271.1.S1_s_at | mito. ETC | ATP synthase epsilon chain | n.s. | n.s. | 0.028 | 0.021 | 0.040 | 0.001 |
| Gma.17344.2.S1_s_at | mito. ETC | ATP synthase gamma chain | n.s. | n.s. | 0.045 | 0.001 | 0.040 | 0.002 |
| Gma.17344.1.S1_at | mito. ETC | ATP synthase gamma chain | n.s. | n.s. | 0.042 | 0.002 | 0.039 | 0.003 |
| GmaAffx.25198.1.S1_at | mito. ETC | ATP synthase, subunit b | n.s. | n.s. | n.s. | n.s. | -0.036 | 0.050 |
| Gma.7397.1.S1_at | mito. ETC | catalytic/ coenzyme binding | n.s. | n.s. | 0.048 | <0.001 | 0.050 | <0.001 |
| GmaAffx.81688.1.S1_at | mito. ETC | catalytic/ coenzyme binding | n.s. | n.s. | 0.046 | 0.001 | 0.050 | 0.001 |
| GmaAffx.93110.1.S1_x_at | mito. ETC | cytochrome c oxidase family | n.s. | n.s. | n.s. | n.s. | 0.037 | 0.009 |
| GmaAffx.93110.1.S1_s_at | mito. ETC | cytochrome c oxidase family | 5.3 | 0.033 | 0.053 | 0.001 | 0.048 | 0.004 |
| GmaAffx.59019.1.S1_at | mito. ETC | cytochrome c oxidase subunit 2 | n.s. | n.s. | n.s. | n.s. | 0.035 | 0.017 |
| Gma.10898.1.S1_at | mito. ETC | cytochrome c oxidase subunit 6b, putative | n.s. | n.s. | 0.055 | 0.005 | 0.060 | 0.003 |
| GmaAffx.88771.1.A1_s_at | mito. ETC | cytochrome c oxidase-related | n.s. | n.s. | 0.047 | <0.001 | 0.047 | <0.001 |
| Gma.17435.1.S1_at | mito. ETC | Cytochrome c, monohaem | 8.6 | 0.006 | 0.039 | 0.039 | n.s. | n.s. |
| Gma.17435.2.S1_at | mito. ETC | Cytochrome c, monohaem | n.s. | n.s. | 0.037 | 0.008 | n.s. | n.s. |
| GmaAffx.43578.1.S1_at | mito. ETC | electron transport SCO1/SenC family protein | -7.3 | 0.045 | 0.067 | 0.021 | n.s. | n.s. |
| Gma.15699.1.S1_at | mito. ETC | electron transport SCO1/SenC family protein | n.s. | n.s. | -0.047 | 0.018 | -0.042 | 0.037 |
| GmaAffx.43578.2.S1_at | mito. ETC | electron transport SCO1/SenC family protein | n.s. | n.s. | 0.077 | 0.026 | n.s. | n.s. |
| GmaAffx.89869.1.S1_s_at | mito. ETC | F1F0-ATPase inhibitor protein, putative | n.s. | n.s. | 0.104 | 0.015 | 0.090 | 0.036 |
| Gma.745.1.S1_a_at | mito. ETC | FRO1 (FROSTBITE1) | n.s. | n.s. | 0.035 | 0.028 | n.s. | n.s. |
| Gma.6372.1.S1_at | mito. ETC | hydrogen ion transporting ATP synthase | 6.7 | 0.039 | n.s. | n.s. | n.s. | n.s. |
| Gma.3832.1.S1_at | mito. ETC | mito. substrate carrier family protein | n.s. | n.s. | -0.166 | <0.001 | -0.105 | 0.014 |
| GmaAffx.82261.1.S1_at | mito. ETC | NAD(P)H dehydrogenase B1 | n.s. | n.s. | 0.040 | 0.013 | 0.037 | 0.022 |
| GmaAffx.4294.1.S1_at | mito. ETC | NAD(P)H dehydrogenase B2 | n.s. | n.s. | 0.034 | 0.017 | 0.046 | 0.002 |
| Gma.3086.1.A1_at | mito. ETC | NAD(P)H dehyrogenase C1 | n.s. | n.s. | 0.060 | 0.042 | n.s. | n.s. |

Table 4.4 (cont)

| Affymetrix Gene ID | Functional Category | Annotation | % change ele[$CO_2$] | p-value | slope at amb [$CO_2$] | p-value | slope at ele[$CO_2$] | p-value |
|---|---|---|---|---|---|---|---|---|
| Gma.1863.1.S1_at | mito. ETC | NADH dehydrogenase | 6.7 | <0.001 | 0.039 | 0.001 | n.s. | n.s. |
| GmaAffx.87851.1.S1_at | mito. ETC | NADH dehydrogenase | n.s. | n.s. | 0.038 | 0.008 | n.s. | n.s. |
| GmaAffx.90872.1.S1_at | mito. ETC | NADH-ubiquinone oxidoreductase 19 kDa subunit | n.s. | n.s. | 0.109 | <0.001 | 0.059 | 0.043 |
| Gma.4356.1.S1_a_at | mito. ETC | NADH-ubiquinone oxidoreductase 20 kDa subunit | n.s. | n.s. | 0.022 | 0.038 | 0.022 | 0.038 |
| GmaAffx.90024.1.S1_s_at | mito. ETC | NADH-ubiquinone oxidoreductase 20 kDa subunit | n.s. | n.s. | 0.026 | 0.032 | n.s. | n.s. |
| Gma.4918.1.S1_at | mito. ETC | NADH-ubiquinone oxidoreductase 23 kDa subunit | n.s. | n.s. | 0.071 | 0.001 | 0.059 | 0.006 |
| Gma.10702.1.S1_at | mito. ETC | NADH-ubiquinone oxidoreductase 51 kDa subunit, putative | n.s. | n.s. | 0.050 | <0.001 | 0.033 | 0.001 |
| Gma.6610.1.S1_s_at | mito. ETC | NADH-ubiquinone oxidoreductase B18 subunit, putative | n.s. | n.s. | n.s. | n.s. | 0.032 | 0.026 |
| Gma.7266.2.S1_at | mito. ETC | NADH-ubiquinone oxidoreductase B8 subunit, putative | n.s. | n.s. | 0.045 | 0.004 | 0.034 | 0.027 |
| Gma.6437.1.S1_at | mito. ETC | NADH-ubiquinone oxidoreductase-related | n.s. | n.s. | n.s. | n.s. | 0.038 | 0.001 |
| Gma.8354.1.S1_s_at | mito. ETC | NADH-ubiquinone oxidoreductase-related | n.s. | n.s. | n.s. | n.s. | 0.038 | 0.046 |
| GmaAffx.90444.1.S1_s_at | mito. ETC | NADPH:quinone oxidoreductase | n.s. | n.s. | 0.073 | 0.016 | 0.073 | 0.018 |
| GmaAffx.91977.1.S1_s_at | mito. ETC | predicted NADH dehydrogenase | n.s. | n.s. | 0.033 | 0.003 | 0.026 | 0.018 |
| GmaAffx.91720.1.S1_s_at | mito. ETC | putative ATP synthase subunit | n.s. | n.s. | n.s. | n.s. | 0.031 | 0.017 |
| Gma.9091.1.S1_at | mito. ETC | Pyridine nucleotide-disulphide oxidoreductase, class I | n.s. | n.s. | 0.131 | 0.001 | 0.109 | 0.006 |
| Gma.9091.2.S1_a_at | mito. ETC | Pyridine nucleotide-disulphide oxidoreductase, class I | n.s. | n.s. | 0.119 | 0.001 | 0.093 | 0.009 |
| Gma.4646.1.A1_s_at | mito. ETC | SURF1 (SURFEIT 1) | -16.4 | 0.018 | n.s. | n.s. | n.s. | n.s. |
| GmaAffx.54104.1.S1_at | mito. ETC | SURFEIT 1 | n.s. | n.s. | 0.063 | 0.004 | n.s. | n.s. |
| GmaAffx.89849.1.S1_at | mito. ETC | ubiquinol-cytochrome C reductase | -9.3 | 0.013 | n.s. | n.s. | n.s. | n.s. |
| Gma.6160.1.S1_at | mito. ETC | ubiquinol-cytochrome C reductase | 5.8 | 0.011 | n.s. | n.s. | n.s. | n.s. |

Table 4.4 (cont)

| Affymetrix Gene ID | Functional Category | Annotation | % change ele[$CO_2$] | p-value | slope at amb [$CO_2$] | p-value | slope at ele[$CO_2$] | p-value |
|---|---|---|---|---|---|---|---|---|
| Gma.6258.1.S1_s_at | mito. ETC | ubiquinol-cytochrome C reductase 14 kDa, putative | n.s. | n.s. | 0.033 | 0.004 | 0.036 | 0.002 |
| Gma.6160.1.S1_s_at | mito. ETC | ubiquinol-cytochrome C reductase family | n.s. | n.s. | 0.047 | 0.020 | 0.040 | 0.049 |
| Gma.5057.2.S1_s_at | mito. ETC | ubiquinol-cytochrome C reductase Fe-S subunit, putative | n.s. | n.s. | 0.040 | <0.001 | 0.039 | <0.001 |
| Gma.5057.2.S1_x_at | mito. ETC | ubiquinol-cytochrome C reductase Fe-S subunit, putative | n.s. | n.s. | 0.033 | 0.016 | 0.031 | 0.026 |
| Gma.5057.2.S1_at | mito. ETC | ubiquinol-cytochrome C reductase Fe-S subunit, putative | n.s. | n.s. | 0.035 | 0.015 | n.s. | n.s. |
| GmaAffx.77958.1.S1_at | mito. ETC | ubiquinone biosynthesis Coq4 family protein | n.s. | n.s. | -0.152 | 0.005 | -0.119 | 0.016 |
| Gma.5276.1.S1_at | TCA cycle | aconitate hydratase family protein | n.s. | n.s. | 0.044 | 0.013 | n.s. | n.s. |
| GmaAffx.93451.1.S1_s_at | TCA cycle | aconitate hydratase, cytoplasmic | n.s. | n.s. | 0.055 | 0.001 | n.s. | n.s. |
| Gma.5618.1.S1_at | TCA cycle | aconitate hydratase, cytoplasmic, putative | n.s. | n.s. | 0.049 | 0.002 | n.s. | n.s. |
| GmaAffx.93250.1.S1_s_at | TCA cycle | ATP-citrate lyase | n.s. | n.s. | -0.029 | 0.028 | -0.033 | 0.015 |
| GmaAffx.80064.1.S1_at | TCA cycle | ATP-citrate lyase A-1 | -13.2 | 0.036 | -0.091 | 0.035 | n.s. | n.s. |
| GmaAffx.93551.1.S1_at | TCA cycle | ATP-citrate lyase A-3 | n.s. | n.s. | -0.103 | 0.004 | n.s. | n.s. |
| GmaAffx.93551.1.S1_s_at | TCA cycle | ATP-citrate lyase A-3 | n.s. | n.s. | -0.080 | 0.010 | n.s. | n.s. |
| Gma.11135.2.S1_at | TCA cycle | ATP-citrate lyase A-3 | n.s. | n.s. | -0.097 | 0.028 | n.s. | n.s. |
| Gma.11135.1.S1_at | TCA cycle | ATP-citrate lyase A-3 | n.s. | n.s. | -0.063 | 0.042 | n.s. | n.s. |
| Gma.15490.3.S1_s_at | TCA cycle | beta carbonic anhydrase 2 | n.s. | n.s. | n.s. | n.s. | 0.053 | 0.030 |
| Gma.16706.1.S1_s_at | TCA cycle | citrate synthase 4 | n.s. | n.s. | 0.048 | 0.002 | 0.038 | 0.017 |
| GmaAffx.91660.1.S1_at | TCA cycle | cytosolic malate dehydrogenase | -41.1 | 0.027 | n.s. | n.s. | n.s. | n.s. |
| Gma.6881.1.S1_at | TCA cycle | dihydrolipoyllysine-residue acetyltransferase | n.s. | n.s. | 0.051 | 0.002 | 0.048 | 0.005 |
| GmaAffx.35011.1.S1_s_at | TCA cycle | dihydrolipoyllysine-residue acetyltransferase | n.s. | n.s. | 0.039 | 0.027 | n.s. | n.s. |
| Gma.4395.1.S1_at | TCA cycle | dihyrdolipoamide acetyltransferase, putative | n.s. | n.s. | 0.043 | 0.005 | 0.038 | 0.016 |
| Gma.8428.1.S1_at | TCA cycle | ferric leghemoglobin reductase | n.s. | n.s. | 0.098 | 0.043 | n.s. | n.s. |
| GmaAffx.64222.1.S1_at | TCA cycle | fumarase 1 | n.s. | n.s. | 0.046 | 0.004 | 0.042 | 0.010 |
| GmaAffx.64222.2.S1_at | TCA cycle | fumarate hydratase | 18.9 | 0.012 | 0.031 | 0.035 | n.s. | n.s. |
| Gma.16566.1.S1_at | TCA cycle | fumarate hydratase, putative | n.s. | n.s. | 0.187 | 0.004 | 0.131 | 0.047 |

Table 4.4 (cont)

| Affymetrix Gene ID | Functional Category | Annotation | % change ele[$CO_2$] | p-value | slope at amb [$CO_2$] | p-value | slope at ele[$CO_2$] | p-value |
|---|---|---|---|---|---|---|---|---|
| Gma.14342.1.S1_at | TCA cycle | isocitrate dehydrogenase (NAD+) | n.s. | n.s. | 0.054 | 0.007 | n.s. | n.s. |
| Gma.3343.1.S1_at | TCA cycle | isocitrate dehydrogenase (NAD+) | n.s. | n.s. | 0.050 | 0.043 | n.s. | n.s. |
| Gma.7096.1.S1_at | TCA cycle | isocitrate dehydrogenase1 (NAD+) | -272.7 | 0.003 | n.s. | n.s. | n.s. | n.s. |
| Gma.1268.1.S1_at | TCA cycle | malate dehydrogenase | n.s. | n.s. | 0.069 | 0.001 | 0.058 | 0.005 |
| Gma.16636.1.S1_s_at | TCA cycle | malate dehydrogenase | n.s. | n.s. | 0.070 | 0.004 | 0.061 | 0.014 |
| Gma.7138.2.S1_a_at | TCA cycle | malate dehydrogenase (NADP), chloroplast, putative | n.s. | n.s. | 0.036 | 0.005 | n.s. | n.s. |
| GmaAffx.90332.1.S1_at | TCA cycle | malate dehydrogenase (NADP+) | 19.7 | 0.005 | n.s. | n.s. | n.s. | n.s. |
| Gma.12311.1.S1_at | TCA cycle | malate oxidoreductase, putative | 25.0 | 0.024 | n.s. | n.s. | n.s. | n.s. |
| GmaAffx.11325.1.S1_at | TCA cycle | malate oxidoreductase, putative | n.s. | n.s. | n.s. | n.s. | 0.034 | 0.012 |
| GmaAffx.60527.1.S1_at | TCA cycle | Malic oxidoreductase | n.s. | n.s. | -0.056 | 0.015 | n.s. | n.s. |
| GmaAffx.92463.1.S1_at | TCA cycle | NADP dependent malic enzyme | n.s. | n.s. | n.s. | n.s. | -0.117 | 0.036 |
| GmaAffx.38558.1.S1_at | TCA cycle | NADP-malate dehydrogenase 1 | n.s. | n.s. | -0.128 | <0.001 | -0.091 | 0.006 |
| Gma.10016.1.S1_at | TCA cycle | pyruvate dehydrogenase complex E1 | 10.8 | 0.008 | n.s. | n.s. | n.s. | n.s. |
| Gma.1111.1.S1_x_at | TCA cycle | pyruvate dehydrogenase complex E1 alpha subunit | n.s. | n.s. | 0.077 | 0.001 | 0.058 | 0.010 |
| Gma.1111.1.S1_at | TCA cycle | pyruvate dehydrogenase complex E1 alpha subunit | n.s. | n.s. | 0.088 | 0.002 | n.s. | n.s. |
| GmaAffx.91418.1.S1_at | TCA cycle | pyruvate dehydrogenase complex E1 alpha subunit | n.s. | n.s. | 0.072 | 0.005 | n.s. | n.s. |
| GmaAffx.73010.1.S1_s_at | TCA cycle | pyruvate dehydrogenase complex E1 alpha subunit | n.s. | n.s. | 0.063 | 0.005 | n.s. | n.s. |
| Gma.5536.1.S1_s_at | TCA cycle | succinate dehydrogenase 2-2 | n.s. | n.s. | 0.037 | 0.010 | 0.047 | 0.001 |
| Gma.5536.1.S1_at | TCA cycle | succinate dehydrogenase 2-2 | n.s. | n.s. | 0.064 | <0.001 | 0.050 | 0.004 |
| Gma.584.3.S1_at | TCA cycle | succinate dehydrogenase subunit 3 | n.s. | n.s. | 0.032 | 0.017 | n.s. | n.s. |
| Gma.16923.1.A1_s_at | TCA cycle | succinate dehydrogenase subunit 4 | n.s. | n.s. | n.s. | n.s. | 0.028 | 0.025 |
| Gma.4267.1.S1_at | TCA cycle | succinate dehydrogenase subunit 4 | n.s. | n.s. | n.s. | n.s. | 0.036 | 0.009 |
| GmaAffx.1301.39.S1_at | TCA cycle | succinyl-CoA ligase alpha-chain, putative | n.s. | n.s. | 0.082 | 0.031 | n.s. | n.s. |

# CHAPTER 5: CONCLUDING REMARKS

This thesis systematically addressed how elevated [$CO_2$], elevated [$O_3$] and a combination of both elevated [$CO_2$] and elevated [$O_3$] affected soybean antioxidant metabolism in a controlled environmental study and in a field system. I first developed small-scale and high-throughput assays to quantitatively assess the variability in the antioxidant system (Chapter 2). The ORAC, ASA and phenolic assays provided accurate, rapid and high-throughput measures of both the general and specific antioxidant action of plant tissue extracts. In soybean leaves, I found a significant positive correlation between ORAC, and total phenolic content and total ascorbate content, which are known major contributors to the total antioxidant capacity in plant leaves. These assays have been subsequently used to investigate how antioxidant capacity varies among soybean cultivars when grown at different [$O_3$] and to test their utility as potential biochemical markers of $O_3$ tolerance (Betzelberger *et al.*, 2010).

In Chapter 3, I investigated how growth environment alters plant antioxidant metabolism and response to an acute oxidative stress. The prevailing view in the literature is that elevated [$O_3$] causes an up-regulation of the antioxidant metabolism in plants (Olbrich *et al.*, 2009; Puckette *et al.*, 2007; Ranieri *et al.*, 1996; Ranieri *et al.*, 2000; Scebba *et al.*, 2003; Xu *et al.*, 2008). However, the direct evidence for this up-regulation has been variable and dependent on the duration and method of $O_3$ fumigation, and the components of antioxidant metabolism investigated (Burkey *et al.*, 2000; Iglesias *et al.*, 2006; Robinson and Britz, 2000). Likewise, reports investigating the effects of growth at elevated [$CO_2$] showed contrasting responses (di Toppi *et al.*, 2002; Polle *et al.*, 1997; Pritchard *et al.*, 2000; Rao *et al.*, 1995), and there is even recent evidence of increased oxidative stress in elevated [$CO_2$] (Qiu *et al.*, 2008). I investigated the antioxidant system at the metabolite, enzymatic and transcriptional levels in order to test

those prevailing views. Chapter 3 confirmed the hypotheses that growth environment alters the antioxidant system, the immediate response to an acute oxidative stress and the timing over which plants return to initial antioxidant levels. I demonstrated that growth in a chronic high [$O_3$] environment increased total antioxidant capacity, while chronic elevated [$CO_2$] decreased total antioxidant capacity. The growth environment also significantly altered the pattern of antioxidant transcript and enzyme response to an acute oxidative stress. Growth at high [$O_3$] increased the basal levels of components of the antioxidant system, which were then unchanged or only slightly increased following an acute oxidative stress, suggesting that growth at chronic elevated [$O_3$] allowed for a primed antioxidant system. Growth at high [$CO_2$] decreased the basal level of antioxidant capacity, increased the response of the existing antioxidant enzymes, but dampened and delayed the transcriptional response. The time-frame across which different components of the plant antioxidant system recovered from the acute $O_3$ spike differed considerably as well, suggesting distinct mechanisms of control in different environments.

Finally, I used a genomic ecology approach to investigate antioxidant metabolism in field-grown soybean at different biological scales, over an entire growing season (Chapter 4). By combining principle components analysis and an analysis of covariance, I was able to explain the effects of [$O_3$] on plants grown at both ambient and elevated [$CO_2$], while also accounting for the variability in other environmental factors. As in Chapter 3, I demonstrated that growth at elevated [$CO_2$] in a field system generally lowered antioxidant metabolism, which was manifested through lower total antioxidant capacity and DHA content, as well as lower total enzyme activity of SOD and MDHAR. Growth at increasing levels of [$O_3$] increased metabolic and genomic components of the antioxidant system, while total activity of the antioxidant enzymes was correlated with changes in other environmental conditions. The results suggest

higher enzyme turnover with increasing [$O_3$] and a role for post-translational control of antioxidant enzymes. In addition, I provide evidence that the soybean antioxidant system responded to chronic elevated [$O_3$] in a similar manner regardless of the [$CO_2$] environment, but that the response was dampened at elevated [$CO_2$], which may be explained by lower flux of [$O_3$] into the leaf. This is in contrast to the transcriptional response to the acute $O_3$ spike in Chapter 3, where plants grown under ambient and elevated [$CO_2$] showed different transcriptional responses. While the terms chronic and acute are subjectively applied to different $O_3$ studies (Fiscus et al., 2005), my results support the notion that acute and chronic [$O_3$] exposures do not promote identical mechanisms of response (Chen *et al.*, 2009).

In addition to increases in antioxidant metabolism with higher [$O_3$], the gene expression results in Chapter 4 implied a coordinated up-regulation of tetrapyrrole synthesis in both ambient and elevated [$CO_2$]. While there were no changes in chlorophyll content, the transcriptional data suggest higher rates of chlorophyll turnover at increasing [$O_3$], which has not been reported in the literature to date and warrants further investigation. The transcriptional data also provided genomic evidence for increases in respiration at higher [$O_3$] in both ambient and elevated [$CO_2$] environments, which would support the energetic costs of antioxidant metabolism and chlorophyll synthesis.

## REFERENCES


**Ainsworth EA, Gillespie KM**. 2007. Estimation of total phenolic content and other oxidation substrates in plant tissues using Folin-Ciocalteu reagent. *Nature Protocols* **2**, 875-877.

**Ainsworth EA, Rogers A, Leakey ADB, Heady LE, Gibon Y, Stitt M, Schurr U**. 2007. Does elevated atmospheric $CO_2$ alter diurnal C uptake and the balance of C and N metabolites in growing and fully expanded soybean leaves? *Journal of Experimental Botany* **58**, 579-591.

**Ainsworth EA, Rogers A, Vodkin LO, Walter A, Schurr U**. 2006. The effects of elevated $CO_2$ concentration on soybean gene expression. An analysis of growing and mature leaves. *Plant Physiology* **142**, 135-147.

**Amthor JS**. 1988. Growth and maintenance respiration in leaves of bean (*Phaseolus-vulgaris L.*) exposed to ozone in open-top chambers in the field. *New Phytologist* **110**, 319-325.

**Amthor JS, Cumming JR**. 1988. Low-levels of ozone increase bean leaf maintenance respiration. *Canadian Journal of Botany-Revue Canadienne De Botanique* **66**, 724-726.

**Asada K**. 1984. Chloroplasts: Formation of active oxygen and its scavenging. Oxygen Radicals in Biological Systems. In: Packer L, ed. *Methods in Enzymology*, Vol. 105. Orlando: Academic Press, 422-429.

**Asada K, Takehashi M**. 1987. Production and scavenging of active oxygen in photosynthesis. In: Kyle DJ, Osmond CB, Amtzen CJ, eds. *Photoinhibition*. Amsterdam, The Netherlands: Elsevier, 227-287.

**Ashmore MR**. 2005. Assessing the future global impacts of ozone on vegetation. *Plant Cell and Environment* **28**, 949-964.

**Badiani M, Dannibale A, Paolacci AR, Miglietta F, Raschi A**. 1993. The antioxidant status of Soybean (*Glycine-max*) leaves grown under natural $CO_2$ enrichment in the field. *Australian Journal of Plant Physiology* **20**, 275-284.

**Badiani M, Paolacci AR, Fusari A, Bettarini I, Brugnoli E, Lauteri M, Miglietta F, Raschi A**. 1998. Foliar antioxidant status of plants from naturally high-$CO_2$ sites. *Physiologia Plantarum* **104**, 765-771.

**Baier M, Kandlbinder A, Golldack D, Dietz KJ**. 2005. Oxidative stress and ozone: perception, signalling and response. *Plant Cell and Environment* **28**, 1012-1020.

**Barth C, De Tullio M, Conklin PL**. 2006. The role of ascorbic acid in the control of flowering time and the onset of senescence. *Journal of Experimental Botany* **57**, 1657-1665.

**Bernacchi CJ, Leakey ADB, Heady LE, Morgan PB, Dohleman FG, McGrath JM, Gillespie KM, Wittig VE, Rogers A, Long SP, Ort DR**. 2006. Hourly and seasonal variation in photosynthesis and stomatal conductance of soybean grown at future $CO_2$ and ozone concentrations for 3 years under fully open-air field conditions. *Plant Cell and Environment* **29**, 2077-2090.

**Betzelberger AM, Gillespie KM, McGrath JM, Koester RP, Nelson RL, Ainsworth EA**. 2010. Effects of chronic elevated ozone concentration on antioxidant capacity, photosynthesis and seed yield of 10 soybean cultivars. *Plant, Cell and Environment **in press***.

**Bienert GP, Moller ALB, Kristiansen KA, Schulz A, Moller IM, Schjoerring JK, Jahn TP**. 2007. Specific aquaporins facilitate the diffusion of hydrogen peroxide across membranes. *Journal of Biological Chemistry* **282**, 1183-1192.

**Bilgin DD, DeLucia EH, Clough SJ**. 2009. A robust plant RNA isolation method suitable for Affymetrix GeneChip analysis and quantitative real-time RT-PCR. *Nature Protocols* **4**, 333-340.

**Bolwell GP, Bindschedler LV, Blee KA, Butt VS, Davies DR, Gardner SL, Gerrish C, Minibayeva F**. 2002. The apoplastic oxidative burst in response to biotic stress in plants: a three-component system. *Journal of Experimental Botany* **53**, 1367-1376.

**Booker FL, Fiscus EL**. 2005. The role of ozone flux and antioxidants in the suppression of ozone injury by elevated $CO_2$ in soybean. *Journal of Experimental Botany* **56**, 2139-2151.

**Bors W, Heller W, Michel C, Saran M**. 1990. Flavanoids as antioxidants - determination of radical-scavenging efficiencies. *Methods in Enzymology* **186**, 343-355.

**Burkey KO, Eason G, Fiscus EL**. 2003. Factors that affect leaf extracellular ascorbic acid content and redox status. *Physiologia Plantarum* **117**, 51-57.

**Burkey KO, Wei CM, Eason G, Ghosh P, Fenner GP**. 2000. Antioxidant metabolite levels in ozone-sensitive and tolerant genotypes of snap bean. *Physiologia Plantarum* **110**, 195-200.

**Cao GH, Prior RL**. 1999. Measurement of oxygen radical absorbance capacity in biological samples. *Oxidants and Antioxidants, Pt A*, Vol. 299, 50-62.

**Carol RJ, Dolan L**. 2006. The role of reactive oxygen species in cell growth: lessons from root hairs. *Journal of Experimental Botany* **57**, 1829-1834.

**Chang A, Scheer M, Grote A, Schomburg I, Schomburg D**. 2009. BRENDA, AMENDA and FRENDA the enzyme information system: new content and tools in 2009. *Nucleic Acids Research* **37**, D588-D592.

**Chu CC, Lee WC, Guo WY, Pan SM, Chen LJ, Li HM, Jinn TL**. 2005. A copper chaperone for superoxide dismutase that confers three types of copper/zinc superoxide dismutase activity in Arabidopsis. *Plant Physiology* **139**, 425-436.

**Cohu CM, Abdel-Ghany SE, Reynolds KAG, Onofrio AM, Bodecker JR, Kimbrel JA, Niyogi KK, Pilon M**. 2009. Copper delivery by the copper chaperone for chloroplast and cytosolic copper/zinc-superoxide dismutases: regulation and unexpected phenotypes in an Arabidopsis mutant. *Molecular Plant* **2**, 1336-1350.

**Conklin PL, Barth C**. 2004. Ascorbic acid, a familiar small molecule intertwined in the response of plants to ozone, pathogens, and the onset of senescence. *Plant Cell and Environment* **27**, 959-970.

**Conklin PL, Saracco SA, Norris SR, Last RL**. 2000. Identification of ascorbic acid-deficient Arabidopsis thaliana mutants. *Genetics* **154**, 847-856.

**Conrath U, Beckers GJM, Flors V, García-Agustín P, Jakab G, Mauch F, Newman M-A, Pieterse CMJ, Poinssot B, Pozo MJ, Pugin A, Schaffrath U, Ton J, Wendehenne D, Zimmerli L, Mauch-Mani B**. 2006. Priming: getting ready for battle. *Molecular Plant-Microbe Interactions* **19**, 1062-1071.

**Croteau R, Kutchan TM, Lewis NG**. 2000. Natural Products (secondary metabolites). In: Buchanan BB, Gruissem W, Jones RL, eds. *Biochemistry and Molecular Biology of Plants*. Beltsville, MD: American Society of Plant Physiologists, 1250-1318.

**Dalton DA, Russell SA, Hanus FJ, Pascoe GA, Evans HJ**. 1986. Enzymatic-reactions of ascorbate and glutathione that prevent peroxide damage in soybran root-nodules. *Proceedings of the National Academy of Sciences of the United States of America* **83**, 3811-3815.

**Dat J, Vandenabeele S, Vranova E, Van Montagu M, Inze D, Van Breusegem F**. 2000. Dual action of the active oxygen species during plant stress responses. *Cellular and Molecular Life Sciences* **57**, 779-795.

**Dat JF, Foyer CH, Scott IM**. 1998. Changes in salicylic acid and antioxidants during induced thermotolerance in mustard seedlings. *Plant Physiology* **118**, 1455-1461.

**De Gara L, de Pinto MC, Tommasi F**. 2003. The antioxidant systems vis-a-vis reactive oxygen species during plant-pathogen interaction. *Plant Physiology and Biochemistry* **41**, 863-870.

**Desikan R, Mackerness SAH, Hancock JT, Neill SJ**. 2001. Regulation of the Arabidopsis transcriptome by oxidative stress. *Plant Physiology* **127**, 159-172.

**Di Baccio D, Castagna A, Paoletti E, Sebastiani L, Ranieri A**. 2008. Could the differences in $O_3$ sensitivity between two poplar clones be related to a difference in antioxidant defense and secondary metabolic response to $O_3$ influx? *Tree Physiology* **28**, 1761-1772.

**di Toppi LS, Marabottini R, Badiani M, Raschi A**. 2002. Antioxidant status in herbaceous plants growing under elevated $CO_2$ in mini-FACE rings. *Journal of Plant Physiology* **159**, 1005-1013.

**Dizengremel P, Le Thiec D, Bagard M, Jolivet Y**. 2008. Ozone risk assessment for plants: Central role of metabolism-dependent changes in reducing power. *Environmental Pollution* **156**, 11-15.

**Dizengremel P, Le Thiec D, Hasenfratz-Sauder MP, Vaultier MN, Bagard M, Jolivet Y**. 2009. Metabolic-dependent changes in plant cell redox power after ozone exposure. *Plant Biology* **11**, 35-42.

**Druart N, Rodriguez-Buey M, Barron-Gafford G, Sjodin A, Bhalerao R, Hurry V**. 2006. Molecular targets of elevated $CO_2$ in leaves and stems of *Populus deltoides*: implications for future tree growth and carbon sequestration. *Functional Plant Biology* **33**, 121-131.

**Dutilleul C, Garmier M, Noctor G, Mathieu C, Chetrit P, Foyer CH, de Paepe R**. 2003. Leaf mitochondria modulate whole cell redox homeostasis, set antioxidant capacity, and determine stress resistance through altered signaling and diurnal regulation. *Plant Cell* **15**, 1212-1226.

**Edwards EA, Enard C, Creissen GP, Mullineaux PM**. 1994. Synthesis and properties of glutathione-reductase in stressed peas. *Planta* **192**, 137-143.

**Edwards EA, Rawsthorne S, Mullineaux PM**. 1990. Subcellular-distribution of multiple forms of glutathione-reductase in leaves of pea (*Pisum-Sativum-L*). *Planta* **180**, 278-284.

**Eltayeb AE, Kawano N, Badawi GH, Kaminaka H, Sanekata T, Shibahara T, Inanaga S, Tanaka K**. 2007. Overexpression of monodehydroascorbate reductase in transgenic tobacco confers enhanced tolerance to ozone, salt and polyethylene glycol stresses. *Planta* **225**, 1255-1264.

**Ewing JF, Janero DR**. 1995. Microplate superoxide dismutase assay employing a nonenzymatic superoxide generator. *Analytical Biochemistry* **232**, 243-248.

**Fedoroff N**. 2006. Redox regulatory mechanisms in cellular stress responses. *Annals of Botany* **98**, 289-300.

**Finkel T, Holbrook NJ**. 2000. Oxidants, oxidative stress and the biology of ageing. *Nature* **408**, 239-247.

**Fiscus EL, Booker FL, Burkey KO**. 2005. Crop responses to ozone: uptake, modes of action, carbon assimilation and partitioning. *Plant Cell and Environment* **28**, 997-1011.

**Fiscus EL, Reid CD, Miller JE, Heagle AS**. 1997. Elevated $CO_2$ reduces $O_3$ flux and $O_3$-induced yield losses in soybeans: Possible implications for elevated $CO_2$ studies. *Journal of Experimental Botany* **48**, 307-313.

**Folin O, Ciocalteu V**. 1927. On tyrosine and tryptophane determinations in proteins. *Journal of Biological Chemistry* **73**, 627-650.

**Foyer C, Rowell J, Walker D**. 1983. Measurement of the ascorbate content of spinach leaf protoplasts and chloroplasts during illumination. *Planta* **157**, 239-244.

**Foyer CH, Halliwell B**. 1976. Presence of glutathione reductase in chloroplasts - proposed role in ascorbic-acid metabolism. *Planta* **133**, 21-25.

**Foyer CH, Lelandais M, Kunert KJ**. 1994. Photooxidative stress in plants. *Physiologia Plantarum* **92**, 696-717.

**Foyer CH, Noctor G**. 2005. Redox homeostasis and antioxidant signaling: A metabolic interface between stress perception and physiological responses. *Plant Cell* **17**, 1866-1875.

**Foyer CH, Noctor G**. 2009. Redox regulation in photosynthetic organisms: Signaling, acclimation, and practical implications. *Antioxidants & Redox Signaling* **11**, 861-905.

**Gandin A, Lapointe L, Dizengremel P**. 2009. The alternative respiratory pathway allows sink to cope with changes in carbon availability in the sink-limited plant *Erythronium americanum*. *Journal of Experimental Botany* **60**, 4235-4248.

**Gillespie KM, Ainsworth EA**. 2007. Measurement of reduced, oxidized and total ascorbate content in plants. *Nature Protocols* **2**, 871-874.

**Gillespie KM, Chae JM, Ainsworth EA**. 2007. Rapid measurement of total antioxidant capacity in plants. *Nature Protocols* **2**, 867-870.

**Gillespie KM, Rogers A, Ainsworth EA**. 2010. Long-term exposure to elevated ozone or elevated carbon dioxide alters antioxidant capacity and response to acute oxidative stress. *Journal of Experimental Biology* ***in review***.

**Grace SC**. 2005. Phenolics as antioxidants. In: Smirnoff N, ed. *Antioxidants and Reactive Oxygen Species in Plants*. Oxford, UK: Blackwell Publishing, 141-168.

**Grace SC, Logan BA**. 2000. Energy dissipation and radical scavenging by the plant phenylpropanoid pathway. *Philosophical Transactions of the Royal Society of London Series B-Biological Sciences* **355**, 1499-1510.

**Grantz DA, Silva V, Toyota M, Ott N**. 2003. Ozone increases root respiration but decreases leaf $CO_2$ assimilation in cotton and melon. *Journal of Experimental Botany* **54**, 2375-2384.

**Griesen D, Su D, Berczi A, Asard H**. 2004. Localization of an ascorbate-reducible cytochrome b561 in the plant tonoplast. *Plant Physiology* **134**, 726-734.

**Griffin KL, Anderson OR, Gastrich MD, Lewis JD, Lin GH, Schuster W, Seemann JR, Tissue DT, Turnbull MH, Whitehead D**. 2001. Plant growth in elevated $CO_2$ alters mitochondrial number and chloroplast fine structure. *Proceedings of the National Academy of Sciences of the United States of America* **98**, 2473-2478.

**Havir EA, McHale NA**. 1987. Biochemical and developmental characterization of multiple forms of catalase in tobacco-leaves. *Plant Physiology* **84**, 450-455.

**He XY, Fu SL, Chen W, Zhao TH, Xu S, Tuba Z**. 2007. Changes in effects of ozone exposure on growth, photosynthesis, and respiration of *Ginkgo biloba* in Shenyang urban area. *Photosynthetica* **45**, 555-561.

**Heath RL**. 2008. Modification of the biochemical pathways of plants induced by ozone: What are the varied routes to change? *Environmental Pollution* **155**, 453-463.

**Held AA, Mooney HA, Gorham JN**. 1991. Acclimation to ozone stress in radish - leaf demography and photosynthesis. *New Phytologist* **118**, 417-423.

**Hertwig B, Streb P, Feierabend J**. 1992. Light dependence of catalase synthesis and degradation in leaves and the influence of interfering stress conditions. *Plant Physiology* **100**, 1547-1553.

**Hewitt EJ, Dickes GJ**. 1961. Spectrophotometric measurements of ascorbic acid and their use for estimation of ascorbic acid and dehydroascorbic acid in plant tissues. *Biochemical Journal* **78**, 384-&.

**Horemans N, Asard H, Caubergs RJ**. 1997. The ascorbate carrier of higher plant plasma membranes preferentially translocates the fully oxidized (dehydroascorbate) molecule. *Plant Physiology* **114**, 1247-1253.

**Horemans N, Foyer CH, Potters G, Asard H**. 2000. Ascorbate function and associated transport systems in plants. *Plant Physiology and Biochemistry* **38**, 531-540.

**Huang DJ, Ou BX, Hampsch-Woodill M, Flanagan JA, Deemer EK**. 2002. Development and validation of oxygen radical absorbance capacity assay for lipophilic antioxidants using

randomly methylated beta-cyclodextrin as the solubility enhancer. *Journal of Agricultural and Food Chemistry* **50**, 1815-1821.

**Huang DJ, Ou BX, Prior RL**. 2005. The chemistry behind antioxidant capacity assays. *Journal of Agricultural and Food Chemistry* **53**, 1841-1856.

**Iglesias DJ, Calatayud A, Barreno E, Primo-Millo E, Talon M**. 2006. Responses of citrus plants to ozone: leaf biochemistry, antioxidant mechanisms and lipid peroxidation. *Plant Physiology and Biochemistry* **44**, 125-131.

**Jahnke LS, Hull MR, Long SP**. 1991. Chilling stress and oxygen metabolizing enzymes in *Zea-Mays* and *Zea-Diploperennis*. *Plant Cell and Environment* **14**, 97-104.

**Janes KA, Yaffe MB**. 2006. Data-driven modelling of signal-transduction networks. *Nature Reviews Molecular Cell Biology* **7**, 820-828.

**Kampfenkel K, Vanmontagu M, Inze D**. 1995. Extraction and determination of ascorbate and dehydroascorbte from plant-tissue. *Analytical Biochemistry* **225**, 165-167.

**Kangasjarvi J, Jaspers P, Kollist H**. 2005. Signaling and cell death in ozone-exposed plants. *Plant Cell and Environment* **28**, 1021-1036.

**Karnosky DF, Zak DR, Pregitzer KS, Awmack CS, Bockheim JG, Dickson RE, Hendrey GR, Host GE, King JS, Kopper BJ, Kruger EL, Kubiske ME, Lindroth RL, Mattson WJ, McDonald EP, Noormets A, Oksanen E, Parsons WFJ, Percy KE, Podila GK, Riemenschneider DE, Sharma P, Thakur R, Sober A, Sober J, Jones WS, Anttonen S, Vapaavuori E, Mankovska B, Heilman W, Isebrands JG**. 2003. Tropospheric $O_3$ moderates responses of temperate hardwood forests to elevated $CO_2$: a synthesis of molecular to ecosystem results from the Aspen FACE project. *Functional Ecology* **17**, 289-304.

**Knight H, Brandt S, Knight MR**. 1998. A history of stress alters drought calcium signaling pathways in Arabidopsis. *Plant Journal* **16**, 681-687.

**Laisk A, Kull O, Moldau H**. 1989. Ozone concentration in leaf intercellular air spaces is close to zero. *Plant Physiology* **90**, 1163-1167.

**Leakey ADB, Ainsworth EA, Bernard SM, Markelz RJC, Ort DR, Placella SA, Rogers A, Smith MD, Sudderth EA, Weston DJ, Wullschleger SD, Yuan SH**. 2009a. Gene expression profiling: opening the black box of plant ecosystem responses to global change. *Global Change Biology* **15**, 1201-1213.

**Leakey ADB, Uribelarrea M, Ainsworth EA, Naidu SL, Rogers A, Ort DR, Long SP**. 2006. Photosynthesis, productivity, and yield of maize are not affected by open-air elevation of CO2 concentration in the absence of drought. *Plant Physiology* **140**, 779-790.

**Leakey ADB, Xu FX, Gillespie KM, McGrath JM, Ainsworth EA, Ort DR**. 2009b. Genomic basis for stimulated respiration by plants growing under elevated carbon dioxide. *Proceedings of the National Academy of Sciences of the United States of America* **106**, 3597-3602.

**Libault M, Thibivilliers S, Bilgin DD, Radwan O, Benitez M, Clough SJ, Stacey G**. 2008. Identification of four soybean reference genes for gene expression normalization. *Plant Genome* **1**, 44-54.

**Littel RC, Milliken GA, Stroup WW, Wolfinger RD, Schabenberger O**. 2006. *SAS for Mixed Models, Second Edition*. Cary, NC: SAS Institute Inc.

**Long SP, Ainsworth EA, Leakey ADB, Nosberger J, Ort DR**. 2006. Food for thought: Lower-than-expected crop yield stimulation with rising $CO_2$ concentrations. *Science* **312**, 1918-1921.

**Long SP, Naidu SL**. 2002. Effects of oxidants at the biochemical, cell and physiological levels. In: Treshow M, ed. *Air Pollution and Plants*. London: John Wiley, 68-88.

**Low M, Haberle KH, Warren CR, Matyssek R**. 2007. $O_3$ flux-related responsiveness of photosynthesis, respiration, and stomatal conductance of adult *Fagus sylvatica* to experimentally enhanced free-air $O_3$ exposure. *Plant Biology* **9**, 197-206.

**Luwe MWF, Takahama U, Heber U**. 1993. Role of Ascorbate in Detoxifying Ozone in the Apoplast of Spinach (Spinacia-Oleracea L) Leaves. *Plant Physiology* **101**, 969-976.

**Mahalingam R, Shah N, Scrymgeour A, Fedoroff N**. 2005. Temporal evolution of the Arabidopsis oxidative stress response. *Plant Molecular Biology* **57**, 709-730.

**Maickel RP**. 1960. A rapid procedure for the determination of adrenal ascorbic acid - application of the Sullivan and Clarke Method to tissues. *Analytical Biochemistry* **1**, 498-501.

**McKee IF, Eiblmeier M, Polle A**. 1997. Enhanced ozone-tolerance in wheat grown at an elevated $CO_2$ concentration: ozone exclusion and detoxification. *New Phytologist* **137**, 275-284.

**McKee IF, Farage PK, Long SP**. 1995. The interactive effects of elevated $CO_2$ and $O_3$ concentration on photosynthesis in spring wheat. *Photosynthesis Research* **45**, 111-119.

**Mittler R**. 2002. Oxidative stress, antioxidants and stress tolerance. *Trends in Plant Science* **7**, 405-410.

**Miyazaki S, Fredricksen M, Hollis KC, Poroyko V, Shepley D, Galbraith DW, Long SP, Bohnert HJ**. 2004. Transcript expression profiles of *Arabidopsis thaliana* grown under

controlled conditions and open-air elevated concentrations of $CO_2$ and of $O_3$. *Field Crops Research* **90**, 47-59.

**Morgan PB, Bernacchi CJ, Ort DR, Long SP**. 2004. An in vivo analysis of the effect of season-long open-air elevation of ozone to anticipated 2050 levels on photosynthesis in soybean. *Plant Physiology* **135**, 2348-2357.

**Nagendra-Prasad D, Sudhakar N, Murugesan K, Mohan N**. 2008. Pre-exposure of calli to ozone promotes tolerance of regenerated *Lycopersicon esculentum cv. PKM1* plantlets against acute ozone stress. *Journal of Plant Physiology* **165**, 1288-1299.

**Niewiadomska E, Polzien L, Desel C, Rozpadek P, Miszalski Z, Krupinska K**. 2009. Spatial patterns of senescence and development-dependent distribution of reactive oxygen species in tobacco (*Nicotiana tabacum*) leaves. *Journal of Plant Physiology* **166**, 1057-1068.

**Noctor G**. 2006. Metabolic signalling in defence and stress: the central roles of soluble redox couples. *Plant Cell and Environment* **29**, 409-425.

**Noctor G, Foyer CH**. 1998. Ascorbate and glutathione: Keeping active oxygen under control. *Annual Review of Plant Physiology and Plant Molecular Biology* **49**, 249-279.

**Okamura M**. 1980. An improved method for determination of L-ascorbic-acid and L-dehydroascorbic acid in blood-plasma. *Clinica Chimica Acta* **103**, 259-268.

**Omaye ST, Turnbull JD, Sauberlich HE**. 1979. Selected methods for the determination of ascorbic acid in animal cells, tissues, and fluids. *Methods Enzymol* **62**, 3-11.

**Overmyer K, Brosche M, Kangasjarvi J**. 2003. Reactive oxygen species and hormonal control of cell death. *Trends in Plant Science* **8**, 335-342.

**Paoletti E, Grulke NE**. 2005. Does living in elevated $CO_2$ ameliorate tree response to ozone? A review on stomatal responses. *Environmental Pollution* **137**, 483-493.

**Pasquer F, Isidore E, Zarn J, Keller B**. 2005. Specific patterns of changes in wheat gene expression after treatment with three antifungal compounds. *Plant Molecular Biology* **57**, 693-707.

**Pastori GM, Mullineaux PM, Foyer CH**. 2000. Post-transcriptional regulation prevents accumulation of glutathione reductase protein and activity in the bundle sheath cells of maize. *Plant Physiology* **122**, 667-675.

**Pei ZM, Murata Y, Benning G, Thomine S, Klusener B, Allen GJ, Grill E, Schroeder JI**. 2000. Calcium channels activated by hydrogen peroxide mediate abscisic acid signalling in guard cells. *Nature* **406**, 731-734.

**Pignocchi C, Foyer CH**. 2003. Apoplastic ascorbate metabolism and its role in the regulation of cell signalling. *Current Opinion in Plant Biology* **6**, 379-389.

**Polle A**. 1996. Mehler reaction: Friend or foe in photosynthesis? *Botanica Acta* **109**, 84-89.

**Polle A**. 2001. Dissecting the superoxide dismutase-ascorbate-glutathione-pathway in chloroplasts by metabolic modeling. Computer simulations as a step towards flux analysis. *Plant Physiology* **126**, 445-462.

**Polle A, Eiblmeier M, Sheppard L, Murray M**. 1997. Responses of antioxidative enzymes to elevated $CO_2$ in leaves of beech (*Fagus sylvatica L.*) seedlings grown under a range of nutrient regimes. *Plant Cell and Environment* **20**, 1317-1321.

**Polle A, Pfirrmann T, Chakrabarti S, Rennenberg H**. 1993. The effects of enhanced ozone and enhanced carbon-dioxide concentrations on biomass, pigments and antioxidative enzymes in spruce needles (*Picea-Abies L*). *Plant Cell and Environment* **16**, 311-316.

**Prentice IC, Farquhar GD, Fasham MJR, Goulden ML, Heimann M, Jaramillo VJ, Kheshgi HS, Le Quere C, Scholes RJ, Wallace DWR**. 2001. The carbon cycle and atmospheric carbon dioxide. In: Houghton JT, Ding Y, Griggs DJ, Noguer M, van der Linden PJ, Dai X, Maskell K, Johnson CA, eds. *IPCC Climate Change 2001: The Scientific Basis*. Cambridge, UK: Cambridge University Press, 183-237.

**Prior RL, Hoang H, Gu LW, Wu XL, Bacchiocca M, Howard L, Hampsch-Woodill M, Huang DJ, Ou BX, Jacob R**. 2003. Assays for hydrophilic and lipophilic antioxidant capacity (oxygen radical absorbance capacity (ORAC(FL)) of plasma and other biological and food samples. *Journal of Agricultural and Food Chemistry* **51**, 3273-3279.

**Prior RL, Wu XL, Schaich K**. 2005. Standardized methods for the determination of antioxidant capacity and phenolics in foods and dietary supplements. *Journal of Agricultural and Food Chemistry* **53**, 4290-4302.

**Pritchard SG, Ju ZL, van Santen E, Qiu JS, Weaver DB, Prior SA, Rogers HH**. 2000. The influence of elevated $CO_2$ on the activities of antioxidative enzymes in two soybean genotypes. *Australian Journal of Plant Physiology* **27**, 1061-1068.

**Puckette MC, Tang YH, Mahalingam R**. 2008. Transcriptomic changes induced by acute ozone in resistant and sensitive *Medicago truncatula* accessions. *BMC Plant Biology* **8**, (23 April 2008).

**Puckette MC, Weng H, Mahalingam R**. 2007. Physiological and biochemical responses to acute ozone-induced oxidative stress in *Medicago truncatula*. *Plant Physiology and Biochemistry* **45**, 70-79.

**Qiu QS, Huber JL, Booker FL, Jain V, Leakey ADB, Fiscus EL, Yau PM, Ort DR, Huber SC**. 2008. Increased protein carbonylation in leaves of Arabidopsis and soybean in response to elevated $CO_2$. *Photosynthesis Research* **97**, 155-166.

**Ranieri A, Durso G, Nali C, Lorenzini G, Soldatini GF**. 1996. Ozone stimulates apoplastic antioxidant systems in pumpkin leaves. *Physiologia Plantarum* **97**, 381-387.

**Rao MV, Hale BA, Ormrod DP**. 1995. Amelioration of ozone-induced oxidative damage in wheat plants grown under high-carbon dioxide - role of antioxidant enzymes. *Plant Physiology* **109**, 421-432.

**Robinson JM, Britz SJ**. 2000. Tolerance of a field grown soybean cultivar to elevated ozone level is concurrent with higher leaflet ascorbic acid level, higher ascorbate-dehydroascorbate redox status, and long term photosynthetic productivity. *Photosynthesis Research* **64**, 77-87.

**Ruijter JM, Ramakers C, Hoogaars WMH, Karlen Y, Bakker O, van den Hoff MJB, Moorman AFM**. 2009. Amplification efficiency: linking baseline and bias in the analysis of quantitative PCR data. *Nucleic Acids Research* **37**.

**Sanmartin M, Drogoudi PD, Lyons T, Pateraki I, Barnes J, Kanellis AK**. 2003. Over-expression of ascorbate oxidase in the apoplast of transgenic tobacco results in altered ascorbate and glutathione redox states and increased sensitivity to ozone. *Planta* **216**, 918-928.

**Scheibe R, Backhausen JE, Emmerlich V, Holtgrefe S**. 2005. Strategies to maintain redox homeostasis during photosynthesis under changing conditions. *Journal of Experimental Botany* **56**, 1481-1489.

**Schmidt M, Dehne S, Feierabend J**. 2002. Post-transcriptional mechanisms control catalase synthesis during its light-induced turnover in rye leaves through the availability of the hemin cofactor and reversible changes of the translation efficiency of mRNA. *Plant Journal* **31**, 601-613.

**Schmutz J, Cannon SB, Schlueter J, Ma JX, Mitros T, Nelson W, Hyten DL, Song QJ, Thelen JJ, Cheng JL, Xu D, Hellsten U, May GD, Yu Y, Sakurai T, Umezawa T, Bhattacharyya MK, Sandhu D, Valliyodan B, Lindquist E, Peto M, Grant D, Shu SQ, Goodstein D, Barry K, Futrell-Griggs M, Abernathy B, Du JC, Tian ZX, Zhu LC, Gill N, Joshi T, Libault M, Sethuraman A, Zhang XC, Shinozaki K, Nguyen HT, Wing RA, Cregan P, Specht J, Grimwood J, Rokhsar D, Stacey G, Shoemaker RC, Jackson SA**. 2010. Genome sequence of the palaeopolyploid soybean. *Nature* **463**, 178-183.

**Schwanz P, Kimball BA, Idso SB, Hendrix DL, Polle A**. 1996. Antioxidants in sun and shade leaves of sour orange trees (*Citrus aurantium*) after long-term acclimation to elevated $CO_2$. *Journal of Experimental Botany* **47**, 1941-1950.

**Sehmer L, Fontaine V, Antoni F, Dizengremel P**. 1998. Effects of ozone and elevated atmospheric carbon dioxide on carbohydrate metabolism of spruce needles. Catabolic and detoxification pathways. *Physiologia Plantarum* **102**, 605-611.

**Singleton VL, Orthofer R, Lamuela-Raventos RM**. 1999. Analysis of total phenols and other oxidation substrates and antioxidants by means of Folin-Ciocalteu reagent. *Oxidants and Antioxidants, Pt A* **299**, 152-178.

**Singleton VL, Rossi JA**. 1965. Colorimetry of total phenolics with phospho-molybdic-phosphotungstic acid reagents. *Am. J. Enol. Vitic.* **16**, 144-158.

**Smirnoff N**. 2000. Ascorbic acid: metabolism and functions of a multi-facetted molecule. *Current Opinion in Plant Biology* **3**, 229-235.

**Smirnoff N**. 2005. Ascorbate, tocopherol and carotenoids: metabolism, pathway engineering and functions. In: Smirnoff N, ed. *Antioxidnts and Reactive Oxygen Species in Plants*. Oxford, UK: Blackwell Publishing, 53-86.

**Solomon S, Qin D, Manning M, Chen Z, Marquis M, Averyt KB, Tignor M, Miller HL, eds.** 2007. *The Physical Science Basis. Contribution of Working Group I to the Fourth Assessment Reprot of the Intergovernmental Panel on Climate Change*. New York, NY: Cambridge University Press.

**Stevens R, Buret M, Garchery C, Carretero Y, Causse M**. 2006. Technique for rapid, small-scale analysis of vitamin C levels in fruit and application to a tomato mutant collection. *Journal of Agricultural and Food Chemistry* **54**, 6159-6165.

**Stitt M, Sulpice R, Keurentjes J**. 2010. Metabolic networks: How to identify key components in the regulation of metabolism and growth. *Plant Physiol.* **152**, 428-444.

**Summermatter K, Sticher L, Metraux JP**. 1995. Systemic responses in *Arabidopsis-thaliana* infected and challenged with *pseudomonas-syringae pv. syringae*. *Plant Physiology* **108**, 1379-1385.

**Tallis MJ, Lin Y, Rogers A, Zhang J, Street NR, Miglietta F, Karnosky DF, De Angelis P, Calfapietra C, Taylor G**. 2010. The transcriptome of Populus in elevated $CO_2$ reveals increased anthocyanin biosynthesis during delayed autumnal senescence. *New Phytologist* **186**, 415-428.

**Tanaka R, Tanaka A**. 2007. Tetrapyrrole biosynthesis in higher plants. *Annual Review of Plant Biology* **58**, 321-346.

**Tausz M, Gonzalez-Rodriguez AM, Wonisch A, Peters J, Grill D, Morales D, Jimenez MSJ**. 2004. Photostress, photoprotection, and water soluble antioxidants in the canopies of five

Canarian laurel forest tree species during a diurnal course in the field. *Flora* **199**, 110-119.

**Taylor G, Street NR, Tricker PJ, Sjodin A, Graham L, Skogstrom O, Calfapietra C, Scarascia-Mugnozza G, Jansson S**. 2005. The transcriptome of Populus in elevated $CO_2$. *New Phytologist* **167**, 143-154.

**The Royal Society**. 2008. Ground-level ozone in the 21st century: future trends, impacts and policy implications. *Science Policy Report 15/08*. London.

**Thimm O, Blasing O, Gibon Y, Nagel A, Meyer S, Kruger P, Selbig J, Muller LA, Rhee SY, Stitt M**. 2004. MAPMAN: a user-driven tool to display genomics data sets onto diagrams of metabolic pathways and other biological processes. *Plant Journal* **37**, 914-939.

**Travers SE, Tang ZW, Caragea D, Garrett KA, Hulbert SH, Leach JE, Bai JF, Saleh A, Knapp AK, Fay PA, Nippert J, Schnable PS, Smith MD**. 2010. Variation in gene expression of *Andropogon gerardii* in response to altered environmental conditions associated with climate change. *Journal of Ecology* **98**, 374-383.

**Van Dingenen R, Dentener FJ, Raes F, Krol MC, Emberson L, Cofala J**. 2009. The global impact of ozone on agricultural crop yields under current and future air quality legislation. *Atmospheric Environment* **43**, 604-618.

**Vapaavuori E, Holopainen JK, Holopainen T, Julkunen-Tiitto R, Kaakinen S, Kasurinen A, Kontunen-Soppela S, Kostiainen K, Oksanen E, Peltonen P, Riikonen J, Tulva I**. 2009. Rising atmospheric $CO_2$ concentration partially masks the negative effects of elevated $O_3$ in silver birch (*Betula pendula Roth*). *Ambio* **38**, 418-424.

**Velikova V, Tsonev T, Pinelli P, Alessio GA, Loreto F**. 2005. Localized ozone fumigation system for studying ozone effects on photosynthesis, respiration, electron transport rate and isoprene emission in field-grown Mediterranean oak species. *Tree Physiology* **25**, 1523-1532.

**Vingarzan R**. 2004. A review of surface ozone background levels and trends. *Atmospheric Environment* **38**, 3431-3442.

**Volin JC, Reich PB**. 1996. Interaction of elevated $CO_2$ and $O_3$ on growth, photosynthesis and respiration of three perennial species grown in low and high nitrogen. *Physiologia Plantarum* **97**, 674-684.

**Wahid A, Perveen M, Gelani S, Basra SMA**. 2007. Pretreatment of seed with $H_2O_2$ improves salt tolerance of wheat seedlings by alleviation of oxidative damage and expression of stress proteins. *Journal of Plant Physiology* **164**, 283-294.

**Wittig VE, Ainsworth EA, Naidu SL, Karnosky DF, Long SP**. 2009. Quantifying the impact of current and future tropospheric ozone on tree biomass, growth, physiology and biochemistry: a quantitative meta-analysis. *Global Change Biology* **15**, 396-424.

**Woo HR, Kim JH, Nam HG, Lim PO**. 2004. The delayed leaf senescence mutants of Arabidopsis, *ore1*, *ore3*, and *ore9* are tolerant to oxidative stress. *Plant and Cell Physiology* **45**, 923-932.

**Wustman BA, Oksanen E, Karnosky DF, Noormets A, Isebrands JG, Pregitzer KS, Hendrey GR, Sober J, Podila GK**. 2001. Effects of elevated $CO_2$ and $O_3$ on aspen clones varying in $O_3$ sensitivity: can $CO_2$ ameliorate the harmful effects of $O_3$? *Environmental Pollution* **115**, 473-481.

**Zimmermann P, Zentgraf U**. 2005. The correlation between oxidative stress and leaf senescence during plant development. *Cellular & Molecular Biology Letters* **10**, 515-534.